**LEVEL**

Report No. AUE-802

# EVALUATION OF ADINA: Part II
## Operating Characteristics

J. Padovan
T. Y. Chang

College of Engineering
The University of Akron
Akron, OH 44325

June 8, 1980

DTIC

MAR 23 1981

C

AD A096681

THE UNIVERSITY OF AKRON
FIAT LUX
1870

81 3 23 014

Report No. AUE-802

EVALUATION OF ADINA. Part II.

Operating Characteristics.

J. Padovan

T. Y. Chang

College of Engineering
The University of Akron
Akron, Ohio 44325

June 8, 1980

Prepared for

Office of Naval Research
Department of the Navy

Contract N00014-78-C-0691

# TABLE OF CONTENTS

i

# TABLE OF CONTENTS

ii

TABLE OF FIGURES

TABLE OF FIGURES (Cont'd)

# TABLE OF FIGURES (Cont'd)

## TABLE OF FIGURES (Cont'd)

## TABLE OF FIGURES (Cont'd)

## I.    Introduction

The purpose of this volume will be to provide an
evaluation of the various algorithmic options inherent to
ADINA (1977).  The main thrust of the work will be to esta-
blish the inherent characteristics of the static, dynamic
and eigenvalue extraction solution branches.  This will
be considered in two steps:

i)    Overview framework of algorithmic options,
and

ii)    Establish computational capabilities and short-
comings.  This is achieved through extensive
benchmarking.

The benchmarking utilized will itself serve two basic
purposes namely:

1)    Establish the algorithmic sensitivities, con-
vergence characteristics and typical solution
failures generic to ADINA and secondarily;

2)    Perform code check out.

For the static and dynamic branches, benchmarks will
be used to quantify the convergence, stability and artificial
propagation characteristics.  In this direction, the results
of several numerical experiments will be employed to check
out the handling of:

a)    Kinematic nonlinearities;

b)    Material nonlinearities and;

c)    Combined geometric and material nonlinearities.

Special emphasis will be given to ascertaining the operating
characteristics in the presence of softening, hardening,

elastic/plastic and load/unload situations. In this context, the major purpose of the benchmarking will be to establish the sensitivity/pathological behavior of the various generic nonlinear algorithms to changes in:

    a) Convergence criteria

    b) Time step size

    c) Load increment size and

    d) Material models etc.
    e) Order of integration of element stiffnesses

To enable the evaluation of the various inherent anomalous behaviorial pathologies, the strain energy will be monitored during the various stages of calculation. This includes both local and global evaluations. Such an approach will allow for the monitoring of the initiation characteristics of pathological behavior which is either local or global in nature.

In addition to testing the purely transient phase, the eigenvalue/vector extraction routine will also be evaluated. The benchmarks used in this phase of evaluation will establish such factors as convergence properties, eigenvalue/vector deterioration, multiplicity and separability etc.

As a natural outgrowth of the foregoing approach, various aspects of the configuration control potential inherent to ADINA will be discussed. This will include such features as:

    i) Equation solver options (eigenvalue extraction routines, integration schemes as well as various nonlinear algorithms) and;

ii) Equation solver parameters (time steps, load increments, tolerance limits iteration counts etc.)

Since many of these features are of significant importance to nonlinear codes, each of the foregoing configuration control options will be examined in detail.

Based on the foregoing, the overall report will be organized in four main sections including:

i) An overview of the basic framework of the non-linear algorithmic solution options;

ii) A detailed benchmarked discussion of algorithmic capabilities and shortcomings;

iii) A discussion of suggested algorithmic improvements and lastly;

iv) A summary of results.

Appendices which include equations for calculating the global and local strain energies, code checkout benchmarks and program listings of code modifications employed in the study and lastly sample problem data input echoes.

## II.    Overview of Framework of Algorithmic Solution Options

As noted earlier, this section will consider the numerical framework of the various algorithmic options available to ADINA. In particular, this will include discussions of the generic/ static nonlinear equation solver, the dynamic and eigenvalue solution branches, the convergence schemes, user I/0 options, adaptive strategies and programmed error stops.

## II.1    Generic/Static Nonlinear Equation Solver

Based on the theoretical framework of the governing field equations outlined in Part I it follows that the Modified Newton Raphson (MNR) algorithm is the generic ADINA nonlinear equation solver.  In particular, it is employed both for the static and dynamic branches of the code.  The algorithm is encoded with three main options namely:

   i)   Load incrementation with iteration and reformation
        (only once);

  ii)   Load incrementation with iteration but no reformation
        and lastly;

 iii)   Load incrementation and reformation.
The overall logic flow associated with such options is defined in Fig. 1.  In particular the reformation loop in ADINA has been specialized so as to provide for nonlinear element stiff- ness updating only at the beginning of a new load or time step. From that point on, iteration proceeds without reformation. Figures (2, 3, and 4) present a graphical representation of the flow of calculation associated with such options.  Note
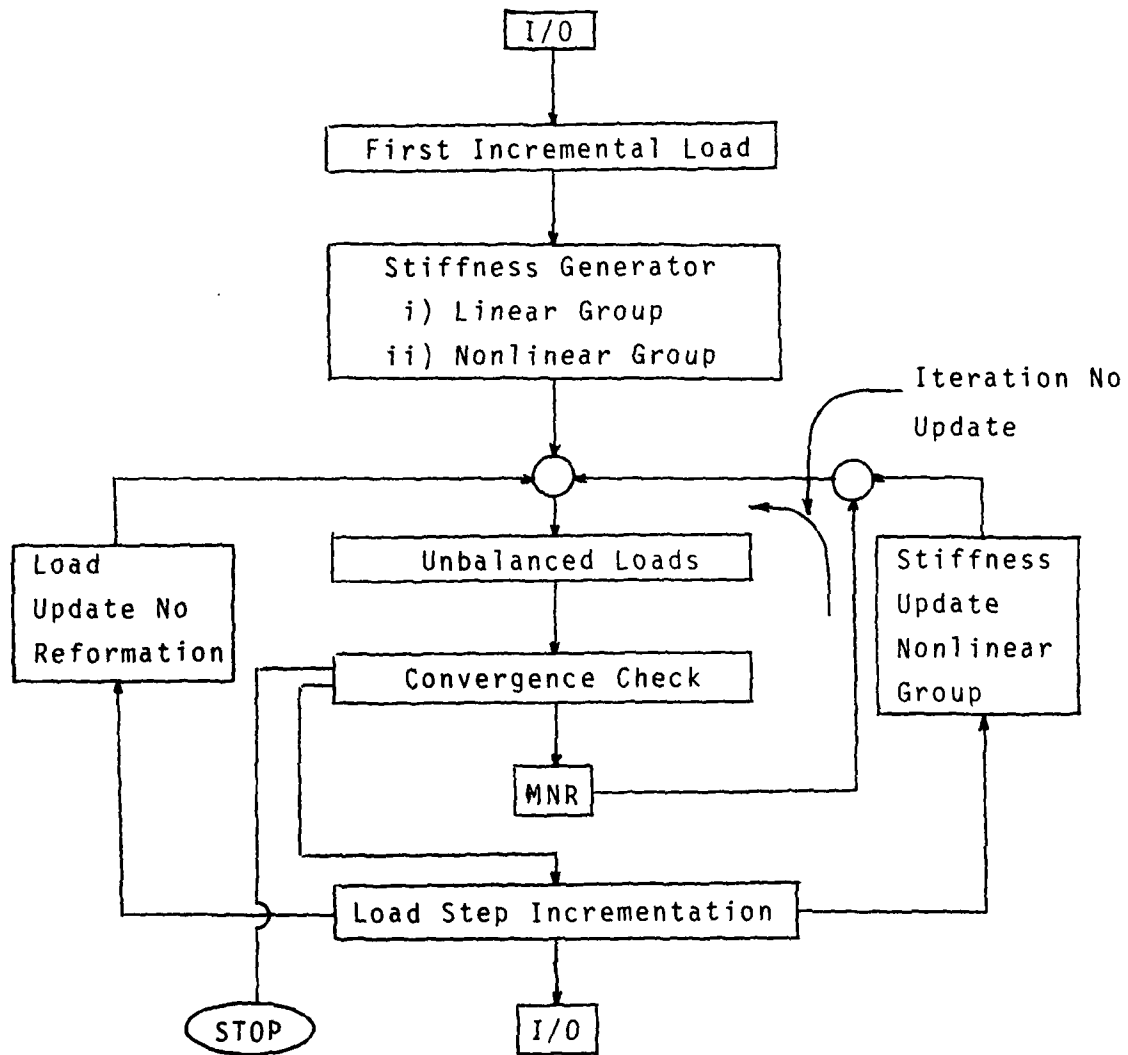
Fig. II.1   Flow Diagram of Newton Raphson Algorithm
            (modified)

$\Delta P$ = Load Increment

$\Delta P$

$||\underset{\sim}{F}||$

$||\underset{\sim}{Y}||$

1. Load Incrementation
2. Reformation
3. Iteration
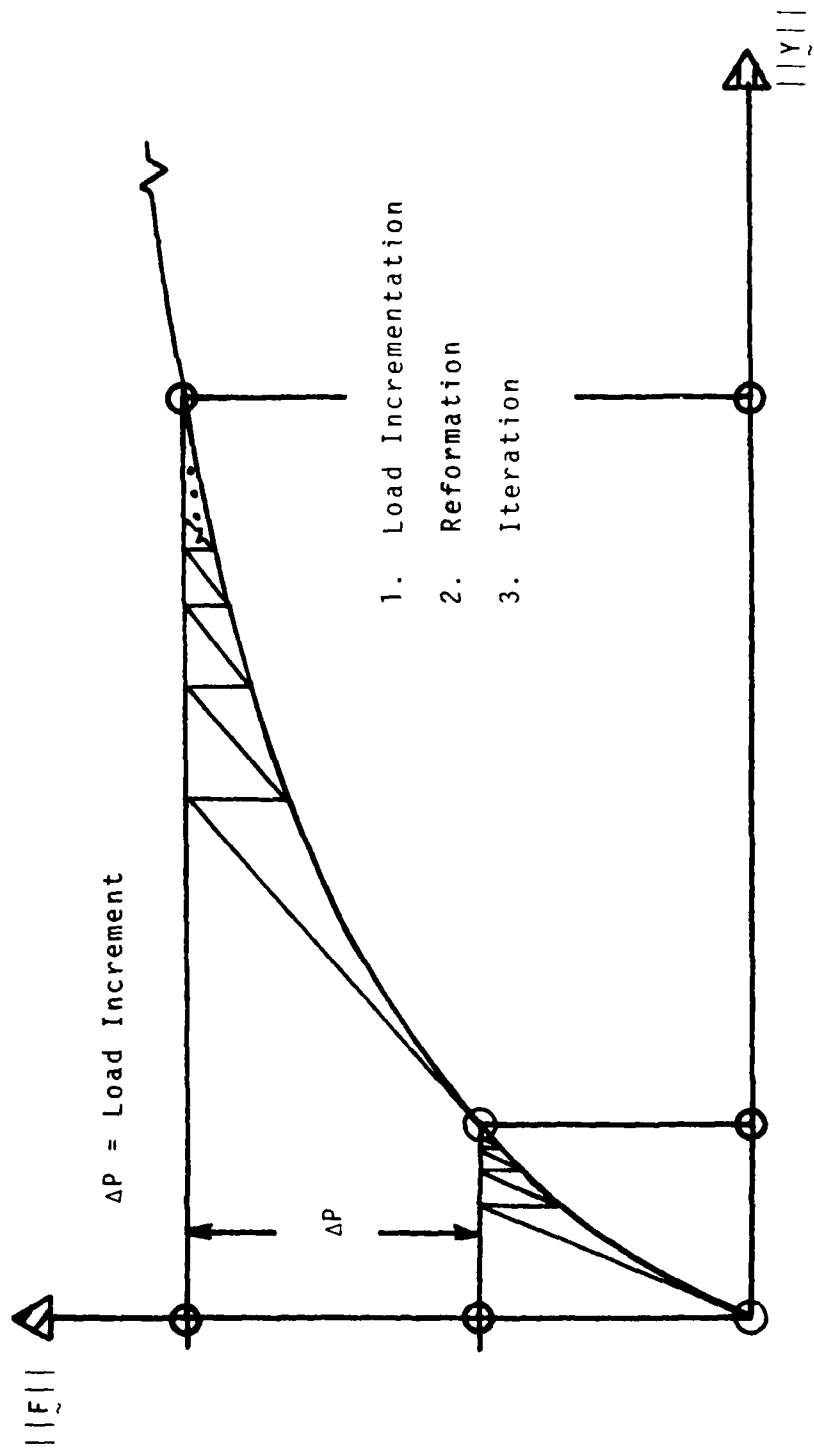
Fig. II-2  Modified NR Procedure with Reformation

1. Load Incrementation
2. No Reformation
3. Iteration

$\Delta P$=Load Increment

$||F||$

$||Y||$
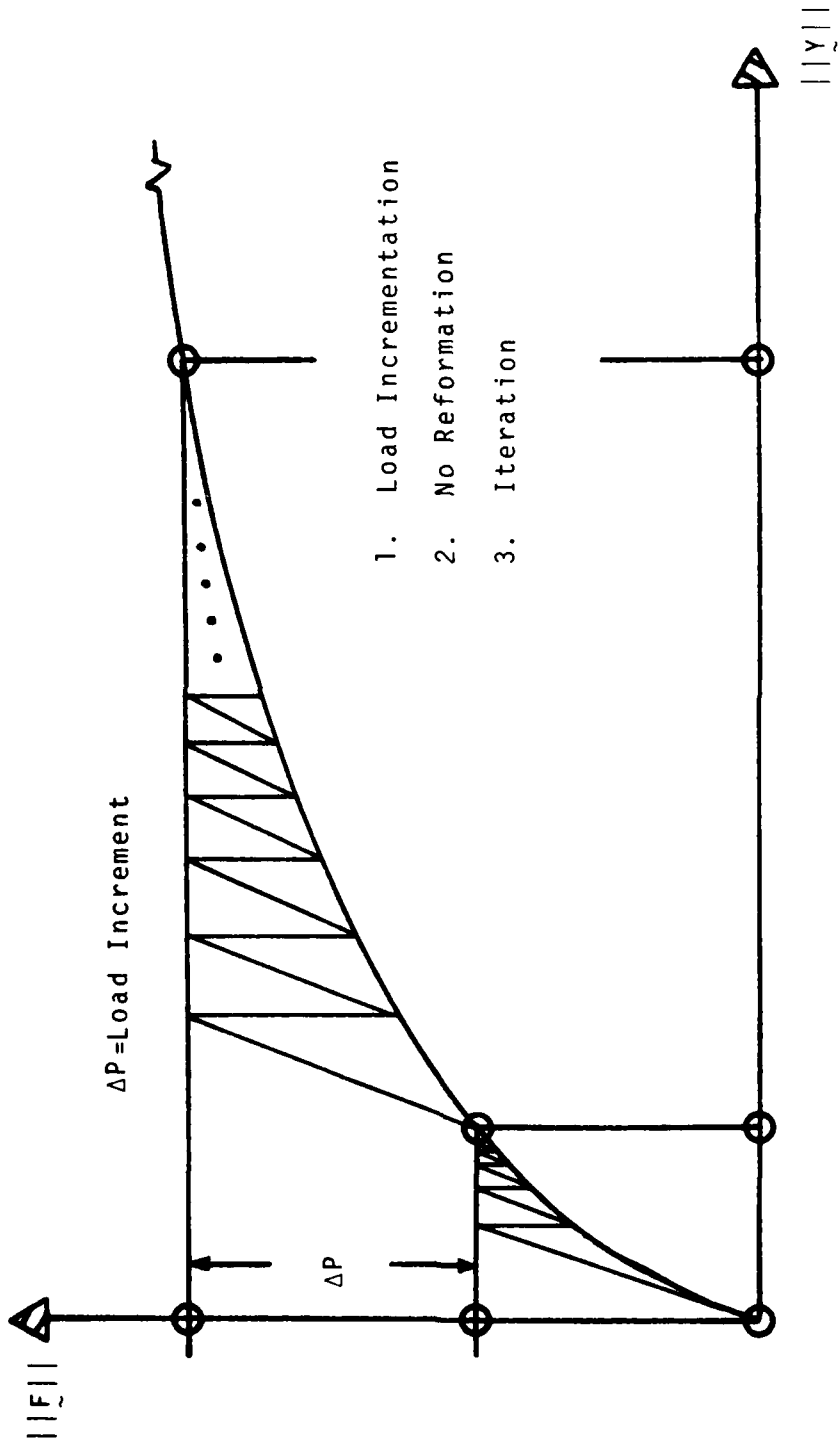
Fig. II-3  Modified NR Procedure with No Reformation
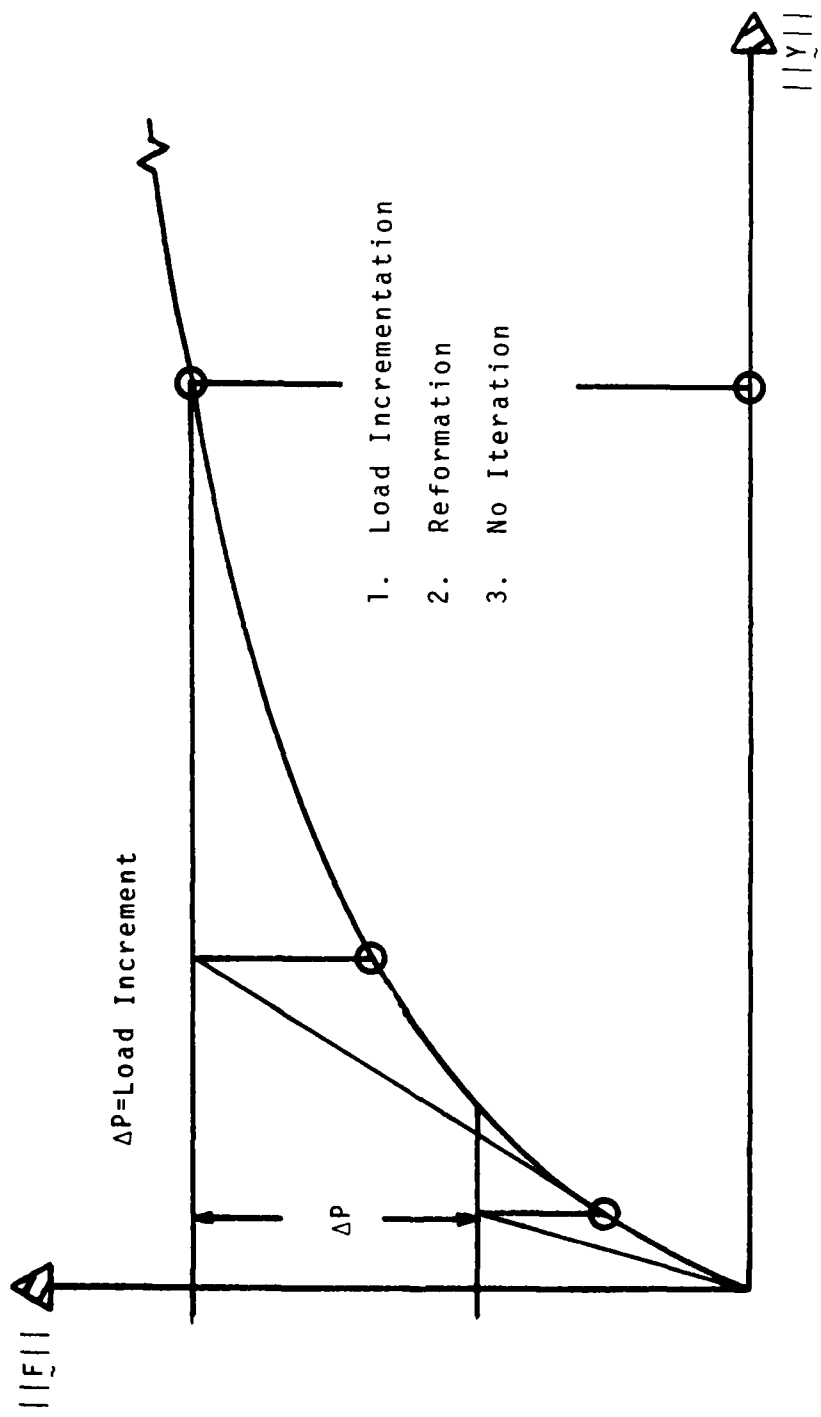
Fig. II-4 Modified NR With Reformation/No Iteration

these options have been programmed for both the static and dynamic branches of ADINA.

The convergence checks associated with the MNR algorithm are two-fold, namely,

1)  A norm test of successive nodal increment vectors as represented by

$$||\underset{\sim}{y}_i||/||\underset{\sim}{y}_{i+1}|| \leq \text{tolerance}$$

2)  A norm test of successive out of balance loads as represented by

$$||R_i|| > ||R_{i+1}||$$

The first test determines whether the solution has converged. The second assures that the tendency of convergence is maintained.

Note while the iteration counter limit can be superceded by a user I/0 option, the out of balance and negative pivot stops do not allow for direct user intervention. This appears appropriate since such events are usually a natural outgrowth of some form of solution divergence. In ADINA, typically such pathologies occur under the following broad category of situations namely:

1)  In the neighborhood of buckling points (Fig. II.5) wherein there is either a significant change or a complete reversal of structural stiffness;

2)  In the neighborhood of plastic unloading zones, Fig. II.6;
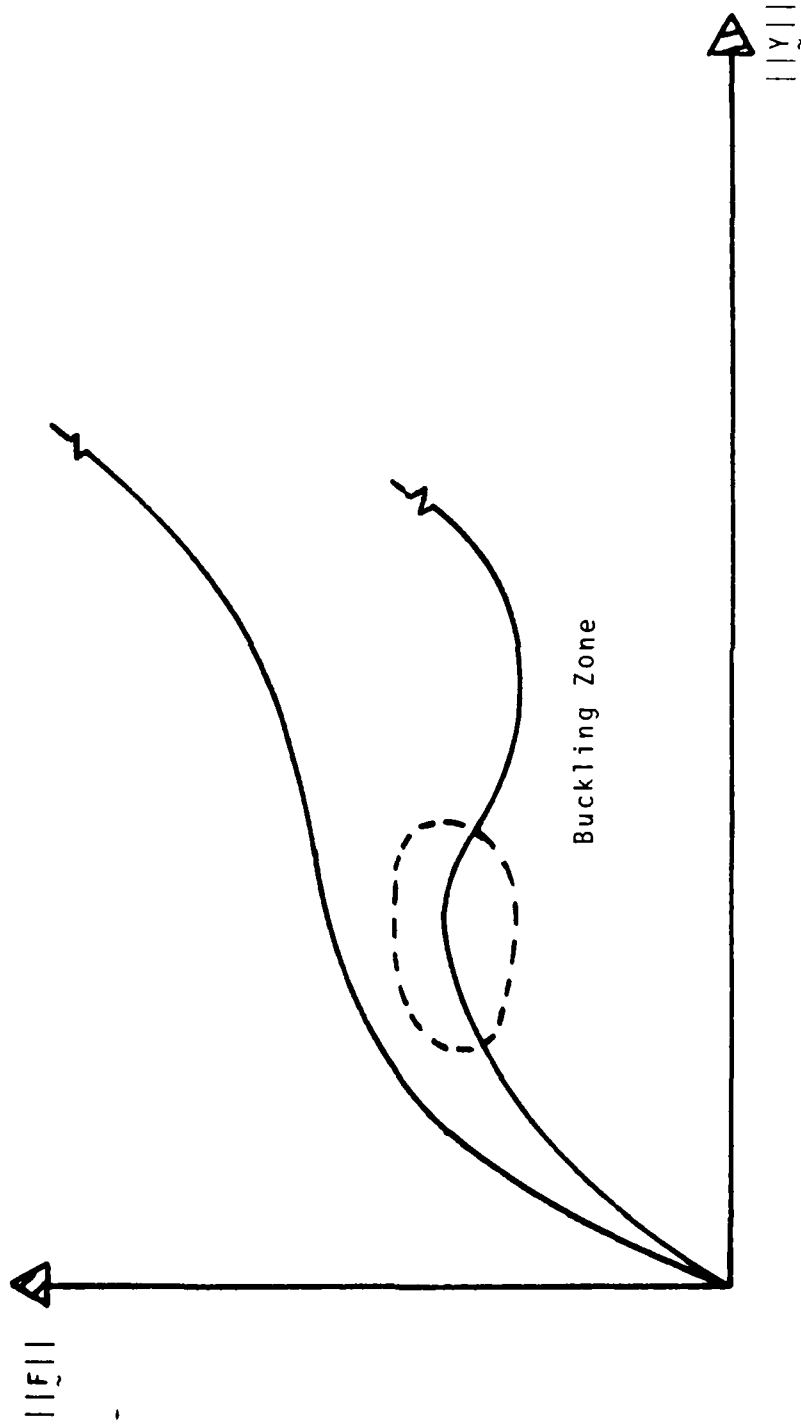
Fig. II-5  Typical Load Deflection Curves in Vicinity of Buckling Zone
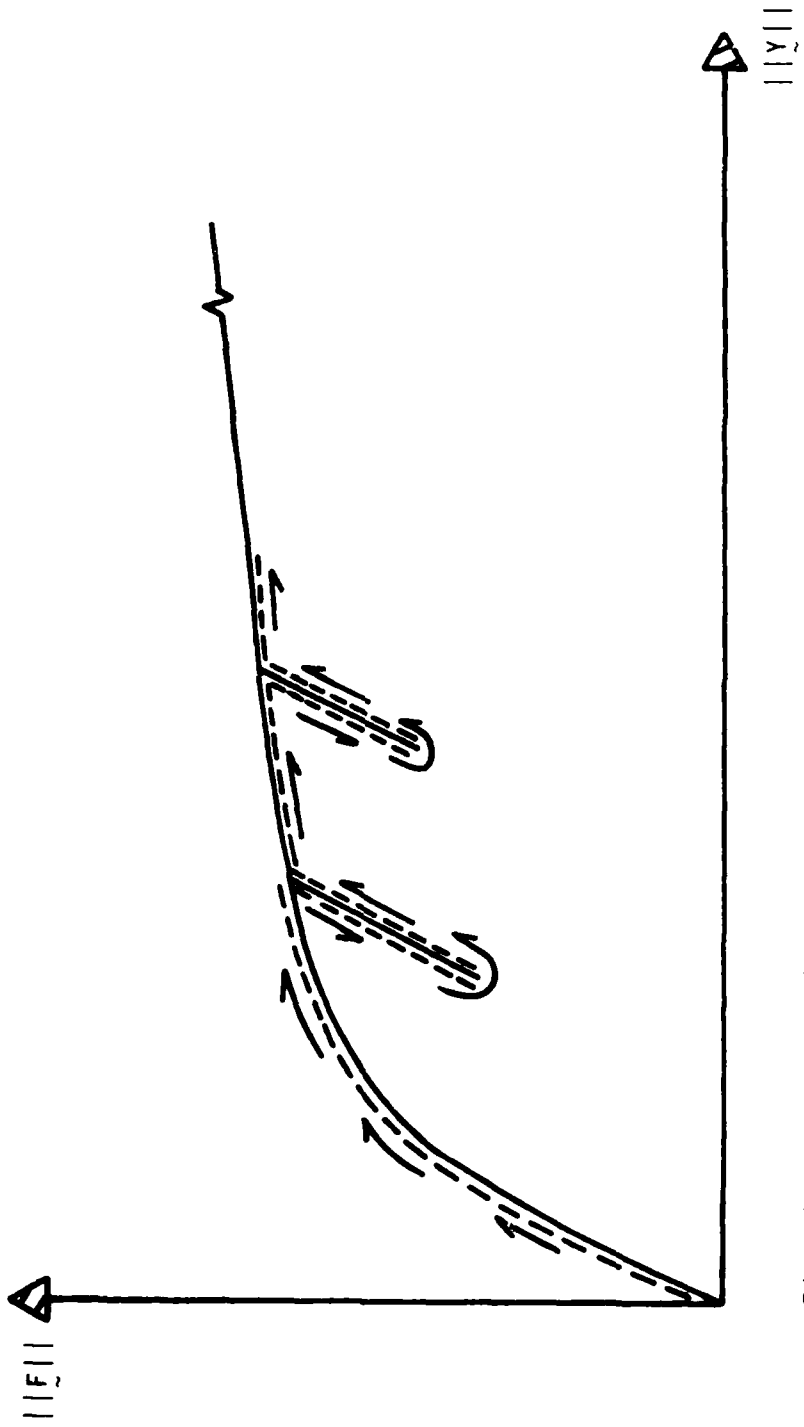
Fig. II-6  Typical Load Deflection Curve for Elastic-Plastic Load-Unload Problem

3)  Use of excessive load step size and;

4)  Use of excessive time step size.

Typically, in the vicinity of buckling points either the out of balance load or negative pivot stop are encountered. As seen from the scenarios depicted in Figs. II.7 and 8, such stops are a direct outgrowth of the use of the MNR operator which is driven by the "tangent hyper-plane" of the solution surface. Note the tangent plane in the neighborhood of buckling points can become quite shallow with possible "slope" reversals. Because of this, as currently programmed, there is no possibility to analyze the post buckling range through the user I/0 intervention capabilities currently available in ADINA. What is obviously necessary is the incorporation of heuristic (adaptive) programming to circumvent the difficulties in such problems. This will be discussed in more detail later in Section IV.

The reason for solution blow ups in the neighborhood of plastic unloading zones is essentially a direct outgrowth of the modified NR algorithm employed by ADINA. As reformation occurs only at the beginning of a load step, if some unloading occurs during the iteration phase, then it is not properly accounted for. As will be seen later, this obviously leads to solution drift and typically out of balance loads.

While the use of excessive load step sizes can lead to solution stops generated by any of the checks, typically the out of balance stop is most often encountered. Generally,
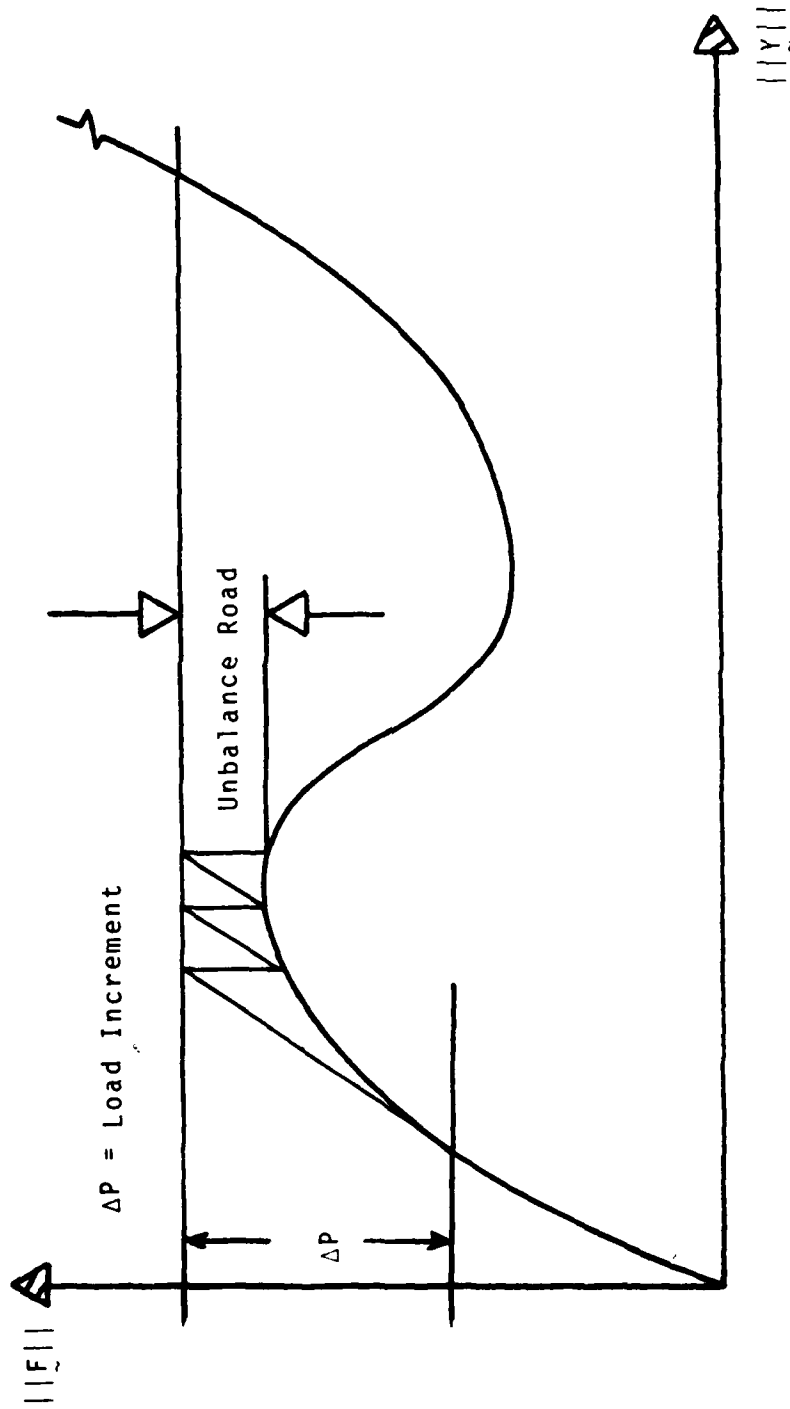
Fig. II-7  Typical Out-of-Balance Load Problem Generated in
Neighborhood of Buckling Zone

14
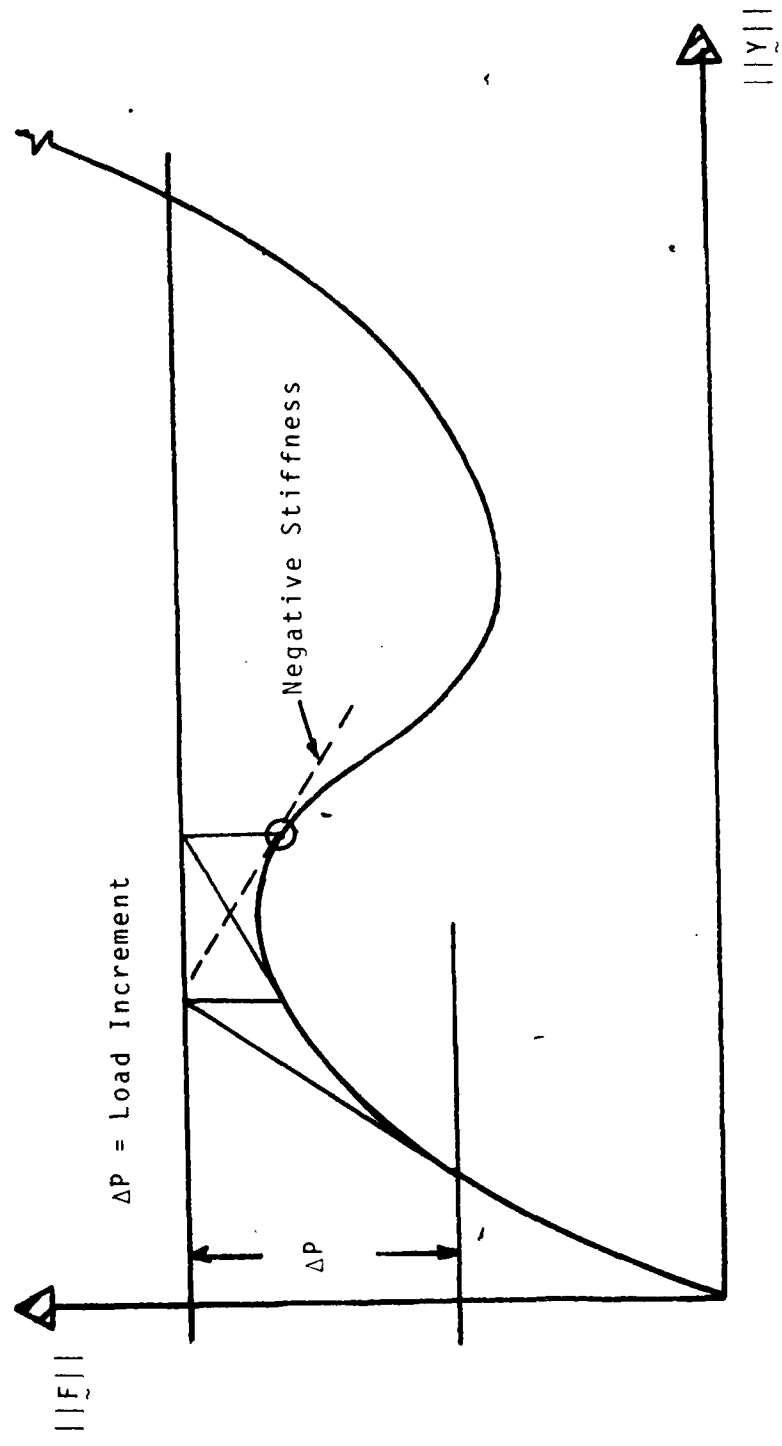
Fig. II-3   Typical Negative Stiffness Generated in Neighborhood of Buckling Zone

excessively large steps tend to lead to solution divergence. Usually this is due to the fact that large load steps may excite significant changes in the stiffness of a given structure. If these changes occur within a given load step, the modified INR employed by ADINA will miss them. Hence since the hyper surface representing the solution is extremely complex, the algorithm will usually drift aimlessly over the surface until typically out of balance loads are excited. In a similar manner, excessive time step sizes may also lead to solution divergence caused by the large changes occurring during a given interval of time.

As was noted earlier, the 1977 version of ADINA does not possess any heuristic programming which can automatically circumvent convergence difficulties. The only recourse open to the ADINA user is to employ:

1) The restart option and/or;

2) The time block option.

With these options, it is possible to either manually reset the algorithmic option and restart or preset the algorithmic choice at a predetermined point in time. Generally the scenario used follows the sequence of events defined below:

1) **Restart option**

    i.  Store all field quantitites generated on tape;

    ii.  When error stop is encountered, manually restart with new algorithmic choice and;

    iii.  Continue process to successful completion.

2) <u>The Block Option</u>

   i. Having employed the restart option to obtain a successful solution, points of unloading can obviously be determined;

   ii. With such information available, the appropriate algorithm can be selected for an estimated time block.

  iii. Once all the time blocks are created, ADINA will automatically use the preselected algorithm for a given time interval.

While the foregoing options are certainly an improvement over the straight primitive algorithmic choices, it presupposes user knowledge of the various solution sensitivities which for *nonlinear problems* are both structure and loading dependent. That is, the solution sensitivities of a given nonlinear structure may shift from load to load. Furthermore, for "one of the kind" problems for which nonlinear codes are oftentimes used, such knowledge can be obtained only after sufficient parametric studies have been completed. As noted earlier, such an approach can oftentimes require significant manpower allocations as well as extensive amounts of computer time.

II.2 <u>Dynamic Equation Solver</u>

As noted in Part I, for time dependent problems numerical integration is required to obtain a solution. In ADINA, this is achieved via the use of either implicit or explicit operators namely:

1) Implicit operators:

    i)   Wilson $\theta$ method[1]

    ii)  Newmark method[2]

2) Explicit: Central Differences[3]

To trace through the algorithmic flow of the transient branch, the use of the Wilson operator will be considered. Its form is given by:[2]

$$\underset{\sim}{^{t+\Delta t}\Delta\ddot{Y}} = (1-\frac{1}{\theta})\ \underset{\sim}{^{t}\Delta\ddot{Y}} + \frac{1}{\theta}\ \underset{\sim}{^{t+\theta\Delta t}\Delta\ddot{Y}} \tag{II.1}$$

$$\underset{\sim}{^{t+\Delta t}\Delta\dot{Y}} = \underset{\sim}{^{t}\Delta\dot{Y}} + \frac{\Delta t}{2}\ (\underset{\sim}{^{t}\Delta\ddot{Y}} + \underset{\sim}{^{t+\Delta t}\Delta\ddot{Y}}) \tag{II.2}$$

$$\underset{\sim}{^{t+\Delta t}\Delta Y} = \underset{\sim}{^{t}\Delta Y} + \Delta t\,\underset{\sim}{^{t}\Delta\dot{Y}} + \frac{(\Delta t)^2}{6}\ (\underset{\sim}{^{t+\Delta t}\Delta\ddot{Y}} + 2\,\underset{\sim}{^{t}\Delta\ddot{Y}}) \tag{II.3}$$

Employing the operators defined by (II.1 - 3), the following sequence of operations is necessary to develop the solution for one time step namely:

1. At beginning of new time step update structural stiffness;
2. Form effective load;
3. Solve for incremental displacements;
4. If required, iterate dynamic algorithm and;
5. Upon convergence, establish final fields for beginning of next time step (displacements, velocities, accelerations, stresses, strains, etc.).

Since the generic nonlinear equation solver employs a modified form of NR algorithm, the iteration process designated by Step 4

involves no reformation of the stiffness. As with the static
solution branch, the convergence check associated with the
iteration process involves the use of norm tests on the dis-
placements and out of balance loads. In short, apart from
the capability of choosing either implicit or explicit opera-
tors, all the iteration options, convergence checks, error
stops, user intervention options (restart, time blocks) etc.
are the same as those of the static branch.

## II. 3  Eigenvalue/vector Algorithm

Since the calculation of the frequencies and associated
mode shapes is important in modal analysis, many general pur-
pose codes have been provided with an extraction algorithm. In
nonlinear codes such as ADINA, the main importance of the eigen-
value/vector algorithm lies in the fact that it can be used to
establish the requisite time increment for dynamic analysis
problems.

In ADINA the algorithm considers the generalized eigen-
value problem defined by

$$[K] \underset{\sim}{V} = \omega^2 [M] \underset{\sim}{V} \qquad (II.4)$$

where

   [K] - is the tangent stiffness matrix at time zero

   [M] - is the mass matrix

   $\underset{\sim}{V}$ - the modal vector

   $\omega$ - the system frequency

Because of the generality of programming, the mass matrices
handled can be either of the lumped or consistent types.

The algorithm programmed in ADINA is the determinant search method as defined in[ 4 ]. The algorithm combines two basic steps namely

   i)  Triangular factorization and

  ii)  Vector inverse iteration.

The eigenvalues are obtained in a sequence starting from the least dominant eigenvalue where it should be noted that the lowest may be zero. Because of this, the algorithm can be employed to calculate the rigid body modes.

Once one eigenvalue/vector is obtained, a fairly efficient accelerated secant iteration procedure is used to obtain a shift near to the next unknown eigenvalue. The eigenvalue separation theorem, Sturm's sequence property, is employed in this iteration. The determinant evalution involves a triangular factorization of the eigenvalue problem defined by Eq. (II.4). Once a shift to the neighborhood of unknown eigenvalue is obtained, inverse iteration is used to calculate the eigenvector. The associated eigenvalue is then extracted accurately by employing the Rayleigh quotient correction to the shift.

The output options available to the user are fairly extensive. The more important of these are defined by:

1.  Any number of frequencies can be calculated up to number of system freedoms and

2.  Cut off frequency option.

### III    Computational Capabilities and Shortcomings

To determine the overall capabilities and shortcomings
of the static and dynamic algorithmic apparatus inherent to ADINA,
several major behavioral traits must first be ascertained,
namely:

1)   The generic algorithmic sensitivities;

2)   The overall convergence characteristics and lastly'

3)   The generic types of solution blow ups encountered.

The evaluation of such algorithmic characteristics will involve
the determination of the effects of several factors.  These
include such items as:

i)    The load increment size;

ii)   The time step size;

iii)  The material properties;

iv)   The kinematic nonlinearity, etc.

In the case of the eigenvalue/vector extraction algorithms,
the major characteristics to be considered include:

1.   Convergence properties;

2.   Eigenvalue/vector deterioration;

3.   Multiplicity and separability.

Since the major thrust of ADINA (1977) is its capability
to handle nonlinear materials and large deformations kinematics,
the main emphasis of the algorithmic check out will involve both
the static and dynamic solution capabilities.  The approach taken
to evaluate the properties of such solution branches will be

essentially three fold in particular:

1)  Establish and perform bench mark tests; 2)  Perform parametric studies to evaluate algorithmic sensitivities and; 3)  Establish comprehensive convergence tests.

As will be seen later, the main purpose of the bench marking will be to establish the algorithmic sensitivities, convergence characteristics and typical solution blow ups generic to ADINA.  In this context, the benchmarks will be chosen so as to establish the characteristic anomalous solution behavior.  Such behavior will be accentuated by performing parametric studies involving such factors as load step size, time step size, material properties, kinematic nonlinearities, etc.

The main purpose of the comprehensive convergence testing will be to monitor solution degradation as the various above mentioned factors are parametrically varied.  The use of such convergence tests in conjunction with the benchmark problems will enable the characterization of the overall solution pathologies inherent to ADINA.

In addition to the foregoing static, dynamic and eigenvalue check outs, several benchmarks will be presented which evaluate the pathological characteristics inherent to the Gaussian quadrature of the isoparametric element stiffnesses.  This will include such considerations as determining how the degree of accuracy is affected by the integration order.

In the context of the foregoing, the subsections to follow will include discussions on the establishment of comprehensive convergence tests, as well as on the results of parametric studies involving a variety of benchmark problems including static, dynamic, eigenvalue and element stiffness integration evaluations.

## III.1  Convergence Tests

To establish the pathologies of the algorithmic sensitivities of ADINA, a comprehensive convergence test which can

monitor both the quality and direction of a given iteration process must be developed. In this context, the standard norm tests on the nodal increment vector and out of balance loads cannot serve in such a capacity. This follows from the fact that the basic structure of such tests is geared primarily to determining outright success or failure of solution rather than the quality of convergence. In particular, what is necessary, is the ability to track both the local as well as global behavior of the iterated solution.

Before developing such a convergence monitor, it is worthwhile to note that for statically loaded problems, the manner of loading holds the key to the direction of proper convergence. For instance, assuming that the loading is monotonically applied, then one would expect essentially monotone behavior in the various field variables. Similar statements can be made of the early stages of the transient response problem. Such behavioral traits should obviously be expected of the iteration process. Namely, monotone loading should always lead to monotone decreasing iterates and monotone field variables. As it is computationally inefficient to track the monotonicity of the various field variables such as displacement, stress or strain, an alternative measure should be employed.

In the context of the foregoing, the local and global strain energy functions are admirably suited for the current purpose. This follows from the fact that in addition to the all important global and load monotonicity properties, the strain energy also has positive or negative definite attributes. Namely, as the calculations proceed for a monotone

loading situation, one would expect a sequence of monotone, positive definite energy iterates. As will be seen in the next section, behavior to the contrary will almost always lead to solution divergence or at best poor convergence characteristics.

Based on applications of the virtual work principle and the incremental approach, the strain energy stored is given by the expression (Derivations given in Appendix A1)

$$E_t = \frac{1}{2} \sum_{i=1}^{I} \sum_{k=1}^{k^i} \left( \int_{0^R} [B \ (\underset{\sim i}{Y}^k)]^T \ \underset{\sim}{\sigma} \ (\underset{\sim i}{Y}^k) \ dV + \int_{0^R} [B \ (\underset{\sim i}{Y}^{k+1})]^T \ \underset{\sim}{\sigma} \ (\underset{\sim i}{Y}^{k+1}) \ dV \right)^T \Delta \underset{\sim i}{Y}^k \qquad \text{(III.1)}$$

where $E_t$ is the total strain energy stored during an iteration cycle involving I loadsteps, $k^i$ the number of iterations required for convergence during $i^{th}$ load increment and $\Delta \underset{\sim i}{Y}^k$ the $k^{th}$ nodal displacement increment of the $i^{th}$ load step. By interpreting the nodal deflection vector $\underset{\sim i}{Y}^k$ as either of an element or global form (III.1) can be used to describe the local element or global strain energies stored. Lastly, due to its generalized form (III.1) can be employed for all the material models inherent to ADINA. For the sake of convenience, the derivation of the expression for $E_t$ is given in Appendix 2.

In order to perform energy checks of the solution, various modification had to be implemented in the ADINA program. So as not to adversely effect core requirements and

dynamic allocation, a new direct access file was defined.
To increase the generality of the energy option, the addi-
tion was programed so as to handle the following possibilities:

1) Multiple element groups;

2) Multiple solution blocks;

3) All material property groups and;

4) All algorithmic options.

## III.2 Benchmarking/Parametric Studies

While the benchmarking discussed in this section serves
the purpose of a check on the accuracy of the programming and
adequacy of the theory inherent to ADINA (1977), its main
function is to determine the computational capabilities and
shortcomings of the algorithmic apparatus. For convenience,
those benchmarks which were run to strictly check out the
code are discussed in Appendix 2 and the input data are
included in Appendix A3. In this context, as noted
earlier, this section will overview the results of extensive
parametric studies involving the effects of such factors as:

i) Load step size;

ii) Time step size;

iii) Material properties;

iv) Kinematic nonlinearities etc.

The main thrust of the parametric studies will be to determine
the pathology of anomalous behavior inherent to the ADINA
algorithmic apparatus.

At this juncture, it should be noted that the field theories and algorithmic approaches are up-to-date and accurately programmed. Hence, the anomalous behavior depicted herein rather than being inherent to ADINA are generic to nonlinear structural analysis in general.

For convenience, the overall section will be divided into several subsections concentrating on such items as the static, dynamic and eigenvalue branches of solution.

### III.2a  Static Solution

This subsection will consider the algorithmic sensitivities of the static solution branches. Because of this emphasis, the geometric configuration of the benchmarks considered will purposely be kept simple yet diverse enough to account for geometric configuration effects.

Interestingly, while such factors as geometry, material properties, boundary conditions, etc. all have some effect on the choice of load increment size, once an excessive value has been chosen, typically similar types of solution degradation are encountered. In this context, the first benchmark chosen will be used to establish much of the generic solution anomalies inherent to situations wherein excessive load step increments are considered. Figure III.1 illustrates the geometry, loading and material properties of a rubber sheet which serves as benchmark 1. This problem combines kinematic, kinetic and material nonlinearity since large deformations and Mooney type materials[5] are admitted in the model. To establish the generic solution anomalies of the static
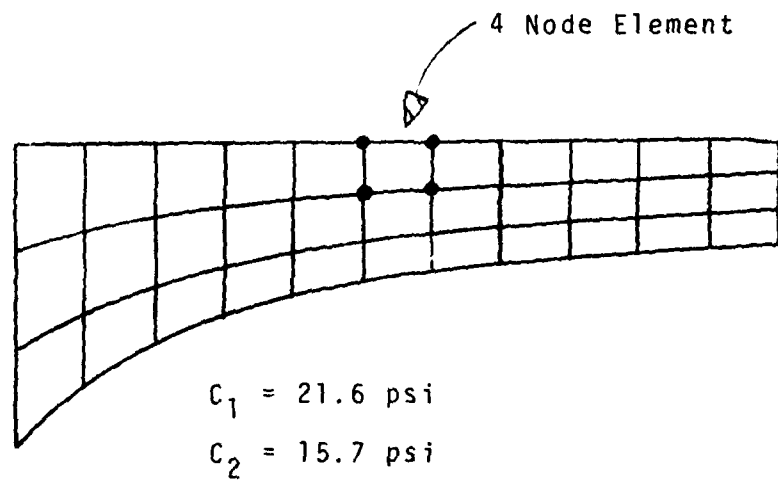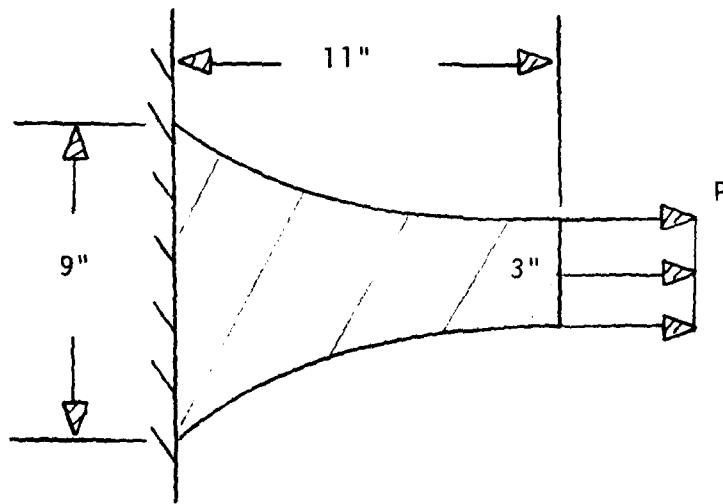
Fig. III-1   Rubber Sheet Geometry, Material Properties
and Element Model

algorithm, three basic scenarios typical of ADINA will be excited namely:

1. Outright solution failure in first load step;

2. Solution failure in successive load steps;

3. Poorly converged solutions.

The actual nature of solution degradation depends on the relative magnitude of incrementation. Typically three basic types of solution pathology occur. These can be categorized by:

1. Immediate and strong nonmonotonicity;

2. Moderate but progressively increasing non-monotonicity and nonpositive definiteness and;

3. Mild monotonicity with either very gradual increases or decreases in solution oscillations.

Note such behavior can be excited either in the first or successive load steps. For example, Fig. III.2 illustrates immediate nonmonotonicity in the first load step caused by excessive incrementation size. While solution failure for the given load step was initiated by a Fortran overflow stop, typically out-of-balance loads are encountered for such problems.

For the given problem, for load increments somewhat lower than those of the proceeding example, typically moderate but progressively increasing nonmonotonicity can be excited either in the first or successive load steps. Figures III.3-5 illustrates such solution degradation. As can be seen, for the given load increment, excellent convergence is
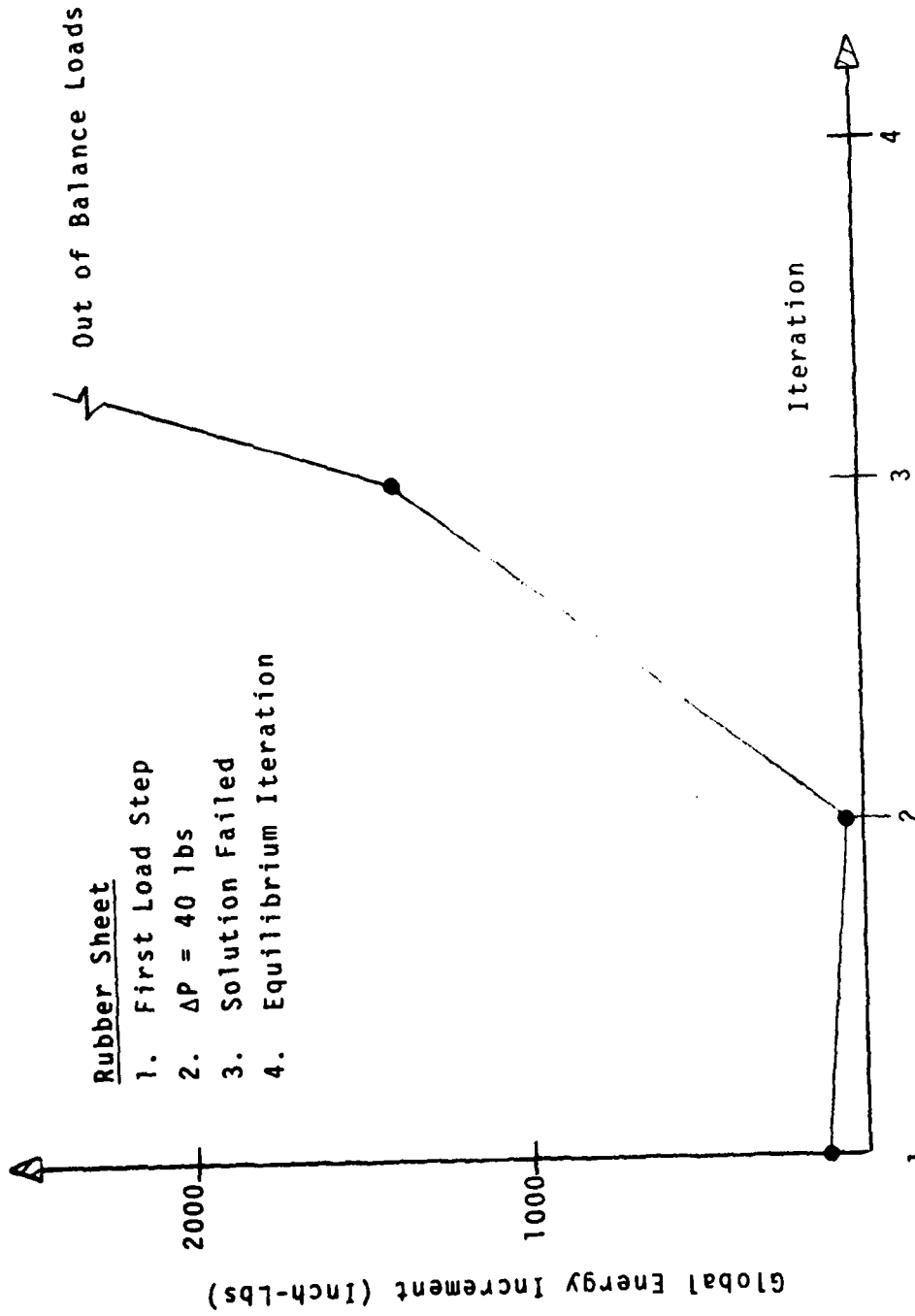
Fig. III-2 Global Energy Increment of Rubber Sheet (1st Load Step)
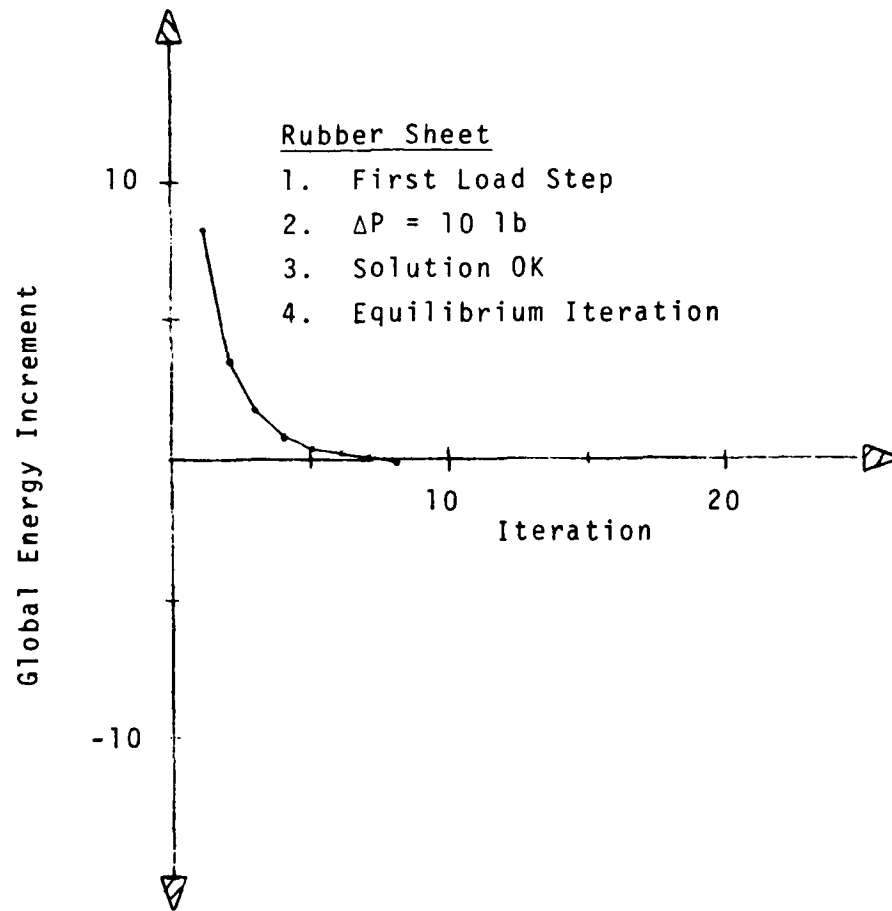
Fig. III-3   Global Energy Increment of Rubber
             Sheet (1st Load Step)
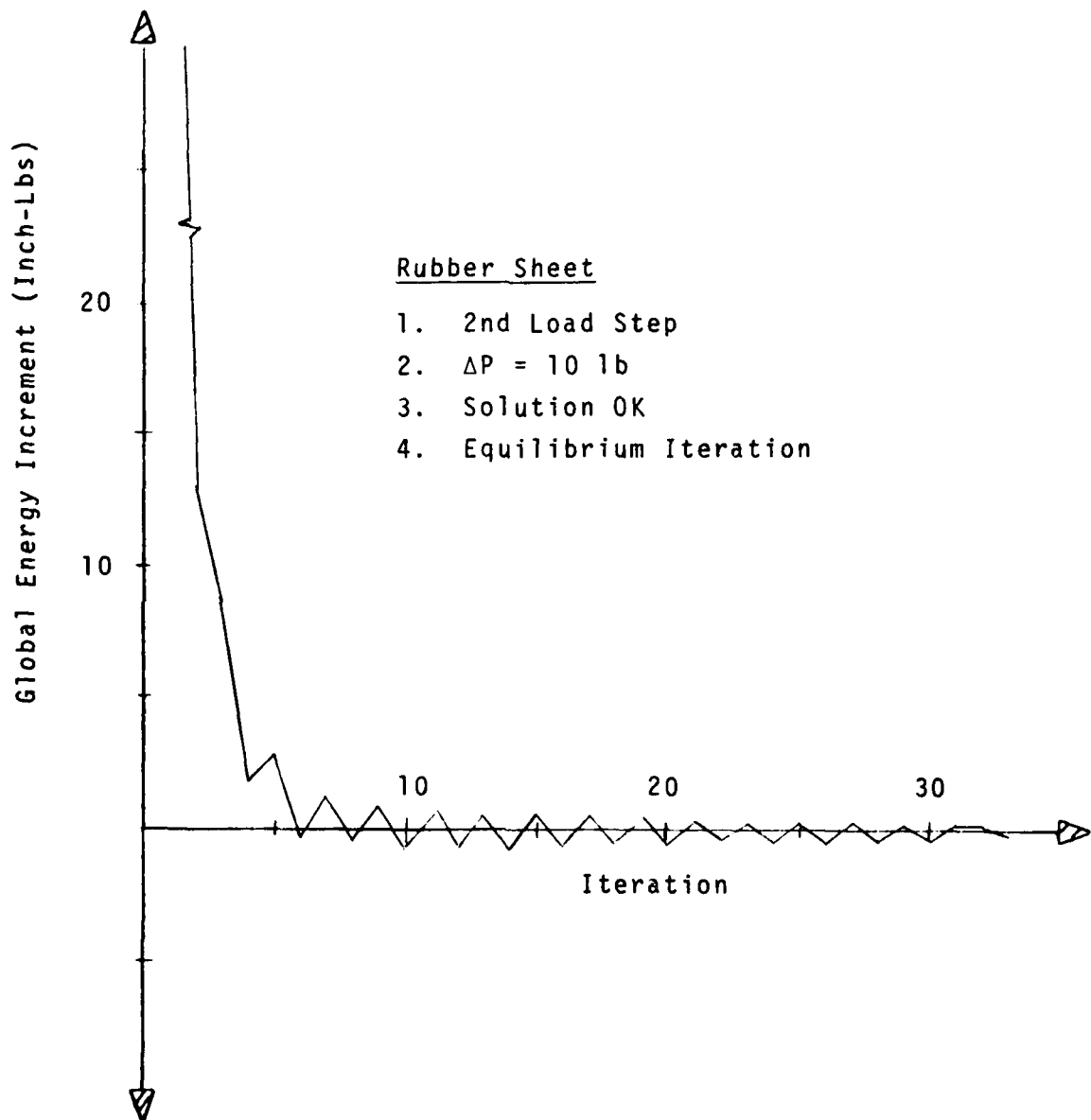
Fig. III-4   Global Energy Increment of Rubber Sheet
(2nd Load Step)
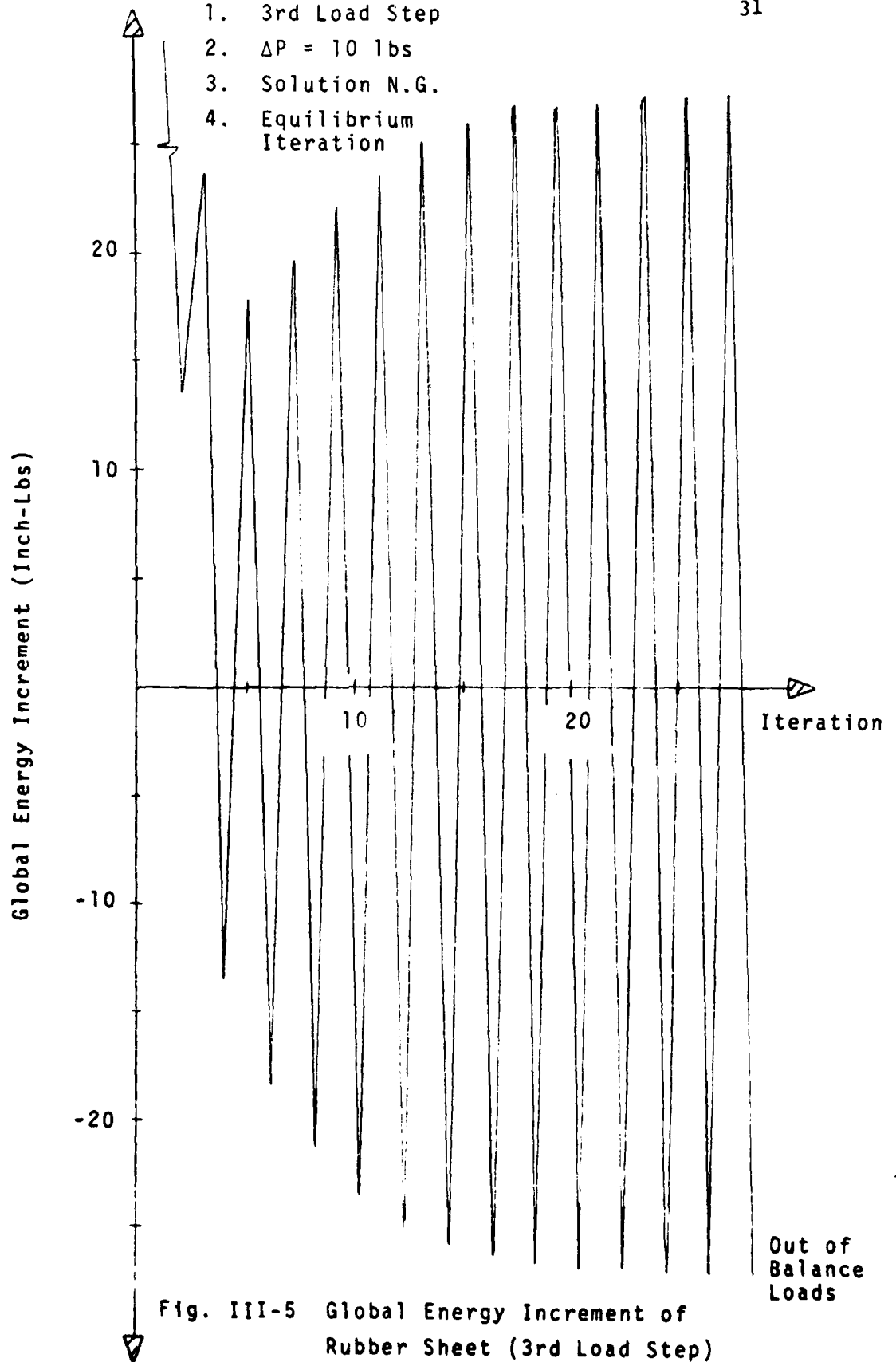
Fig. III-5  Global Energy Increment of
Rubber Sheet (3rd Load Step)

obtained in the first load step. In the second, a mild
form of nonmonotonicity and nonpositive definiteness is en-
countered. Since this increment required a large number
iterations, to enable the solution to proceed further, the
iteration count limit was raised. In this context, strong
and progressively increasing nonmonotonicity and nonpositive
definiteness is encountered in the third load step as illu-
strated in Fig. III.5. Here solution failure is due to out-of-
balance loads.

A better perspective of the foregoing behavior can be
obtained by a juxtaposition of results. This is given in Fig.III
6. The scenario of solution degradation depicted is typical
of excessive load incrementation. Note as can be seen from
these results, the onset of such behavior is signalled by
the initiation of nonmonotonicity.

In the preceding discussion, emphasis was given to
global considerations. Additional insights can be obtained
by studying the behavior of the local element energies. Such
an approach will enable the tracking of the progressive solu-
tion degradation from a purely local point of view. In this
context, Figures III.7-13 illustrate selected local conver-
gence characteristics for the global results depicted in
Figures III.3-6. As can be seen, the solution degradation is
initially localized but gradually spreads to the entire struc-
ture as the iteration process continues. Because of this, it
appears quite plausible that the choice of increment size
should reflect local solution characteristics so as to con-
trol the growth of localized degradation.
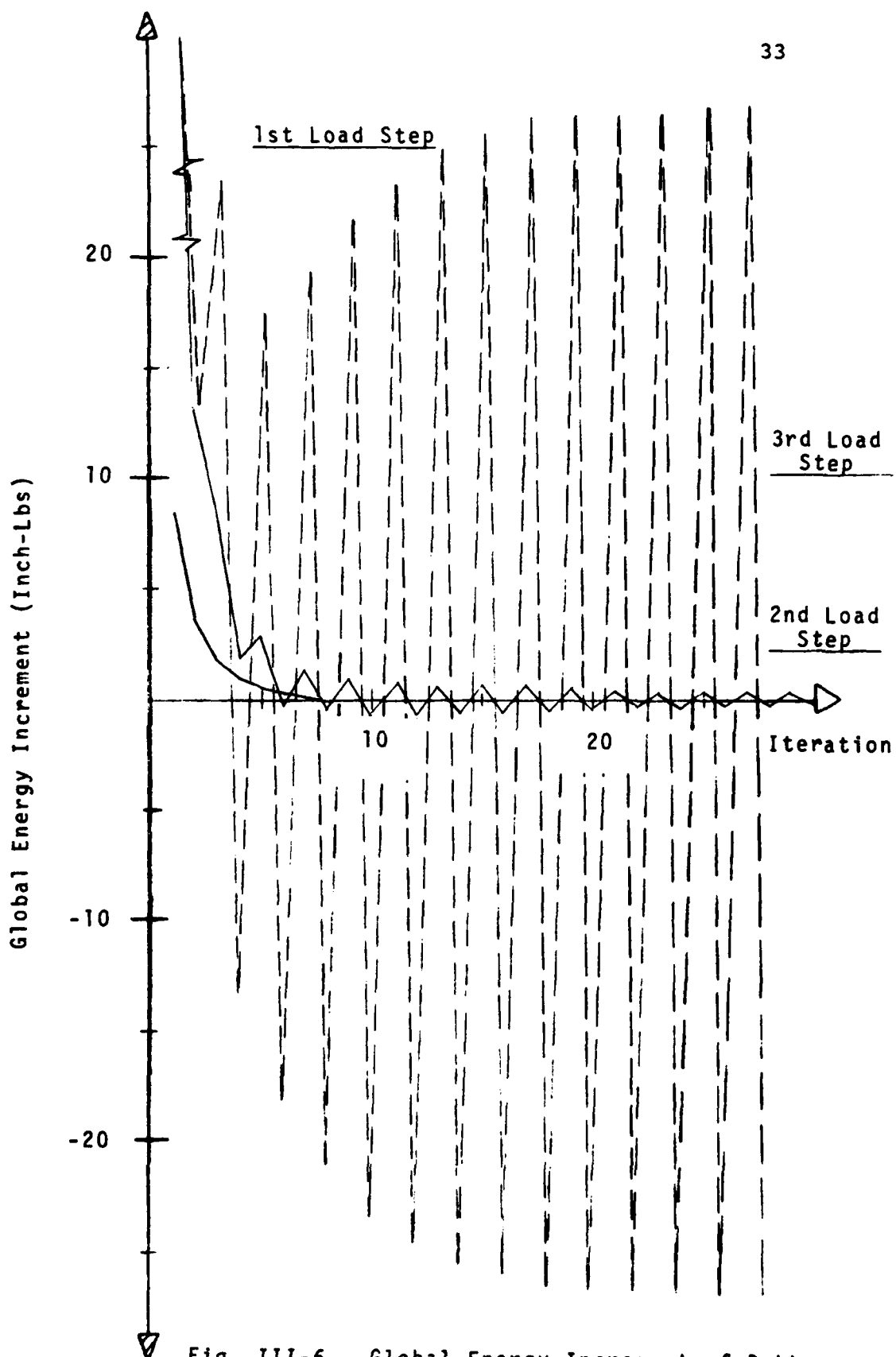
Fig. III-6    Global Energy Increment of Rubber
              Sheet (1st, 2nd, and 3rd Load Steps)
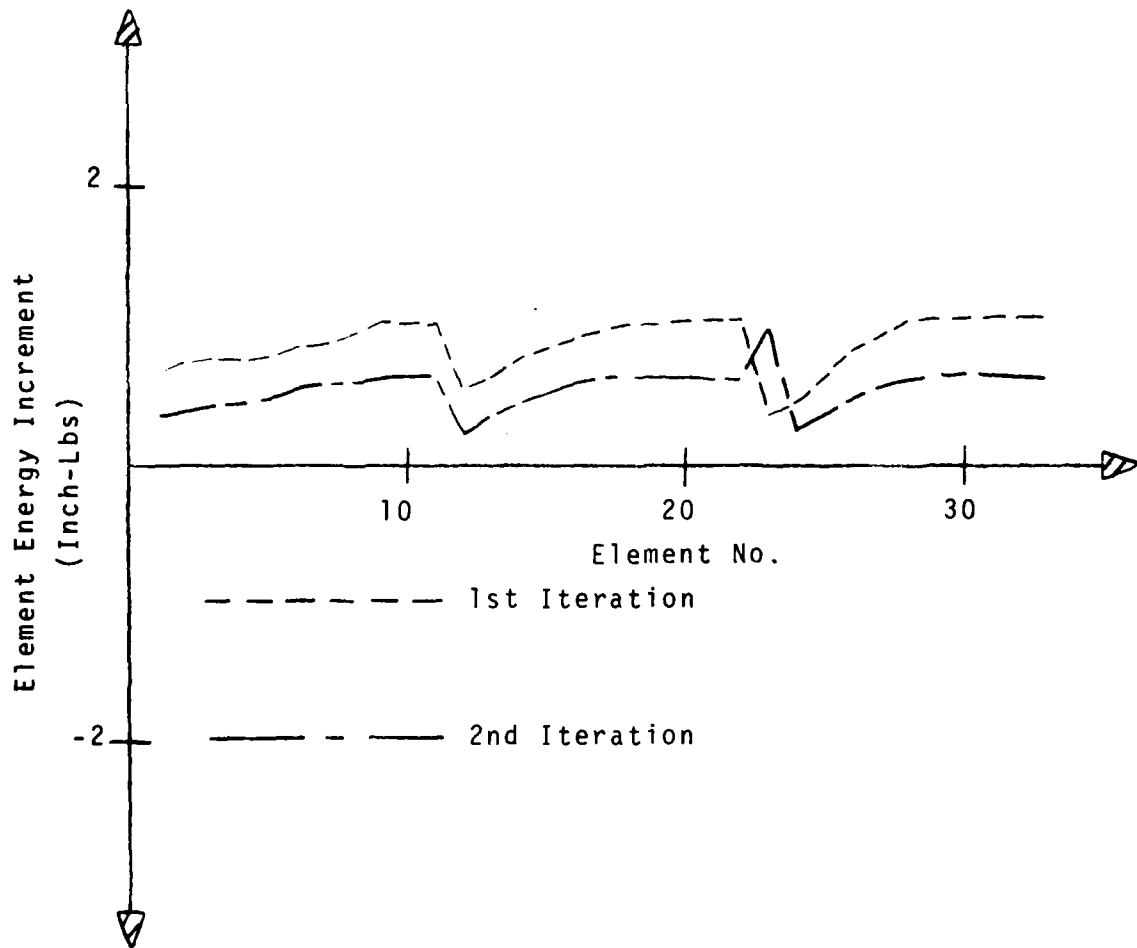
Fig. III-7   Incremental Element Energies of Rubber Sheet
             (3rd Load Step)
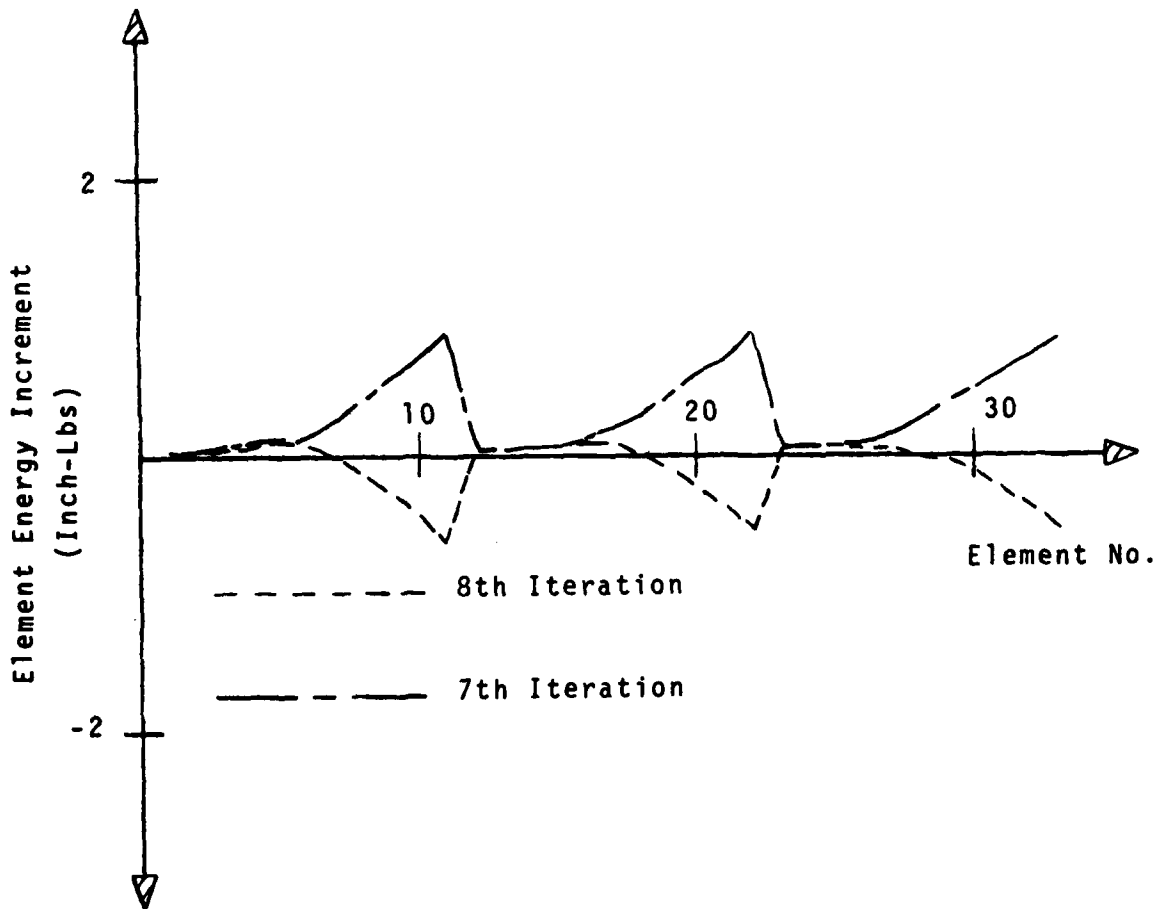
Fig. III-8  Incremental Element Energies of Rubber Sheet
(3rd Load Step)
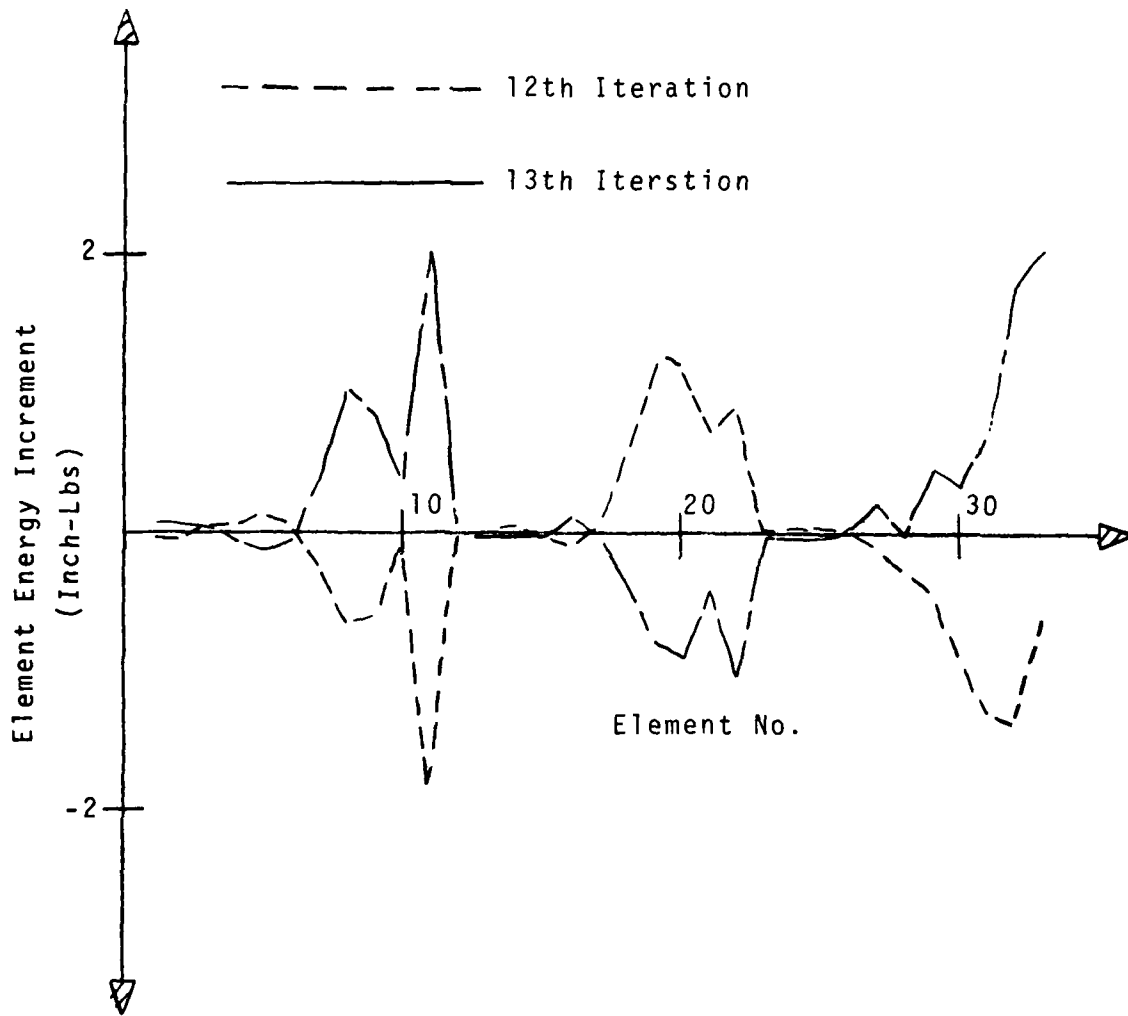
Fig. III-9  Incremental Element Energies of Rubber Sheet
(3rd Load Step)
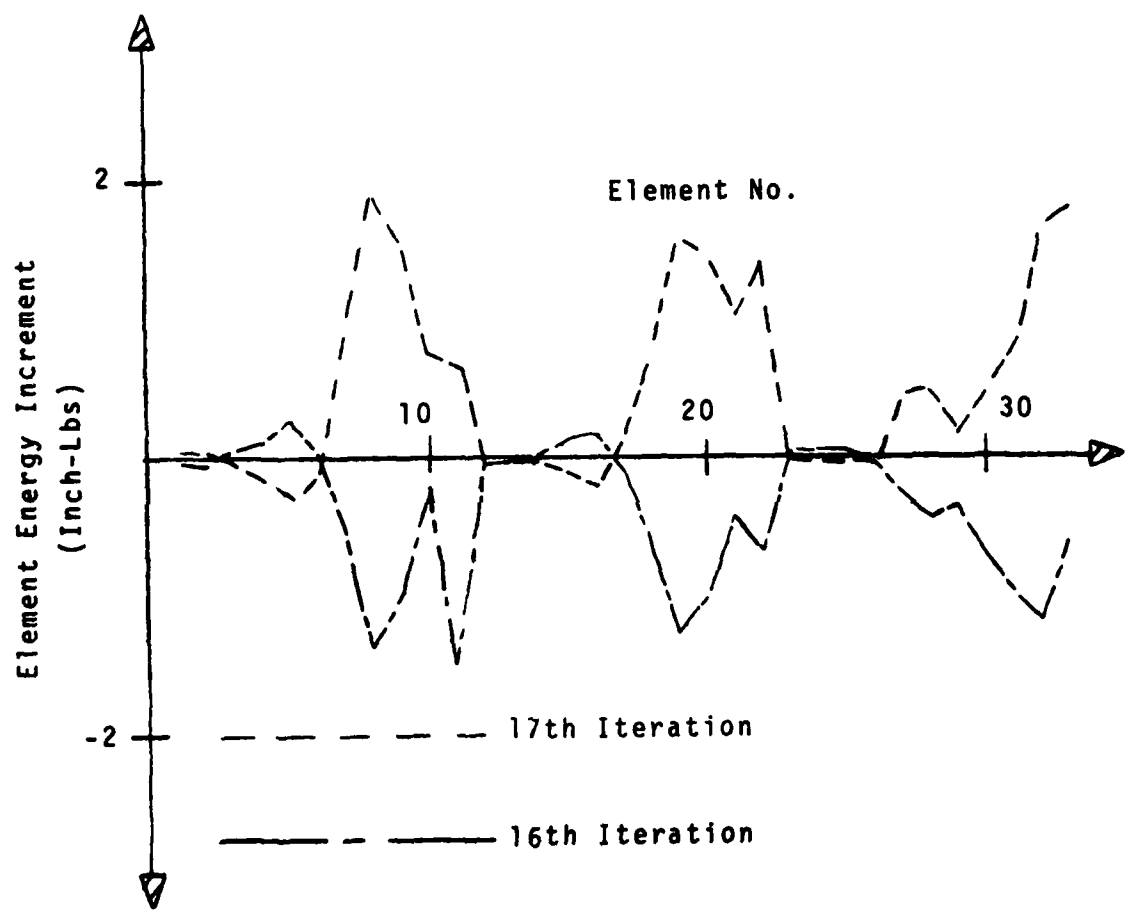
Fig. III-10   Incremental Element Energies of Rubber Sheet
(3rd Load Step)
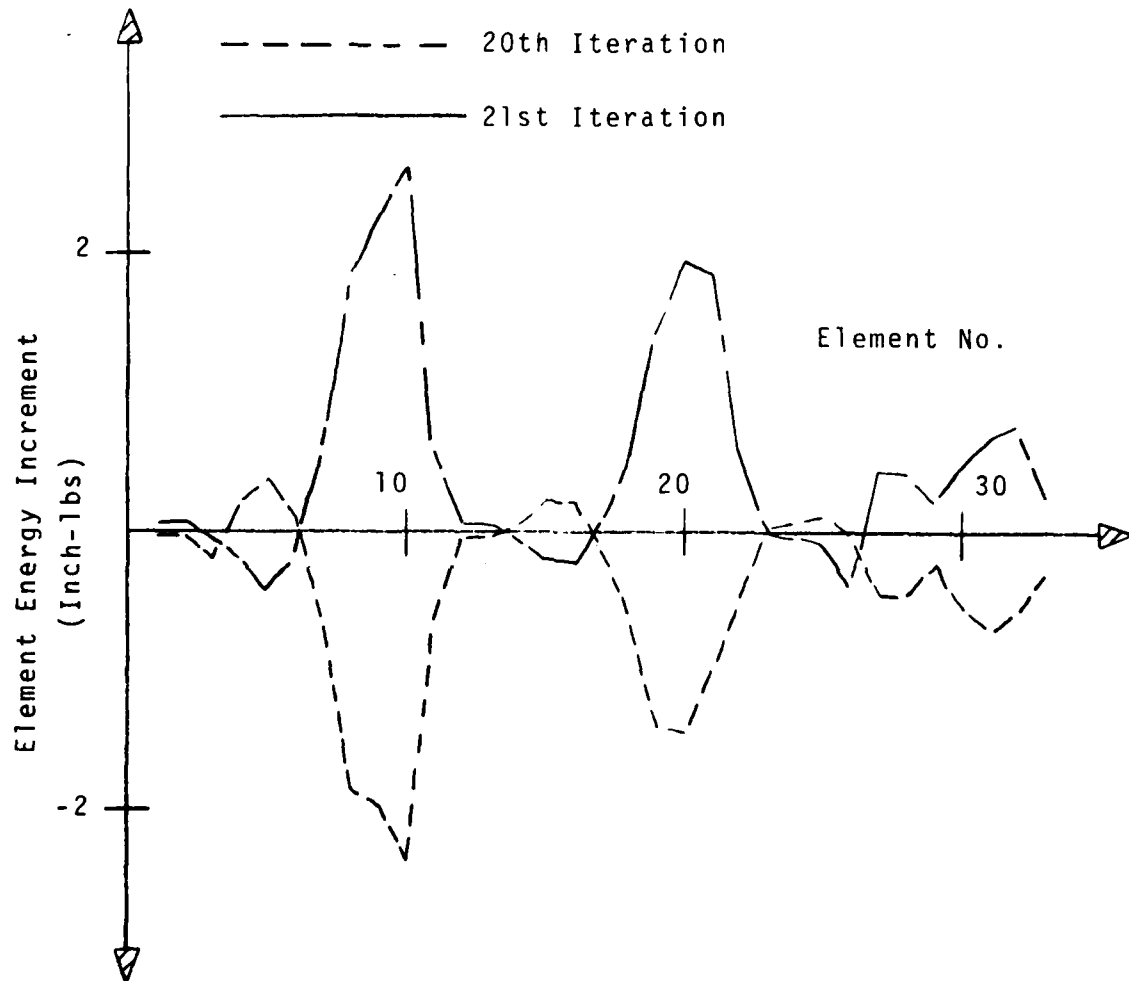
Fig. III-11    Incremental Element Energies of Rubber Sheet
(3rd Load Step)
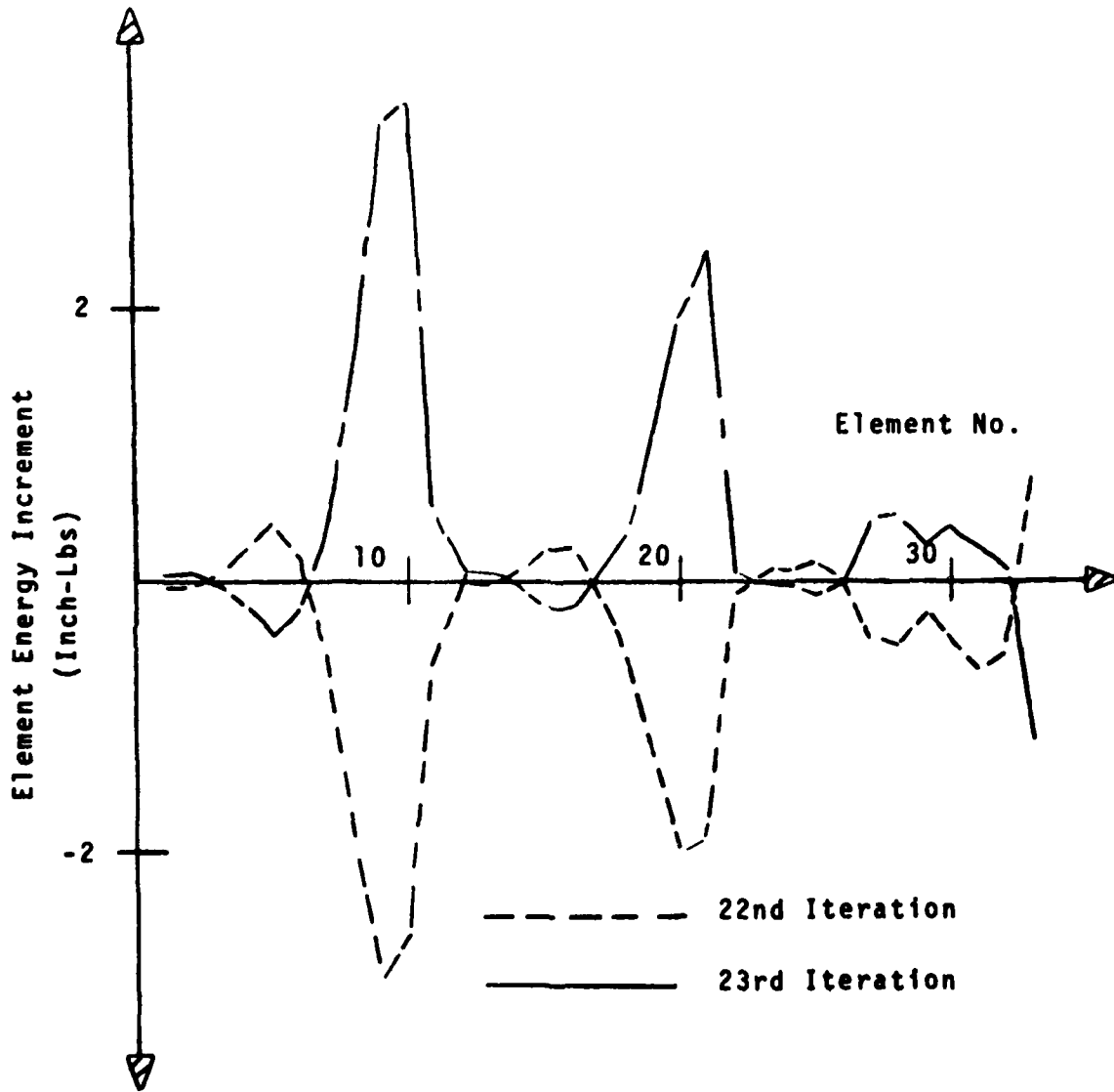
Fig. III-12   Incremental Element Energies of Rubber Sheet
(3rd Load Step)
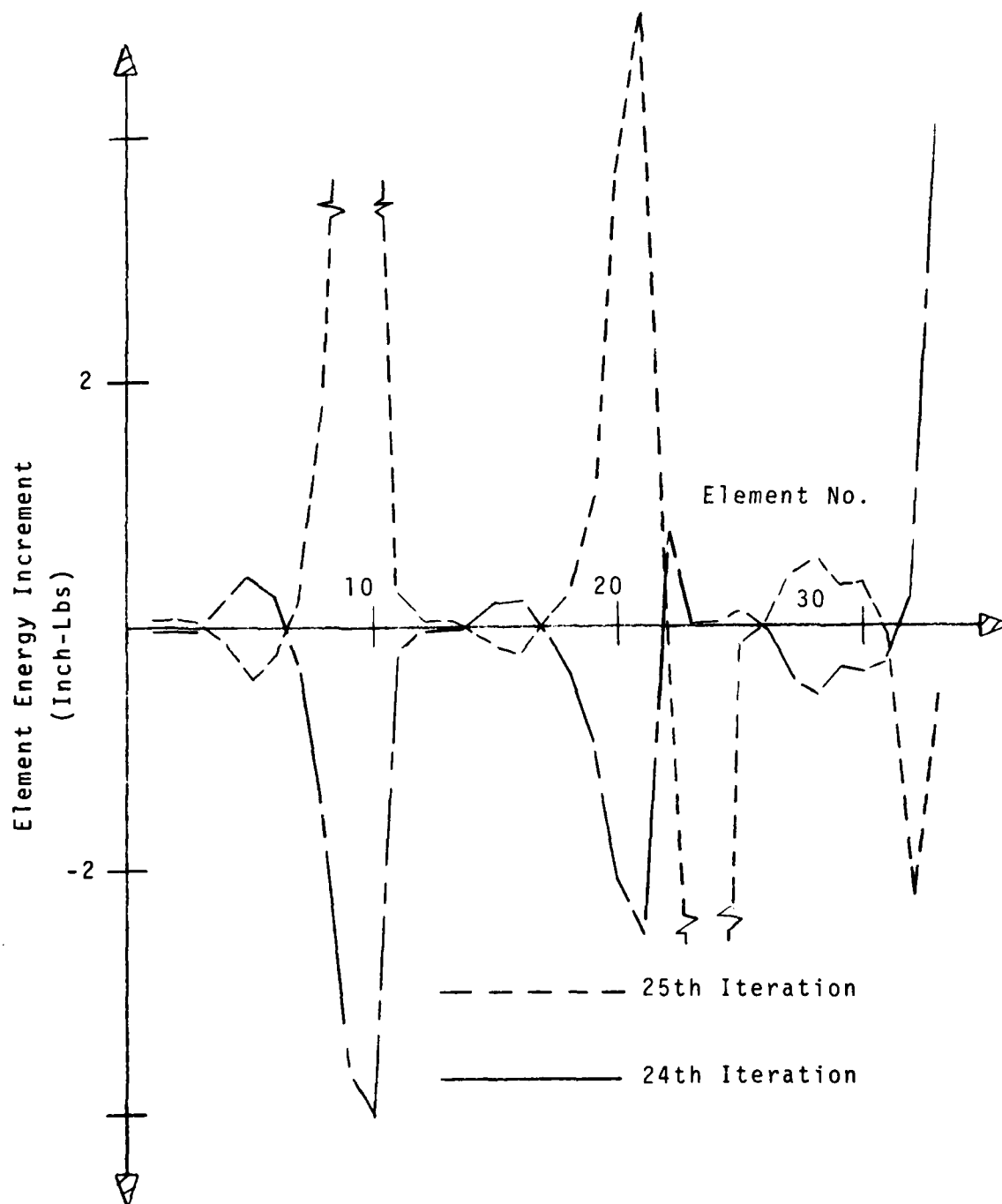
Fig. III-13   Incremental Element Energies of Rubber Sheet
              (3rd Load Step)

Figure III.14 illustrates the geometry, loading and material properties of a fixed arch which serves as benchmark 2. This problem involves geometric (kinematic) nonlinearity which is strongly influenced by the geometry of the arch. As noted earlier, improper incrementation and algorithmic choice can lead to solution failure. This is particularly true for arch problems which are subject to snap through if excessively loaded. While anomalous solution behavior will always occur in the vicinity of buckling and bifurcation points, improper incrementation will make the accurate estimation of such points impossible.

As with the previous benchmark, choosing excessively large load steps can lead to various types of solution degradation. For the current example problem, such behavior can be exacted far in advance of bifurcation or buckling zones. In particular, Figures III.15 and III.16 illustrate typical types of solution breakdowns in various of the load steps. Interestingly, while the nature of the nonlinearity of the arch and rubber sheet problems are inherently different, the pathology of solution failure appears qualitatively the same. This is essentially an outgrowth of the fact that the MNR algorithm is slope driven.

In addition to monitoring global energy, local element characteristics were also tracked. Here again, solution degradation was found to be initially localized but spreads to neighboring elements as the iteration process continues. The rate of such spreading is associated with the topology of the solution space. In this context, as was
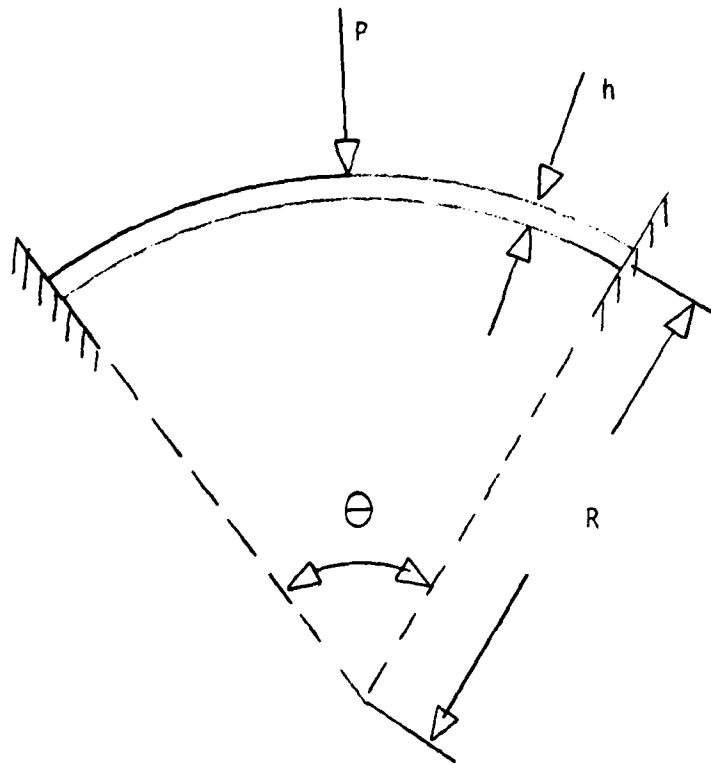
$$E = .10 \times 10^8 \text{ psi}$$
$$\nu = .3$$
$$\rho = .245 \times 10^3 \text{ lbm/in}^3$$
$$R = 4.8 \text{ inch}$$
$$h = .016 \text{ inch}$$

Fig. III-14    Geometry and Material Properties of A
Ring Loaded at Crown
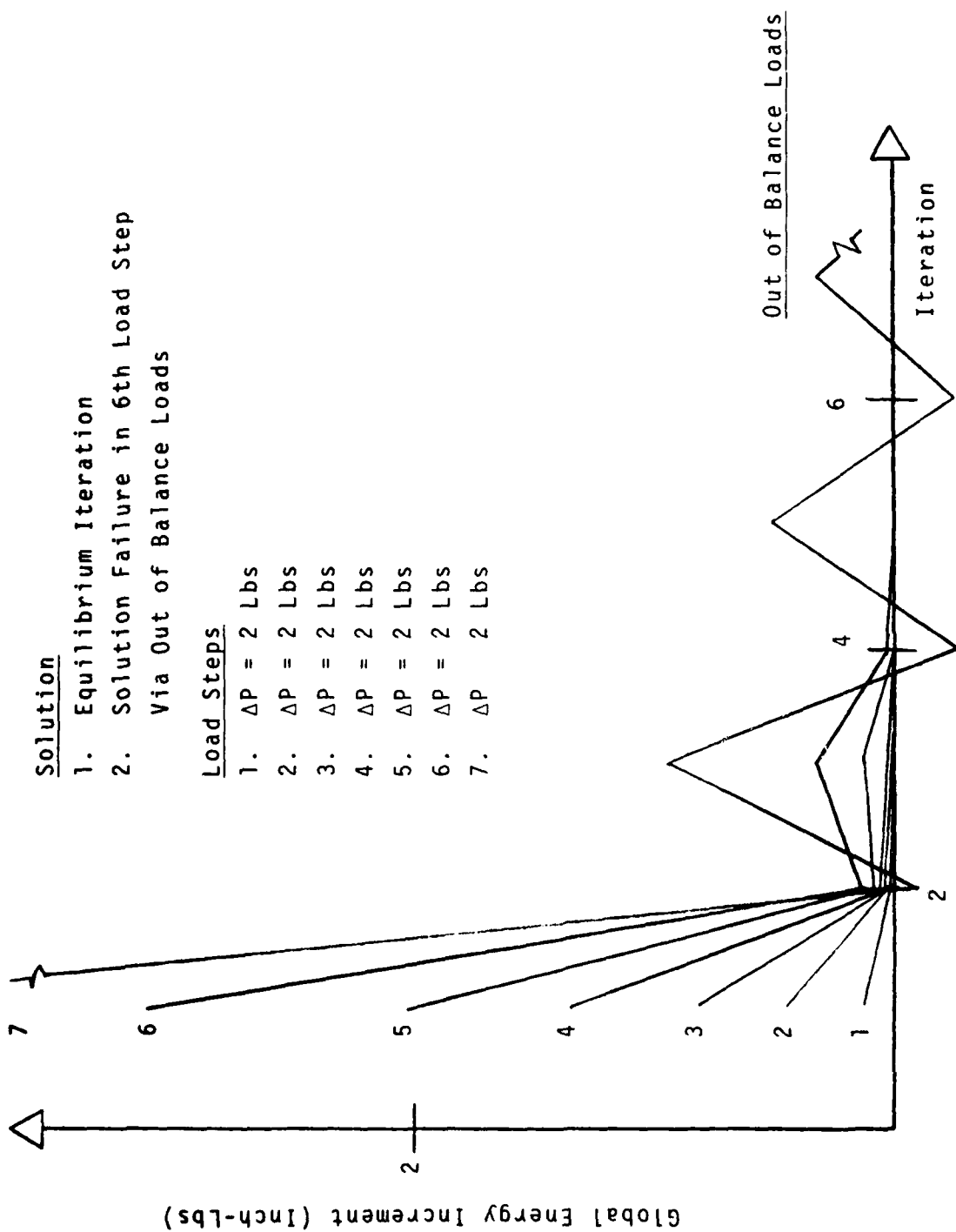
Solution

1. Equilibrium Iteration
2. Solution Failure in 6th Load Step
   Via Out of Balance Loads

Load Steps

1. $\Delta P = 2$ Lbs
2. $\Delta P = 2$ Lbs
3. $\Delta P = 2$ Lbs
4. $\Delta P = 2$ Lbs
5. $\Delta P = 2$ Lbs
6. $\Delta P = 2$ Lbs
7. $\Delta P = 2$ Lbs

Out of Balance Loads

Iteration

Global Energy Increment (Inch-Lbs)

Fig. III-15   Global Energy Increment of Arch (Modified NR Employed)

Fig. III-16 Global Energy Increment of Arch (Modified NR Employed)

noted earlier, to improve local solution characteristics,
the load incrementation process should involve the use of
localized information concerning element stiffness behavior
namely positive, negative definiteness,monotonicity, etc.
Note, waiting until local solution anomalies spread to the
entire structure may lead to restart difficulties. Namely
since localized solution breakdowns can occur earlier in the
iteration process, all successive iterates tend to drift
from the true solution. Hence upon restart, difficulties
arise as to what portion of the solution is valid. Obviously,
the constant monitoring of local behavior can mitigate such
restart problems.

As can be seen from the foregoing benchmarks, for static
problems excessive incrementation leads most frequently to
error stops involving out-of-balance loads or out of iteration
counts. Such solution difficulties can under the proper circum-
stances be circumvented by the use of improved iteration pro-
cedures. For example, Figures III.17 and 18 illustrate re-
sults obtained for benchmarks 1 and 2 wherein an NR algorithm
employing constant updating was used. Note while the modified
NR approach yields divergent solutions for such problems,
the constantly updated version succeeded in either proceeding
further or outrightly obtaining the final solution. An al-
ternative to the straight update approach is yielded by al-
lowing the solution to proceed via the modified INR algorithm
until solution degradation is initiated either locally or
globally. Once this is encountered, the algorithm can then
be switched to the constant update approach to finish out the
solution.
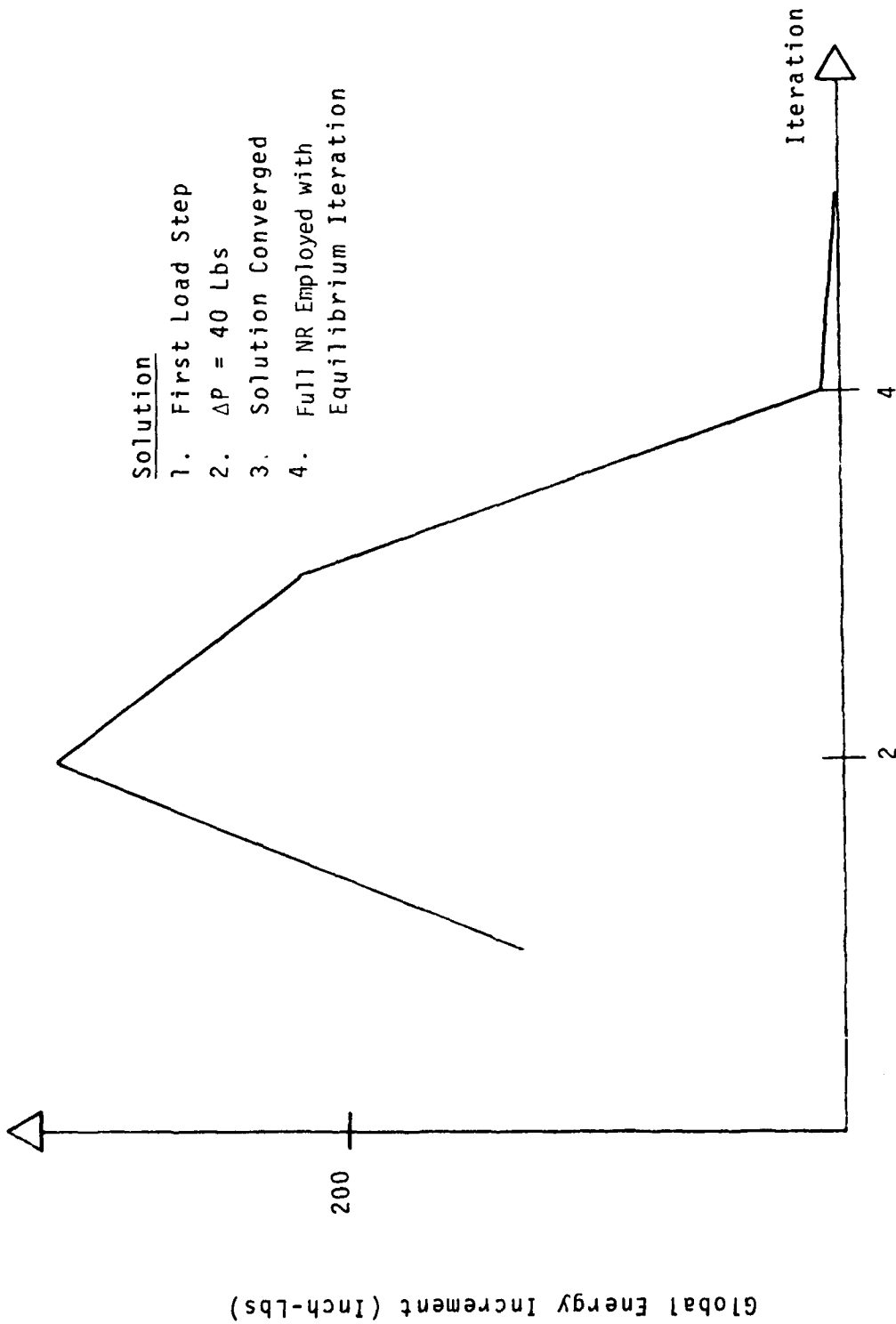
Fig. III-17  Global Energy Increment of Rubber Sheet (1st Load Step, Full NR Employed)
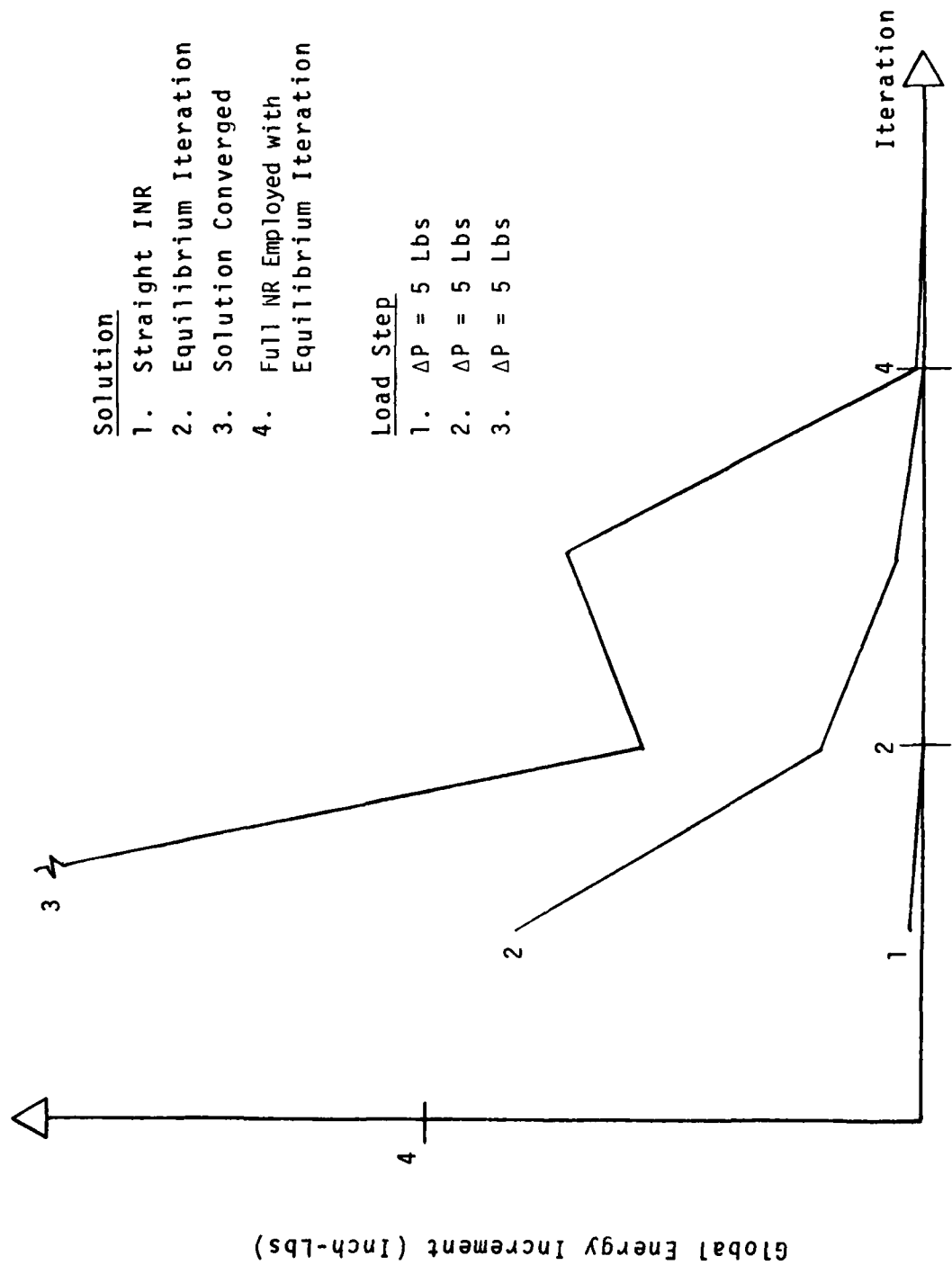
Fig. III-18  Global Energy Increment of Arch (Full NR Employed)

Further, static benchmarking involving different
geometries (beams, plates, spherical shells/caps and mate-
rial properties (plasticity) also initiated similar static
solution pathologies.  The common denominator to all such
solution breakdowns was the initiation of localized non-
monotonicity.  Once encountered, typically such behavior
spreads to the entire structure either in the given load
step or in successive load steps.  Note such solution ano-
malies are not generic to ADINA but rather are an outgrowth
of the use of MNR algorithms which are based on tangent stiff-
ness properties.  Hence, all general purpose nonlinear codes
employing such algorithmic approaches should encounter such
anomalous behavior if improper load incrementation is attempted.
Section IV discusses several possible improvements which can
be implemented into the ADINA program to diminish such dif-
ficulties.

### III.2b  Dynamic Solution

Before considering the algorithmic sensitivities of
the dynamic solution branch, several important points must
first be clarified.  The most important of these is the need
to define the manner in which the inertial, stiffness and
damping effects interact to control the overall dynamic res-
ponse of a structure.  As a starting point, we shall first
consider the purely linear case.  Next, the effects of struc-
tural nonlinearity (kinematic, kinetic & material) will be
considered.  Such insights will enable us to establish the
proper framework from which to evaluate the dynamic solution
algorithm.

As noted earlier, the main thrust oi this work will be to evaluate the algorithmic sensitivities of ADINA (1977). As with the static branch, this will be accomplished by exciting the various forms of pathological behavior inherent to the algorithms.

Since the dynamic branch of ADINA employs direct numerical integration to yield the transient solution, the problem of central importance involves the matter of time step size. This question itself consists of two major points namely:

1. System dynamic characteristics and;

2. Characterization of exciting fields.

The problem of dynamic system characterization can generally be answered by considering the properties of its natural frequencies. This includes such questions as spectral spacing, size of lowest frequencies, modal participation factors, etc. In the case of linear systems, once such characteristics are defined, they undergo no changes during the calculation phase.[6] This is obviously a direct outgrowth of the linearity of the governing differential operators characterizing such problems.

The characterization of the exciting fields also in essence requires the definition of its spectral properties. In this context, several possible situations may arise namely:

1. A profusion of frequencies may be present;

2. Small numbers of frequencies are present or;

3. Selected frequencies dominate behavior.

Regardless of which situation exists, once the spectral

characteristics of the structural system and exciting fields are established, the proper time step increment can be selected so that the participation of the dominant system frequencies can be accounted.

For situations in which a profusion of exciting frequencies exist, the explicit procedure must be employed. In ADINA the central difference algorithm can be used to handle such situations. In the case where small numbers of frequencies or selected frequencies dominant the behavior, implicit operators are employed to handle the response. For such situations, the Wilson[2] and Newmark[3] integration schemes are available in ADINA.

Regardless of the approach employed, once the full spectrum of excitation and system frequencies are accounted for, due to the stationarity of the spectral properties of linear systems, no changes need be implemented in the time step to capture the response. Such is not the case for non-linear systems. In particular for nonlinear systems, major changes in the spectral properties can occur from moment to moment during the excitation. Generally, three basic types of changes can occur in the structural behavior. These can be categorized by:

    i)   global/localized structural stiffening;

    ii)   global/localized structural softening or;

    iii)   combined structural stiffening/softening.

For problems which are characterized by material nonlinearity, generally softening behavior is usually encountered.

A good example of such behavior can be seen in structure undergoing small plastic type deformations. During the development of plastic flow, such structure behave softer than their purely elastic counterparts. Interestingly, while the initial time step chosen for the elastic version of such structure can capture the inertial effects of either the linear or nonlinear situations, it is possible that the level of nonlinearity excited by plasticity can be severe enough to cause solution difficulties. Note the problems which are typically encountered for such situations are a direct outgrowth of the inability to handle the nonlinearity via MNR type algorithms. That is, if extensive softening is encountered during a given time step, the various solution pathologies depicted for the static case can be excited. This follows from the fact that the level of nonlinear excited during a given time step can be likened to that encountered during an excessively large static load step. In either case, the solution degradation follows the same pattern as the static case namely, out of balance loads or iteration count stops can be initiated. Since the time step size controls the degree of nonlinearity excited, the only approach available to remedy this situation is to decrease the time step size. In ADINA such modifications can be established for selected times via the block option. If the adjustment of time step size cannot stem the occurrence of out of balance loads or out of iteration stops, the reformation but no iteration option can be employed. Solution failure under this option generally involves the initiation of negative pivots.

This follows from the fact that without the out of balance load check inherent to the iteration option, there is no bound on the growth of load imbalance.

For plastic problems, perhaps the most severe form of material nonlinearity occurs in the neighborhood of load unload zones. In such situations, as noted in Fig. II.8, transitions between softening to hardening to softening behavior can be encountered. The major solution difficulty which arises from such behavior is the fact that the modified NR algorithm can miss the need to unload during the iteration phase of a given load step. This usually leads to solution drift and typically out of balance loads. To bypass such difficulties, the only avenue open to the ADINA user is to stop equilibrium iteration in the neighborhood of unloading. This obviously can be initiated through the use of the restart and block options. While such an approach can handle the load/unload problem, the apriori knowledge of the existence of such behavior is usually not immediately available. Hence such information must be ascertained by extensive and oftentimes costly parametric studies involving the restart and block options.

In the case of structure with severe hardening characteristics, the modified NR algorithm inherent to ADINA is destined to either converge poorly or initiate out of balance loads as depicted in Fig. III.19. The only way to avoid such difficulties is to employ the reformation option without iteration. This obviously can lead to solution drift as the solution proceeds.
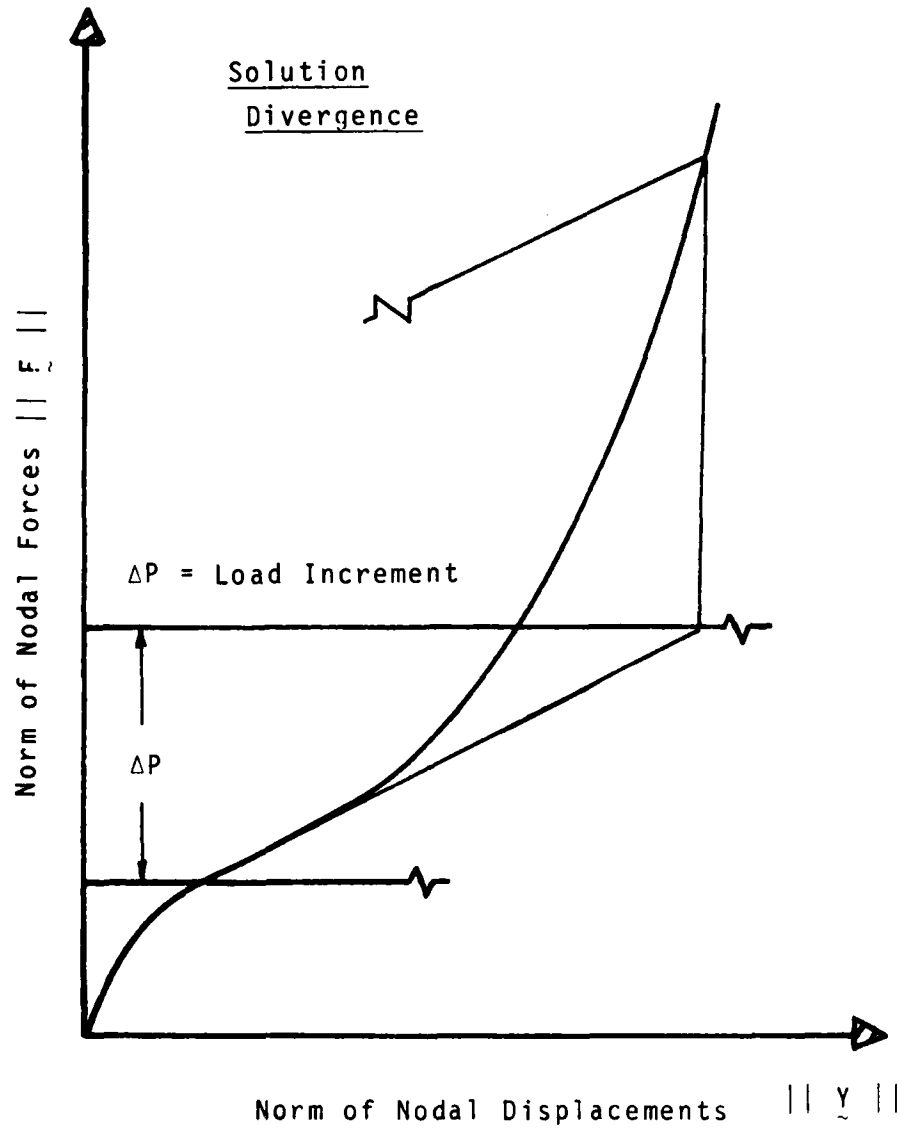
Fig. III-19    Typical Solution Drift for Softening/Hardening
               Problems

In the context of the foregoing discussion, the benchmarking of the dynamic solution branch of ADINA discussed in this section will attempt to establish the various forms of pathological behavior intrinsic to the direct integration algorithm. Note the main emphasis of such numerical experiments will be to establish the important effects of nonlinearity on the generation of anomalous solution behavior. This emphasis follows from the fact that the main thrust of ADINA is its ability to handle both material and geometric nonlinearity. As with the static branch, because of this emphasis, the geometric configuration of the benchmarks considered will purposely be kept simple yet diverse enough to account for geometric configuration effects.

As will be seen from the following discussion, while such factors as geometry, material properties and boundary conditions all have varying effects on the choice of time step size, once an excessive value has been chosen, typically similar types of anomalous solution behavior are encountered. For instance, once such a situation is excited, the iteration loops tend to initiate either out of balance load or out of iteration stops. For the noniterative loop, typically the negative pivot check is encountered.

Figure III.20 illustrates the geometry and material properties of a  cantilevered beam which serves as the first benchmark of the dynamic solution branch. Since large deformations and either elastic or plastic (strain hardening) material properties are employed, this problem combines the
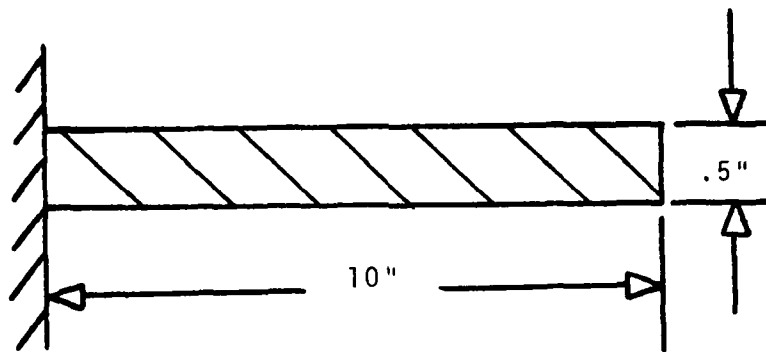
$E = .30 * 10^8$ psi

$\nu = .27$

$\rho = .7305 * 10^{-3}$ lbm/in$^3$

$\sigma_y = 44. * 10^3$ psi

$E_p = .3 * 10^6$ psi

Fig. III-20   A Cantilever Beam

effects of kinematic, kinetic and material nonlinearity.
Since we are primarily concerned with the characterization
of algorithmic behavior, to establish the validity of model
employed, runs were performed involving 20, 40, 80 and 160
elements for selected problems. This enabled the deter-
mination of whether modelling difficulties initiated solution
degradation as opposed to algorithmically generated ano-
malous behavior.

To establish the anomalous behavior of the various
options of the transient algorithms, the problems run in-
volved increasing orders of severity. This enabled the
evaluation of the sources of degradation. In this context,
Figs. III. 21-26 illustrate the various characteristics of
the displacements, velocities and accelerations associated
with the large deformation responses of an elastic canti-
levered beam subject to a concentrated step load. These
were run with the Newmark option. Similar results were ob-
tained via the Wilson operator. As can be seen from the
velocity and acceleration fields depicted, because of the
lack of damping, numerous higher order spectral modes par-
ticipate in the overall response. This necessitates the
selection of an extremely small time increment namely
$\Delta t \sim. 5 \times 10^{-4}$ sec. While such behavior eventually initiates
long term solution drift, for the first few cycles of time,
good accuracy is maintained.

To increase the degree of severity, plasticity is ad-
mitted in the model. As noted earlier, this initiates sof-
tening type behavior. Namely, the apparent period of the

57
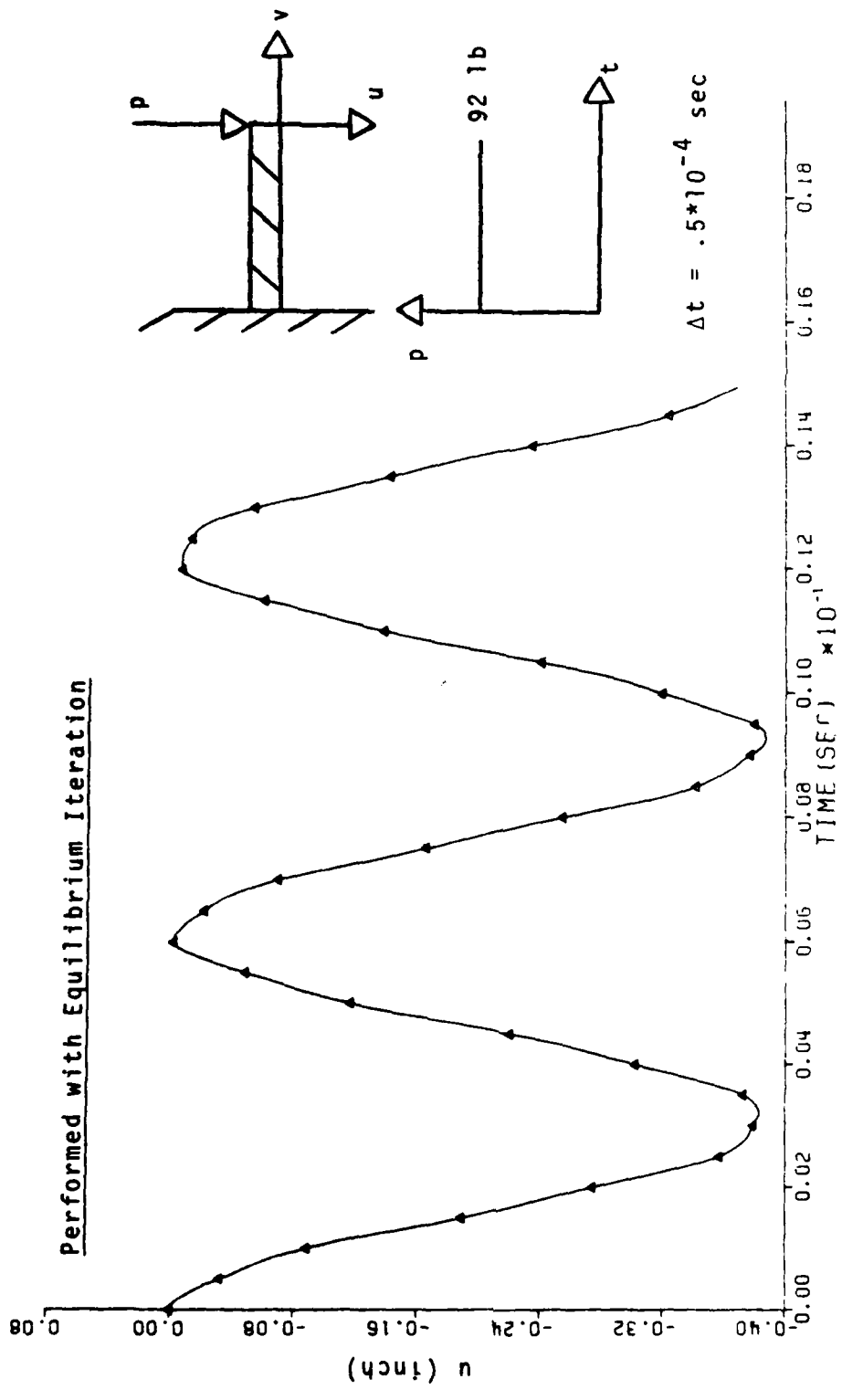


Fig. III-21   Vertical End Deflection of Step Loaded Elastic Cantilevered Beam (80 elements)
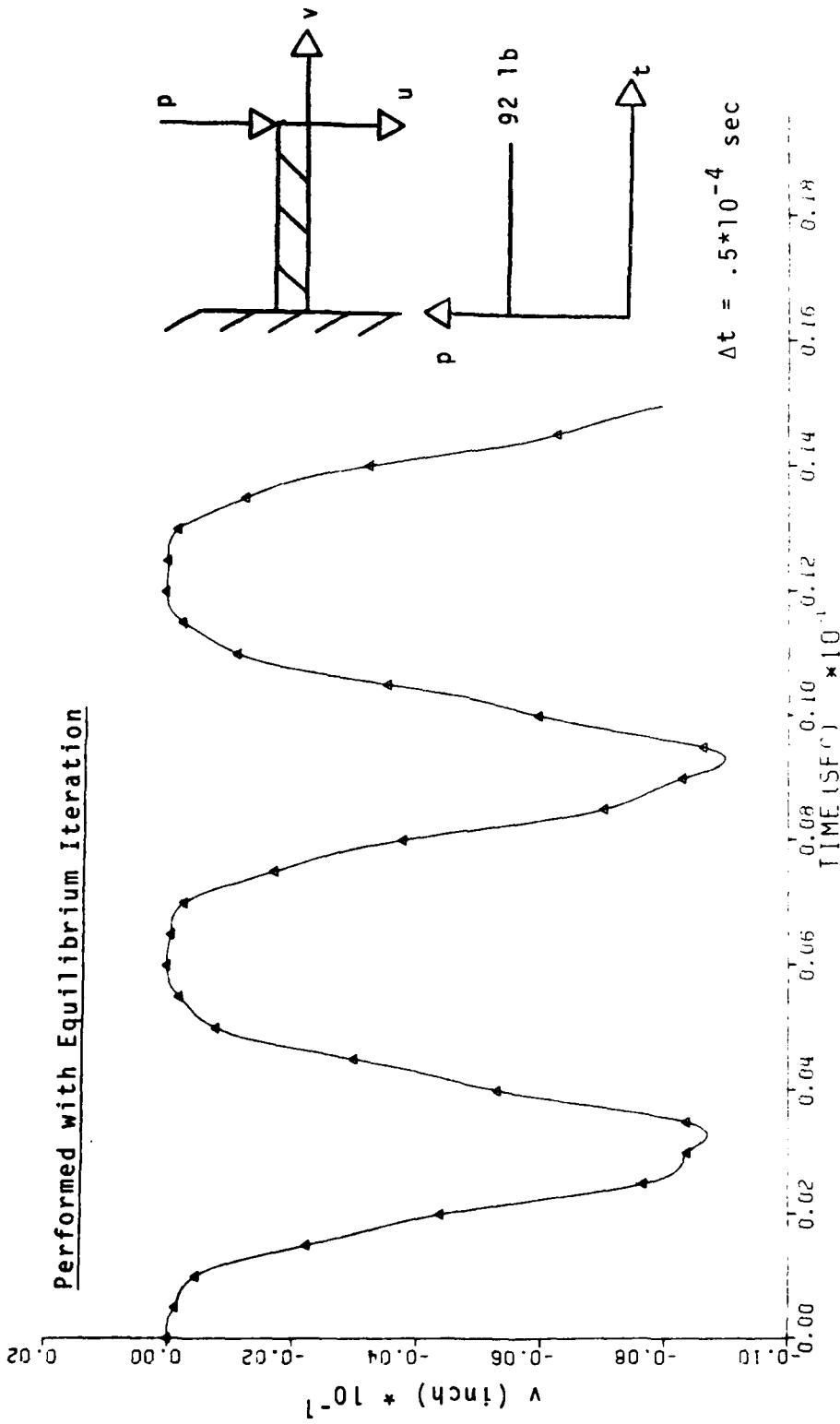
Fig. III-22 Horizontal End Deflection of Step Loaded Elastic Cantilevered Beam (80 elements)

59
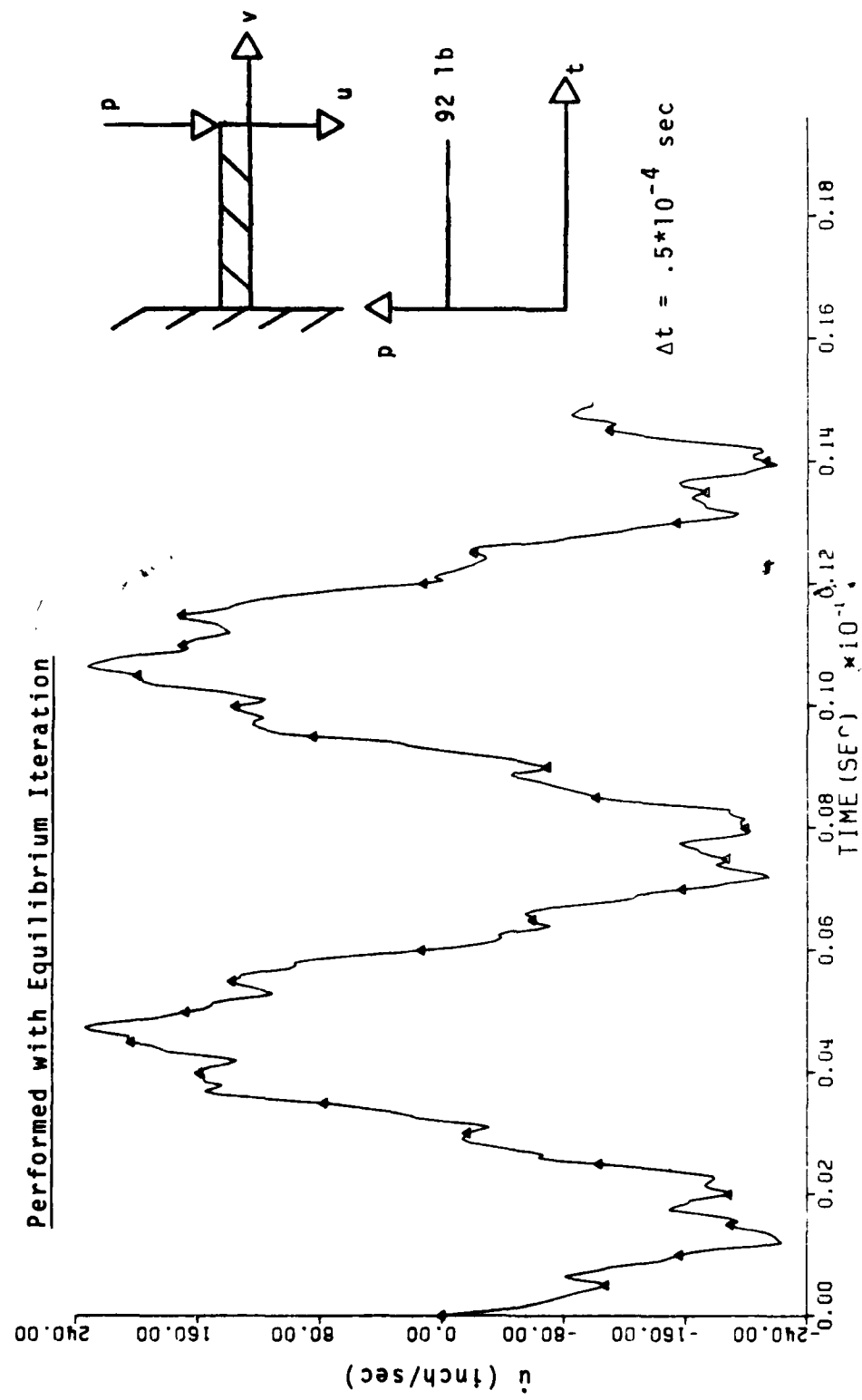


Fig. III-23  Vertical End Velocity of Step Loaded Elastic Cantilevered Beam
(80 elements)
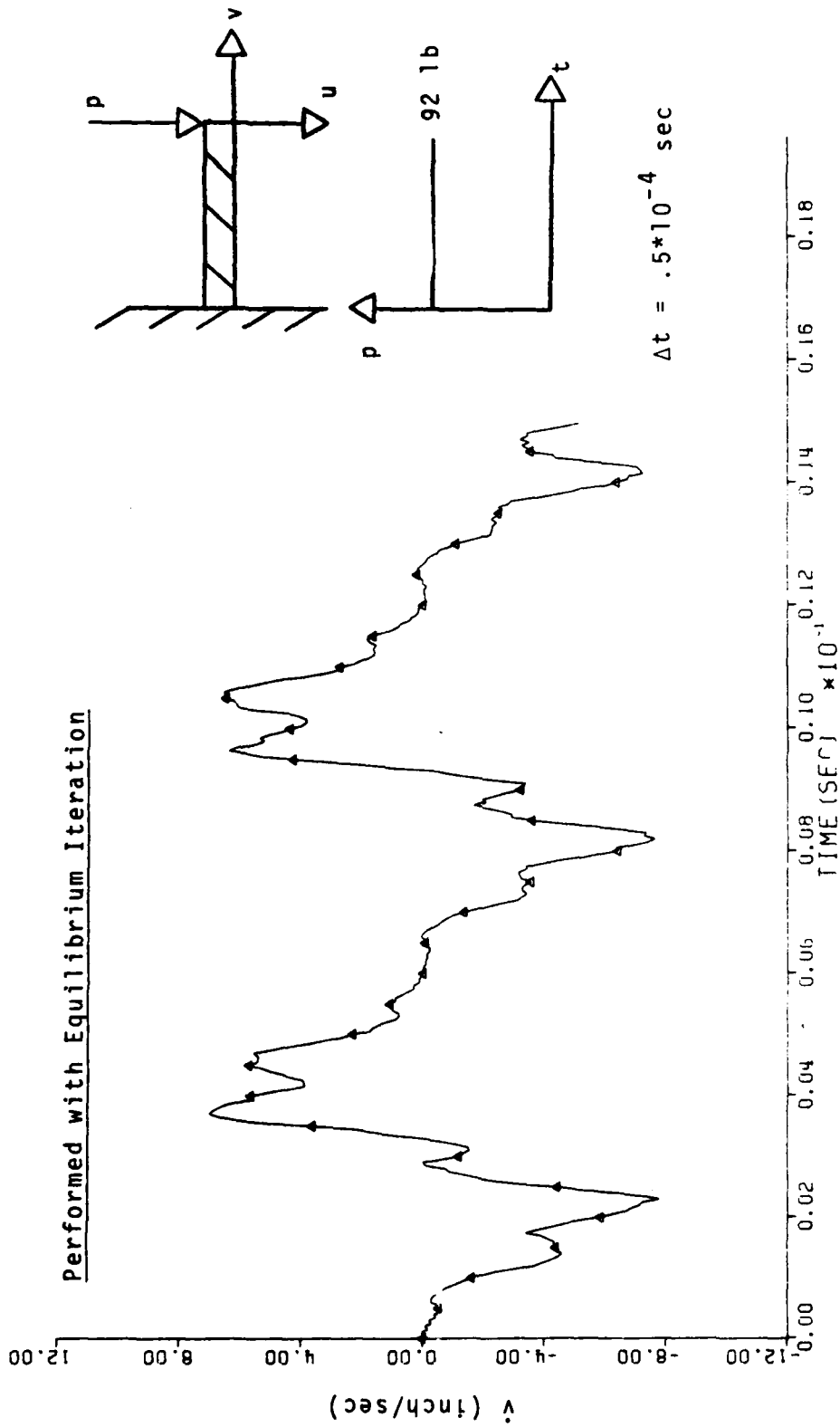
Fig. III-24  Horizontal End Velocity of Step Loaded Elastic Cantilevered Beam
(80 elements)

Performed with Equilibrium Iteration

92 lb

$\Delta t = .5*10^{-4}$ sec

120.00   80.00   40.00   -0.00   -40.00   -80.00   -120.00

$\ddot{u}$ (inch/sec$^2$)*10$^4$

0.00   0.02   0.04   0.06   0.08   0.10   0.12   0.14   0.16   0.18

0.10 *10$^{-1}$

TIME (SEC)
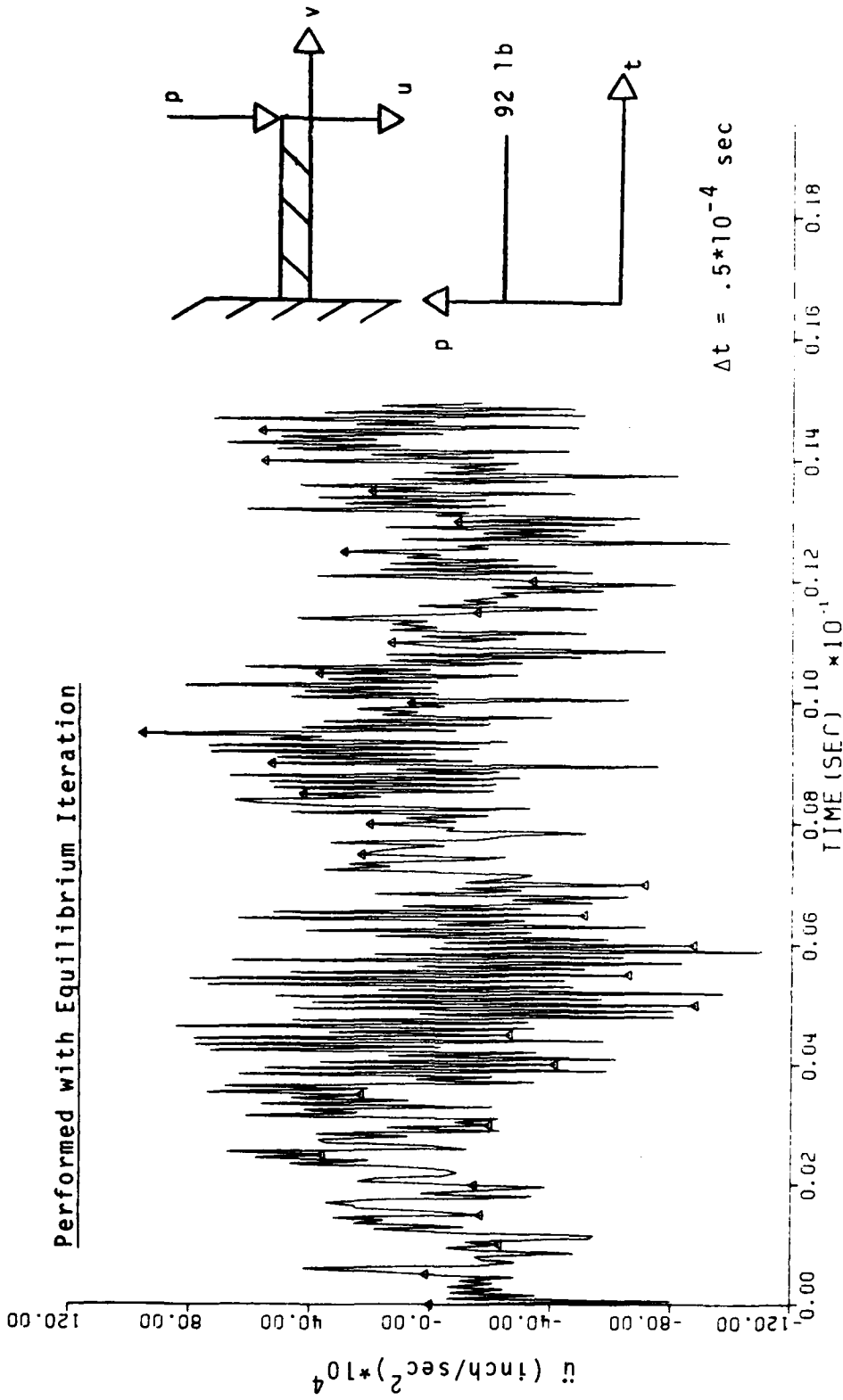
Fig. III-25   Vertical End Acceleration of Step Loaded Elastic Cantilevered Beam (80 elements)
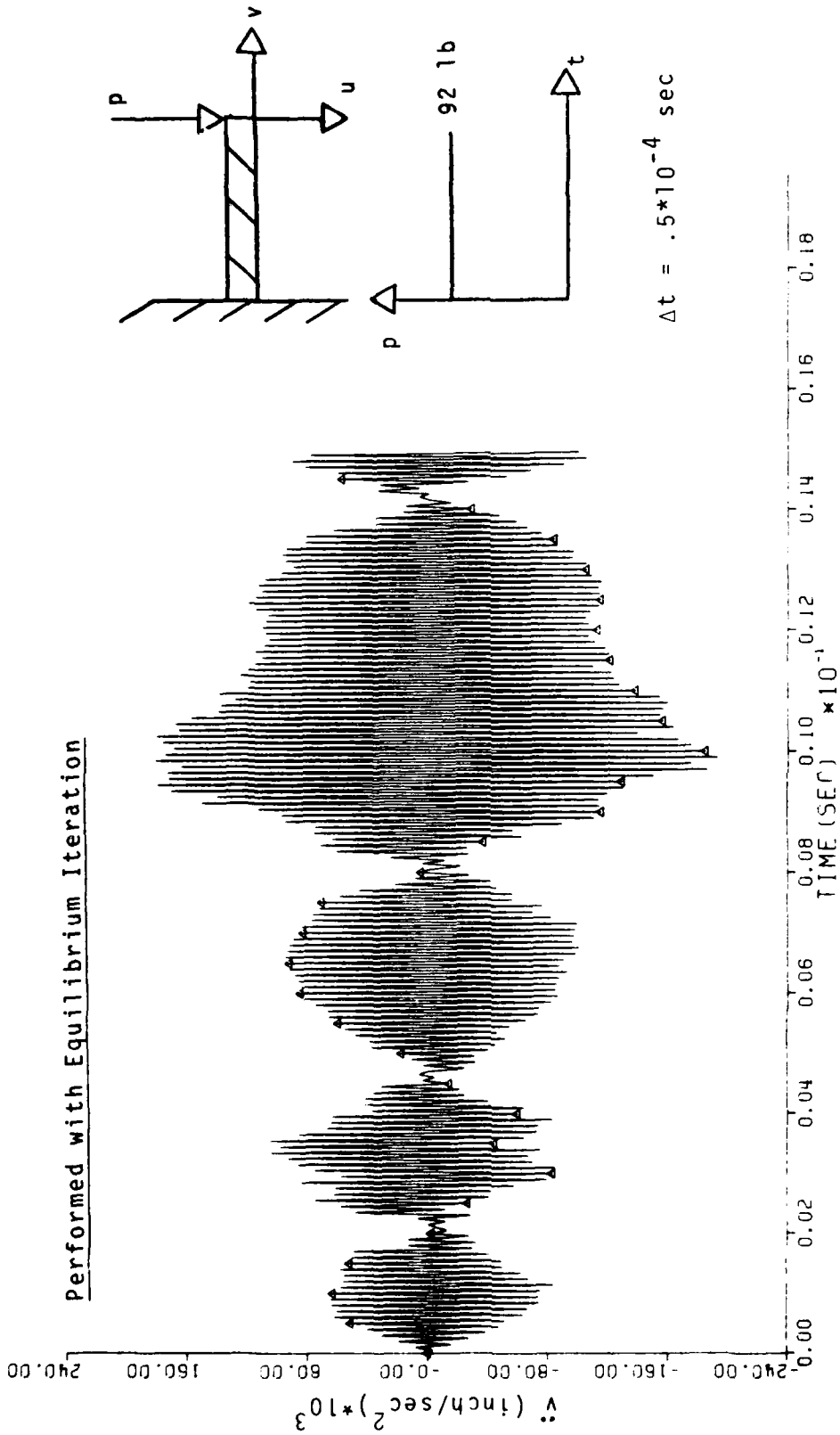
Fig. III-26    Horizontal End Acceleration of Step Loaded Elastic Cantilevered Beam
(80 elements)

62

response tends to increase because of the softening structural
stiffness initiated by plastic transitions.  Since such a
trend tends to improve the inertia following characteristics
of the numerical integration, this enables a good check on
the stiffness following capabilities of the algorithm.  The
first attempt at this problem employed the use of the equi-
librium option and a distributed type loading.  The results
are depicted in Figs. III.27-32.  As noted earlier, the ite-
ration option of the NR algorithm inherent to ADINA does not
reform the stiffness during the iteration cycle.  Hence upon
unloading which typically occurs at cycle limits, such an
algorithm misses the transition from plastic back to elastic
during the iteration phase.  This can lead to solution de-
gradation.  An example of such anomalous behavior is il-
lustrated in Figs. III.27-32.  The actual cause of failure
is the initiation of the out of balance load stop.  In ADINA,
such difficulties can be circumvented by employing the no
iteration option.

Figures III.33-38 illustrate the elastic-plastic (strain-
harding) distributed load response as obtained by the no
iteration option.  As can be seen, the imbalance loads encoun-
tered earlier during the first cycle limit were not monitored
through the use of this option.  Note while the solution ap-
pears successful when viewed strictly from the displacement
point of view, Figs. III.33 and 35, such a simplistic approach
can be dangerous.  This is clearly seen by considering the
behavior of the velocity and acceleration fields depicted in
Figs. III.35-38.  As can be seen from these figures, once
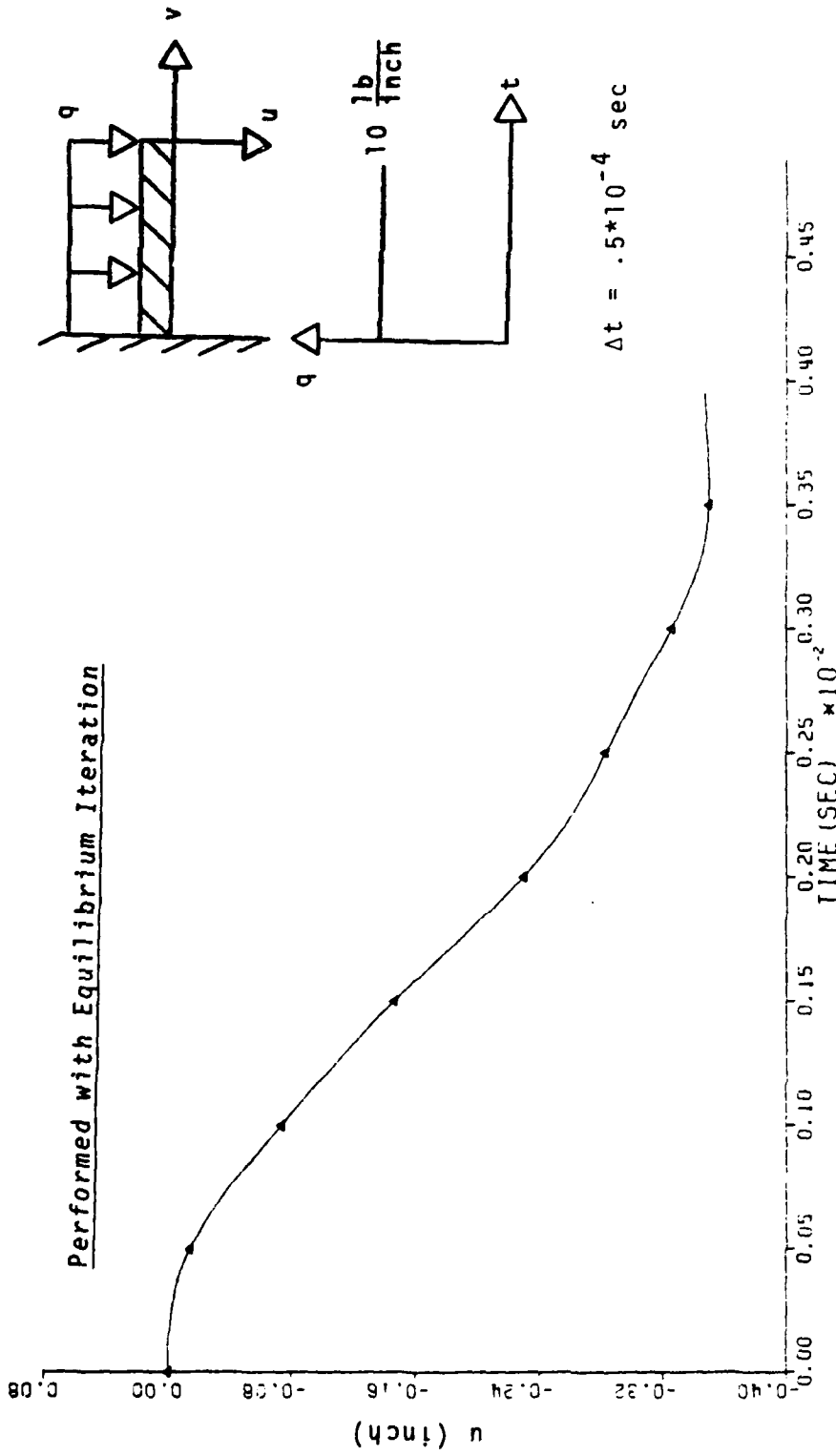
Fig. III-27   Vertical End Deflection of Step Loaded Elastic-Plastic (Strain Hardening) Cantilevered Beam (80 elements)
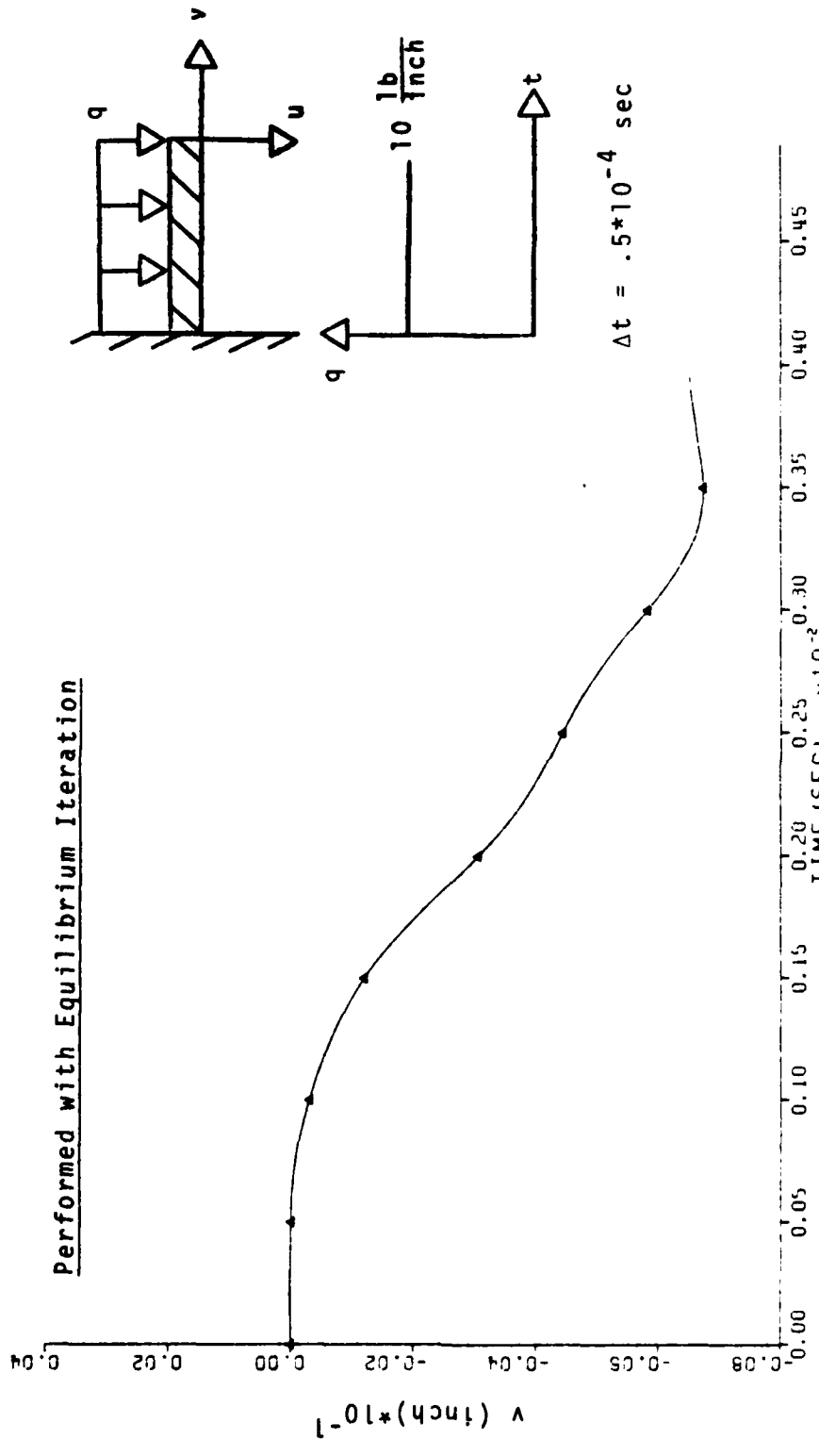
Fig. III-28   Horizontal End Deflection of Step Loaded Elastic-Plastic (Strain Hardening) Cantilevered Beam (80 elements)
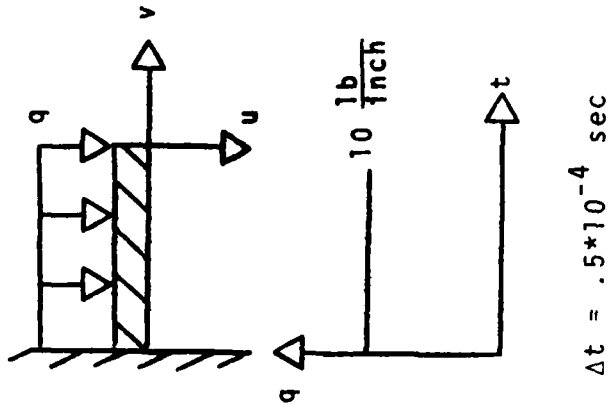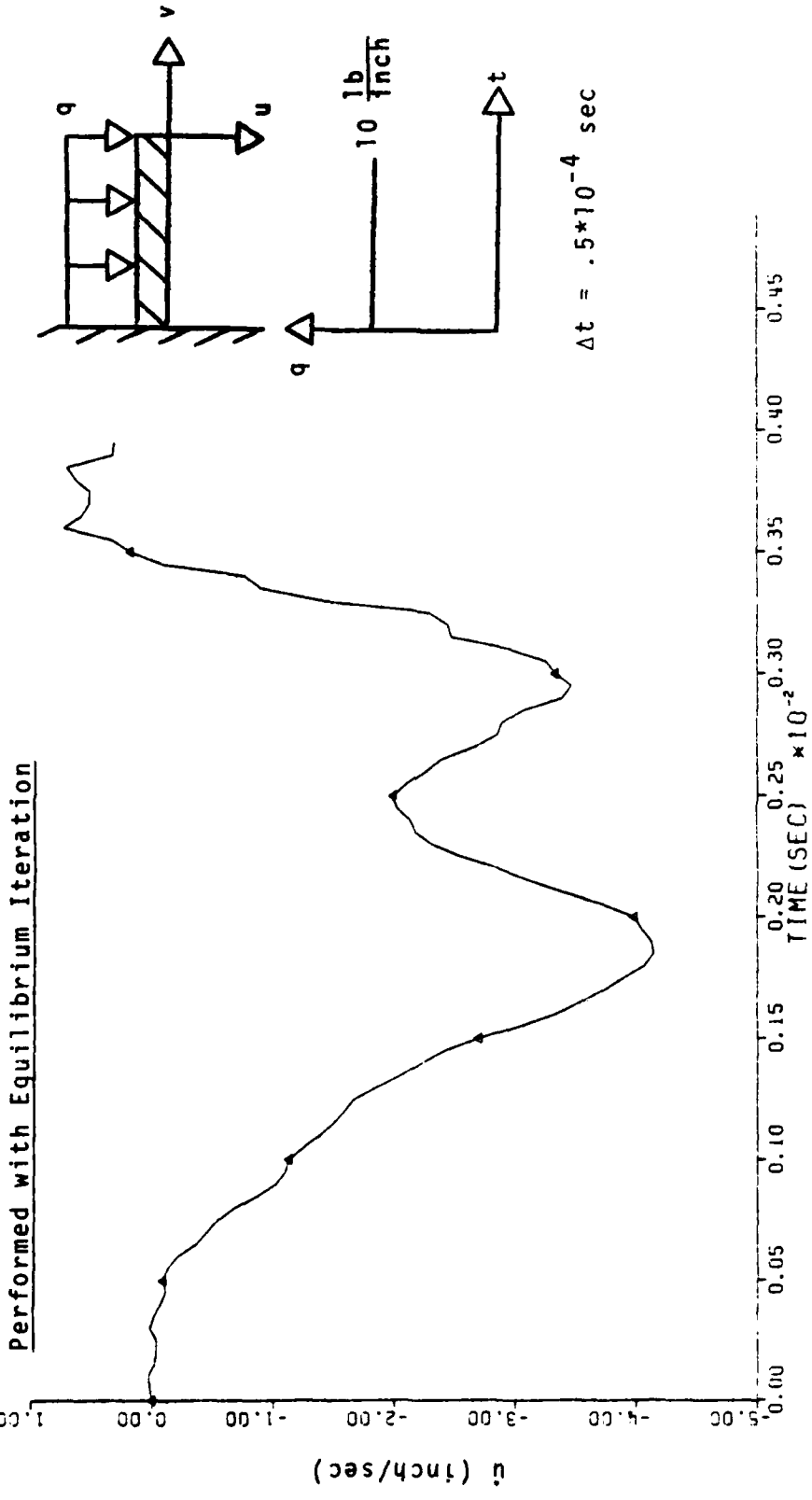
Fig. III-29  Vertical End Velocity of Step Loaded Elastic-Plastic
(Strain Hardening) Cantilevered Beam  (80 elements)
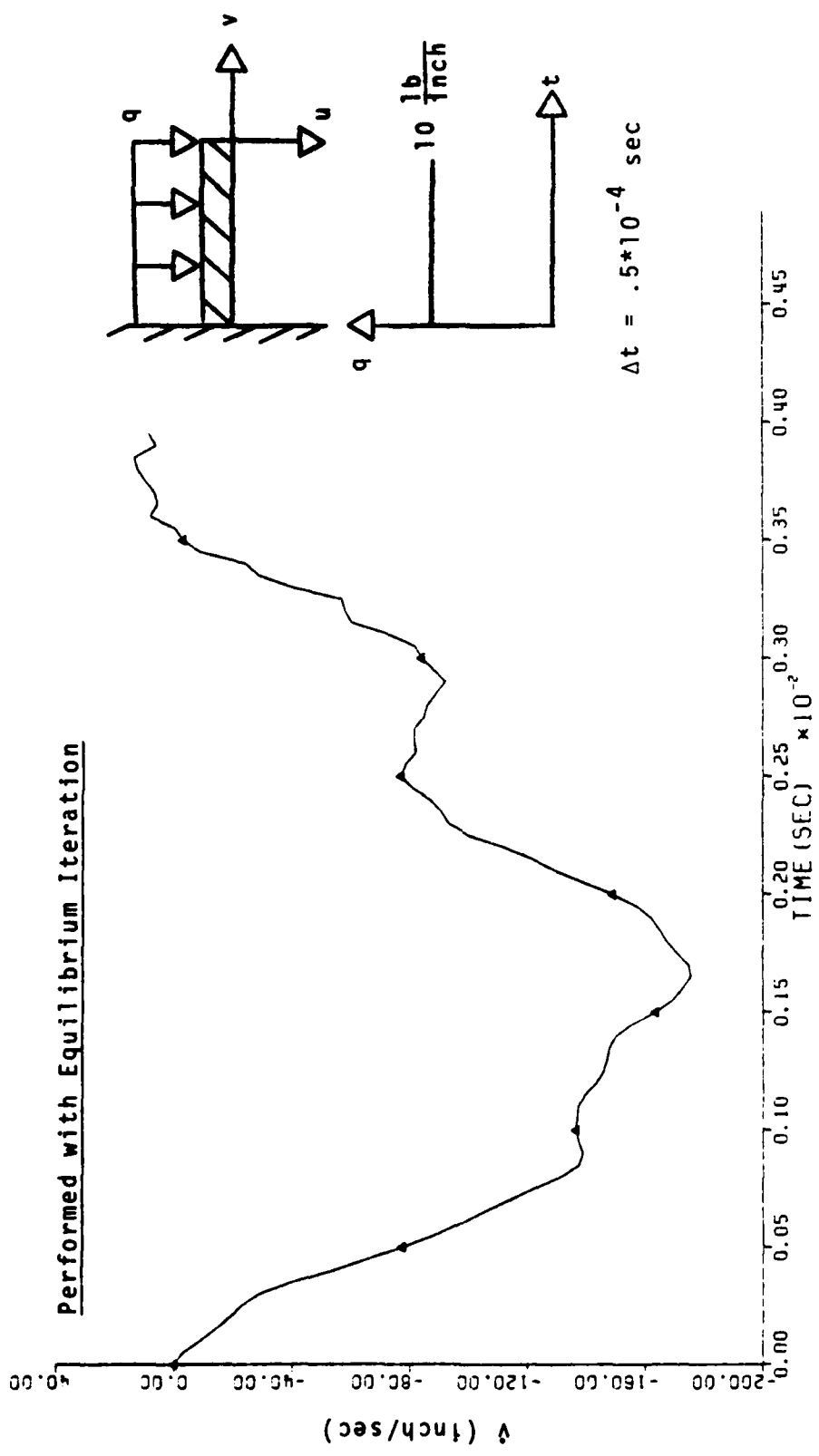
Fig. III-30  Horizontal End Velocity of Step Loaded Elastic-Plastic
(Strain Hardening) Cantilevered Beam  (80 elements)
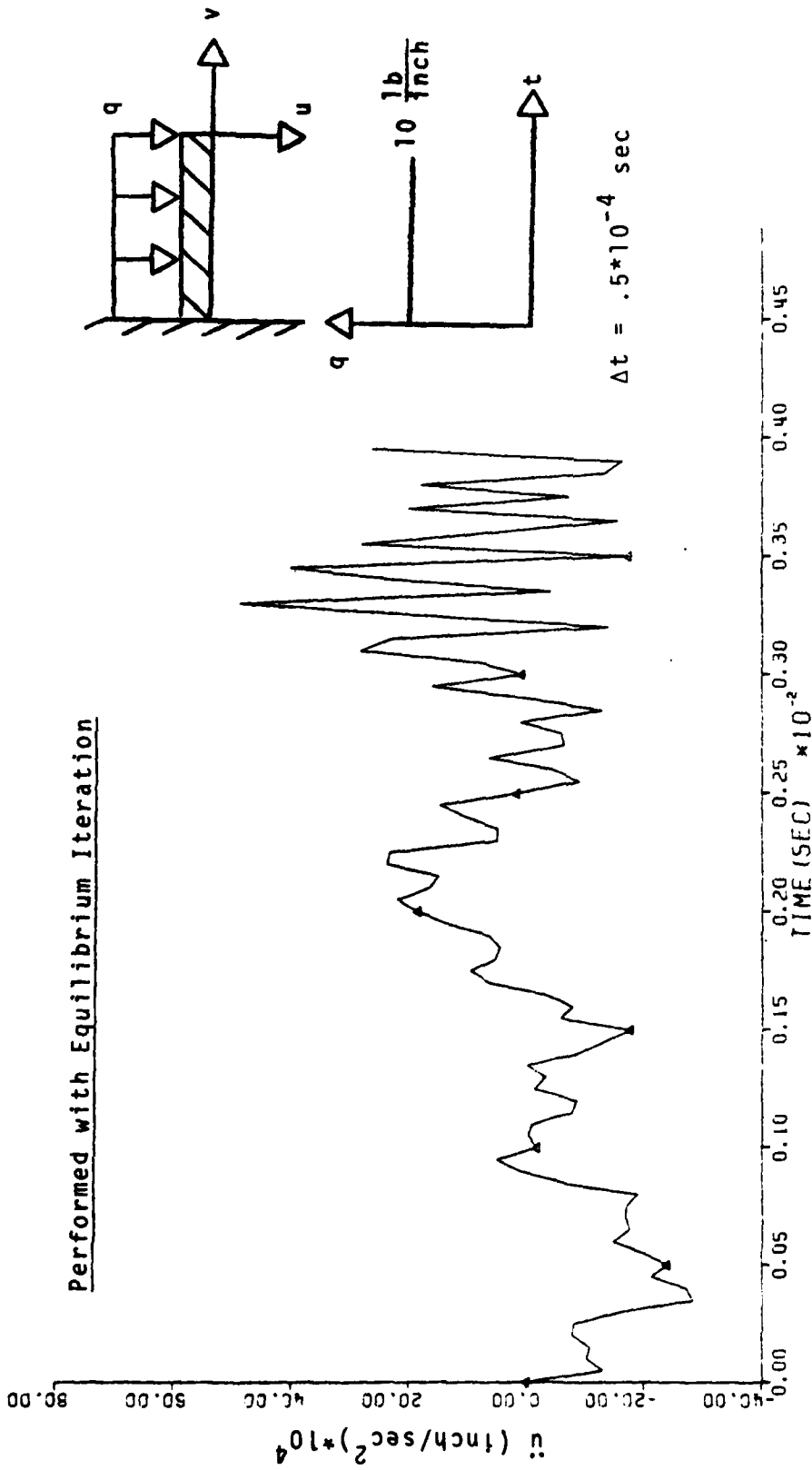
Fig. III-31   Vertical Acceleration of Step Loaded Elastic-Plastic (Strain
Hardening) Cantilevered Beam  (80 elements)
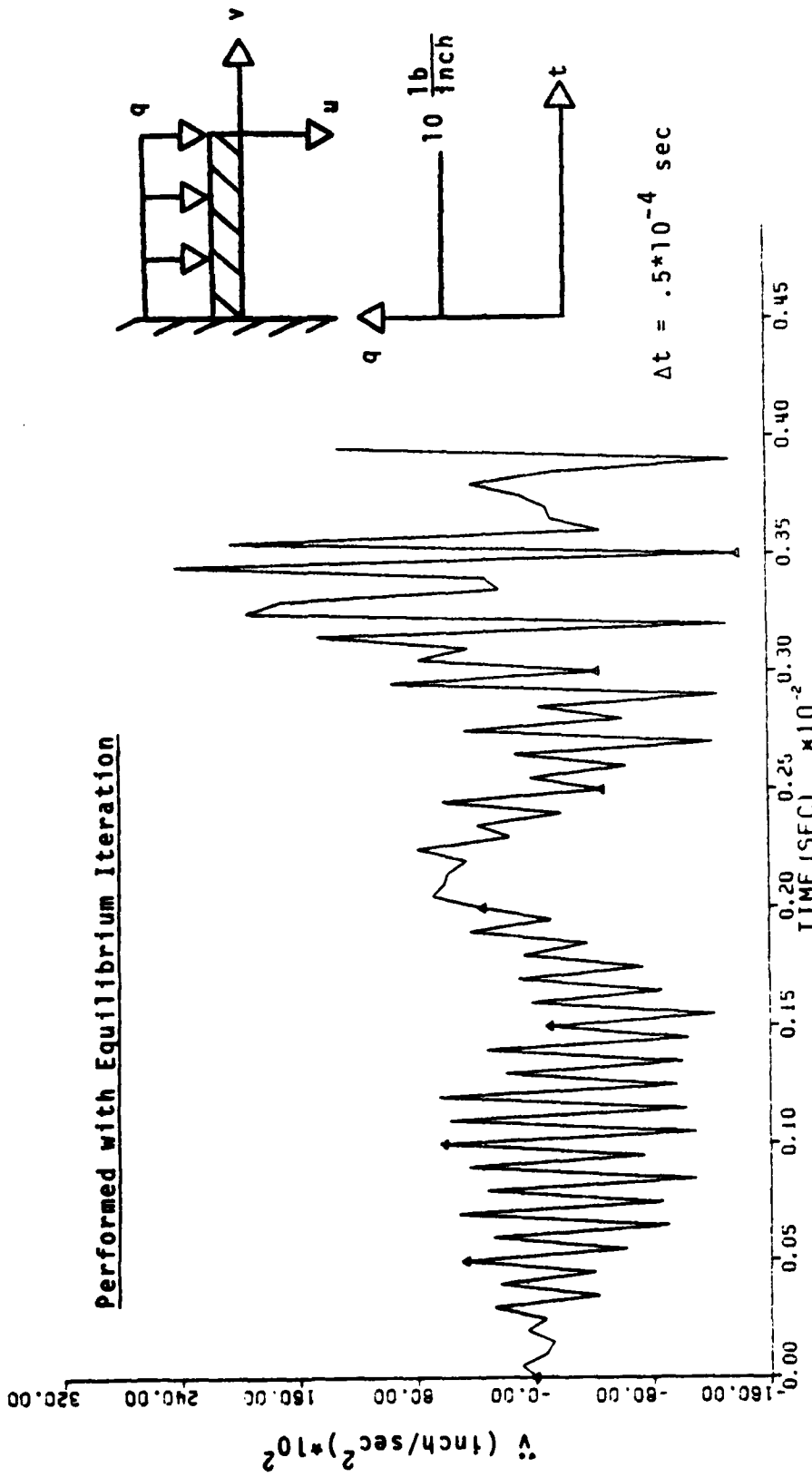
Fig. III-32    Horizontal Acceleration of Step Loaded Elastic-Plastic
(Strain Hardening) Cantilevered Beam    (80 elements)

Performed with Equilibrium Iteration

69
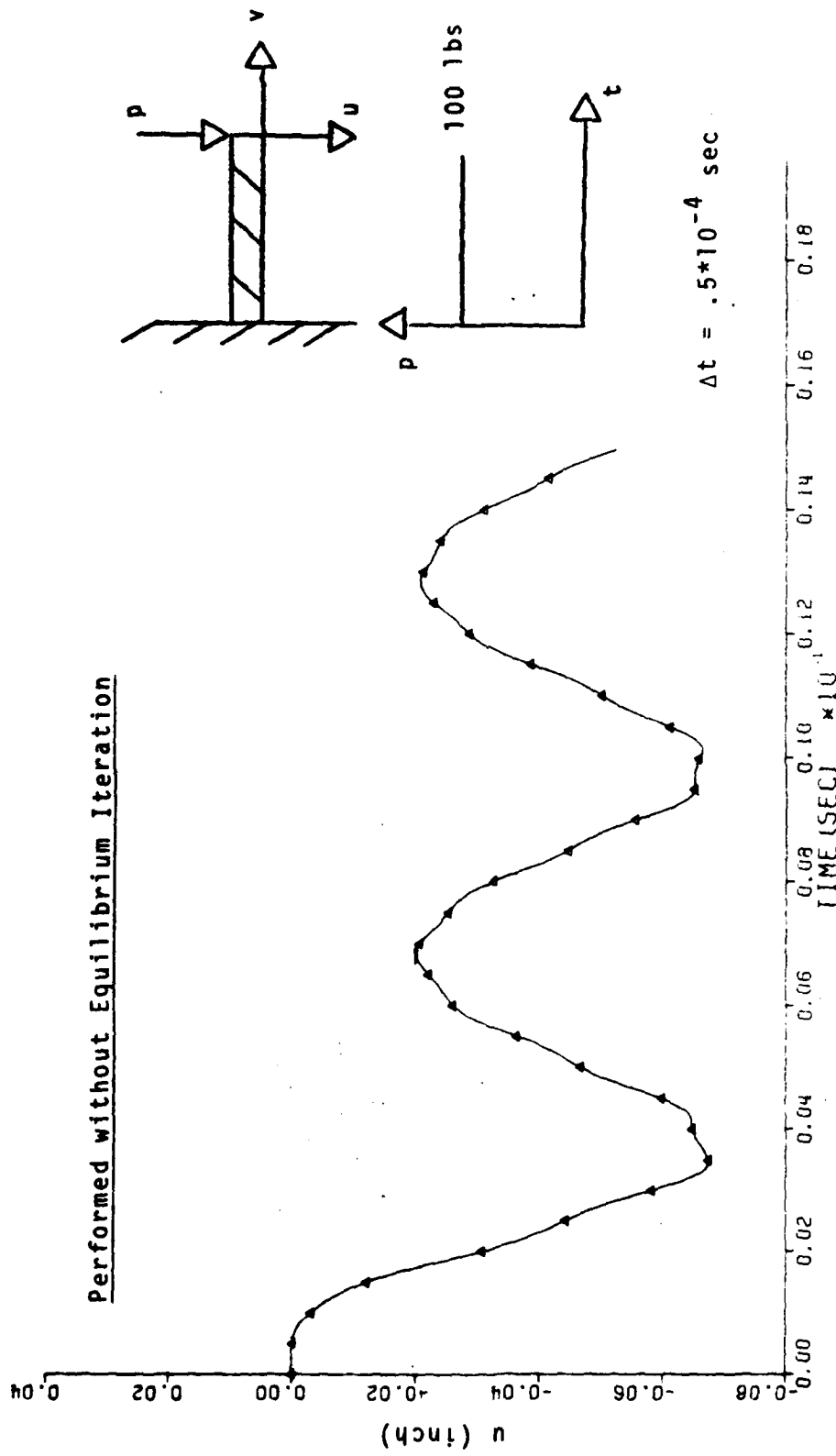
Fig. III-33  Vertical End Deflection of Step Loaded Elastic-Plastic
(Strain Hardening) Cantilevered Beam  (80 elements)

70
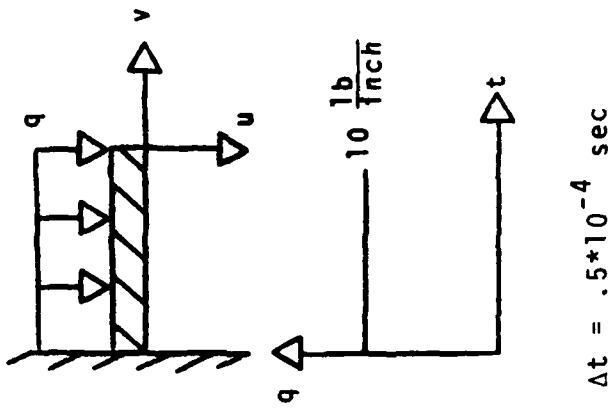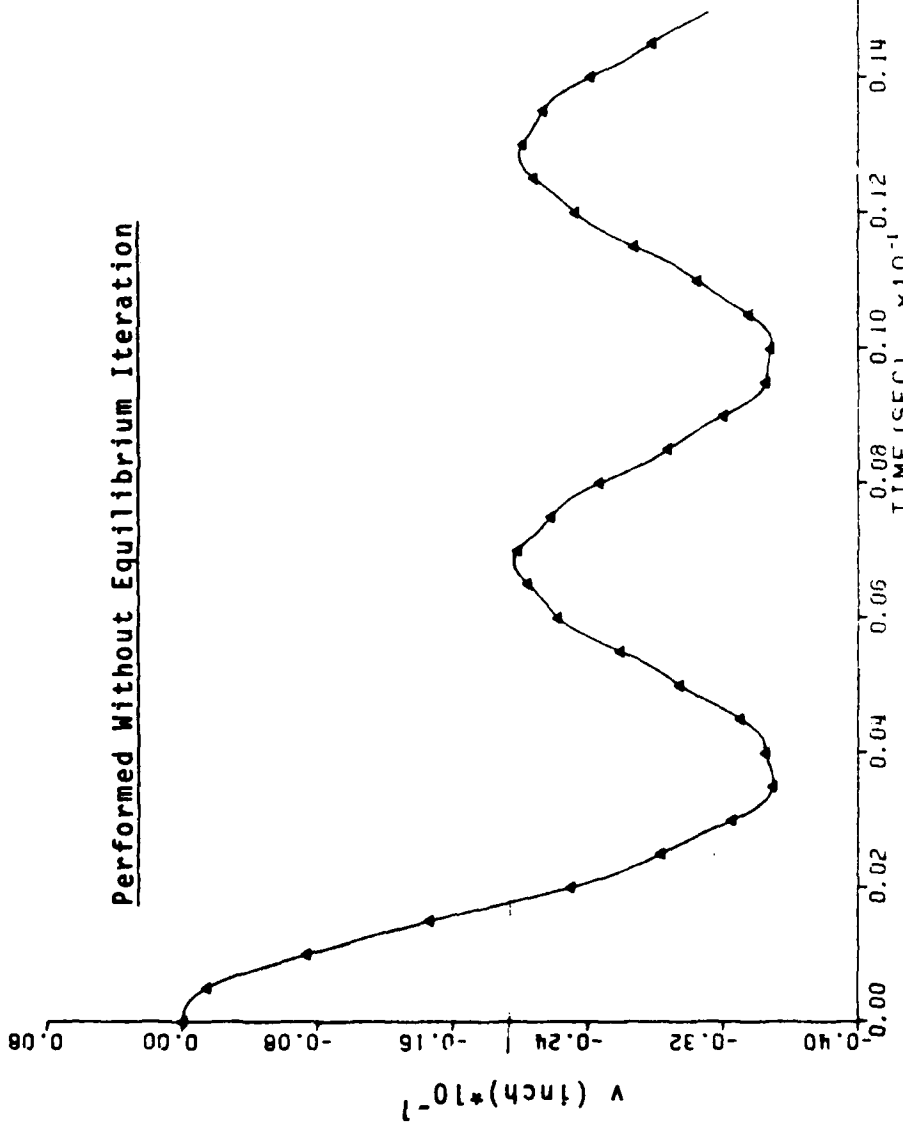
Fig. III-34  Horizontal End Deflection of Step Loaded Elastic-Plastic
(Strain Hardening) Cantilevered Beam  (80 elements)

Performed Without Equilibrium Iteration

$q$

$v$

$u$

$10 \frac{lb}{inch}$

$q$

$t$

$q$

$\Delta t = .5*10^{-4}$ sec

ů (inch/sec)

100.00   50.00   0.00   -50.00   -100.00   -150.00   -200.00

0.00   0.02   0.04   0.06   0.08   0.10   0.12   0.14   0.16   0.18

TIME (SEC)   $*10^{-1}$
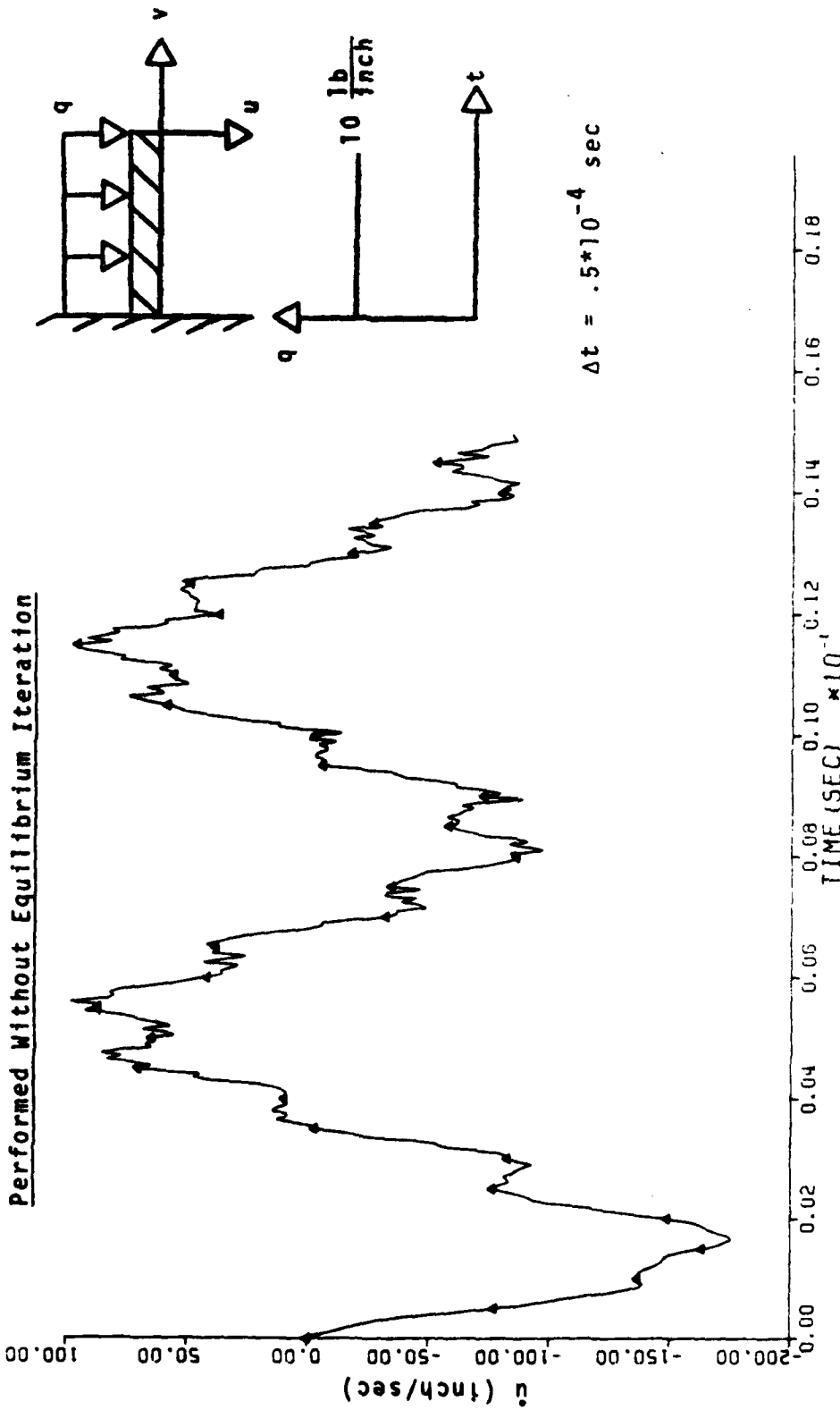
Fig. III-35   Vertical End Velocity of Step Loaded Elastic-Plastic
(Strain Hardening) Cantilevered Beam   (80 elements)

Performed Without Equilibrium Iteration

10 $\frac{lb}{inch}$

$\Delta t = .5*10^{-4}$ sec

$\dot{v}$ (inch/sec)

6.00  4.00  2.00  0.00  -2.00  -4.00  -6.00

0.00  0.02  0.04  0.06  0.08  0.10  0.12  0.14  0.16  0.18

TIME (SEC) $\times 10^{-1}$
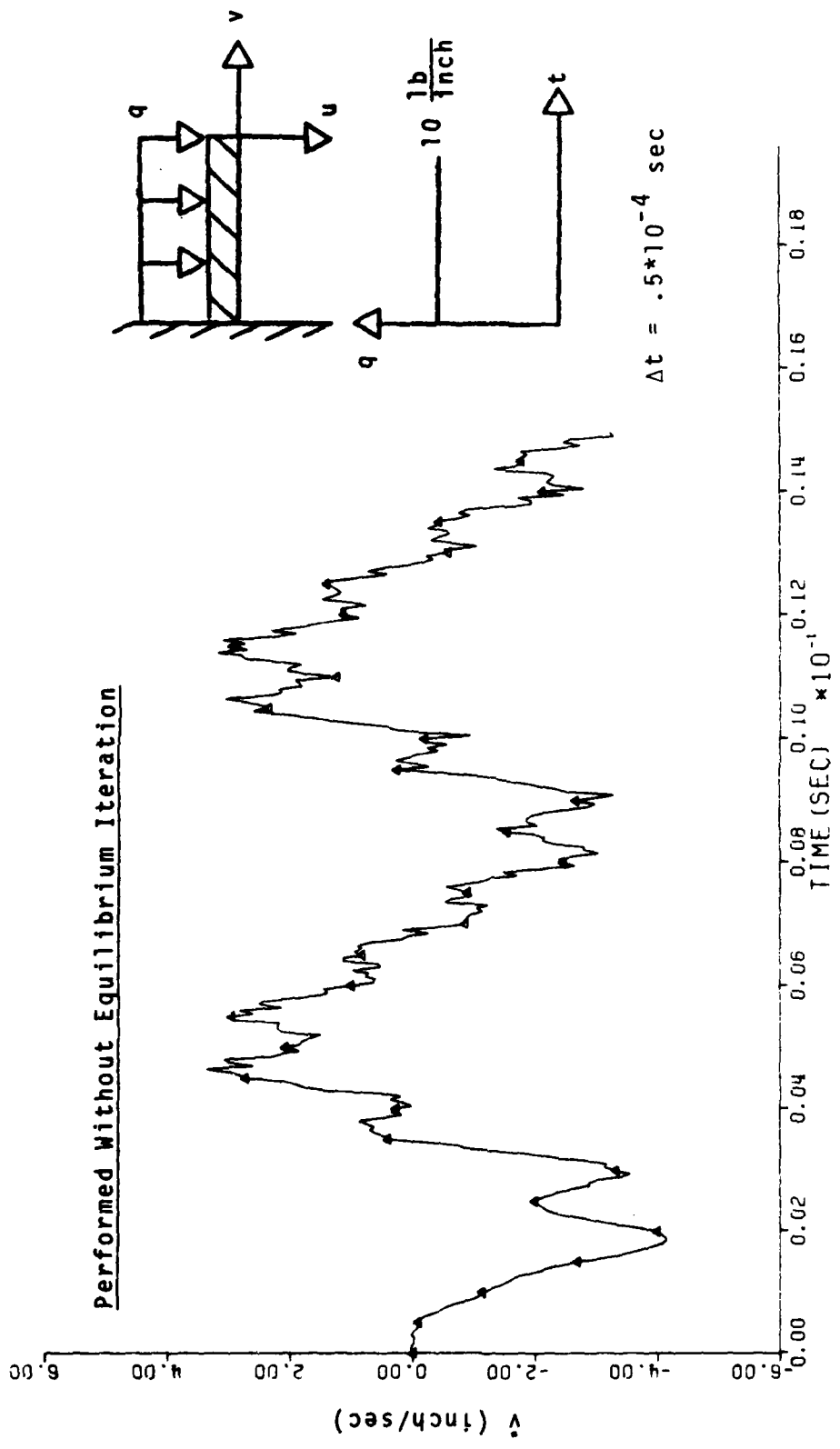
Fig. III-36  Horizontal End Velocity of Step Loaded Elastic-Plastic (Strain-Hardening) Cantilevered Beam (80 elements)
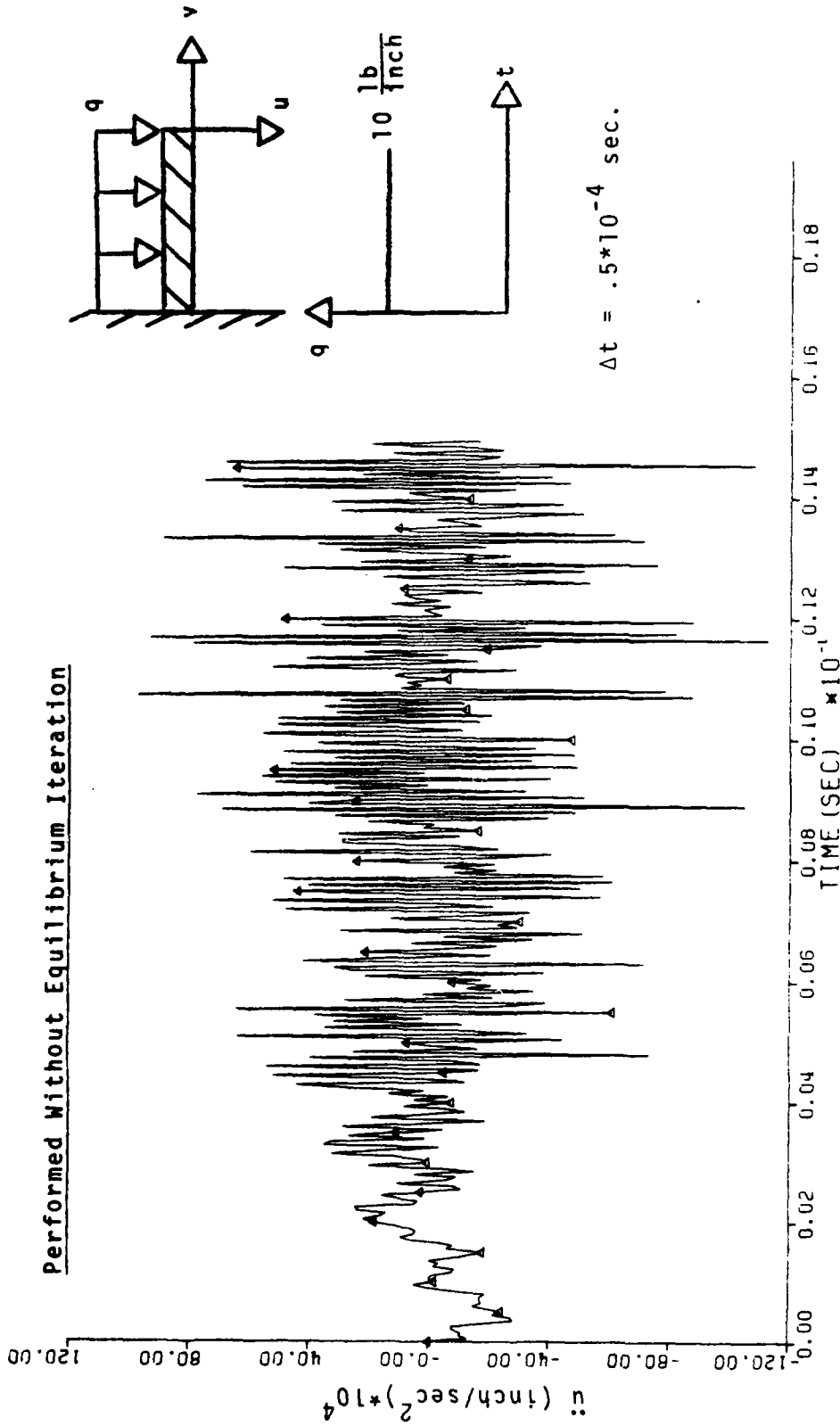
Fig. III-37   Vertical End Acceleration of Step Loaded Elastic-Plastic
(Strain Hardening)  Cantilevered Beam  (80 elements)

75
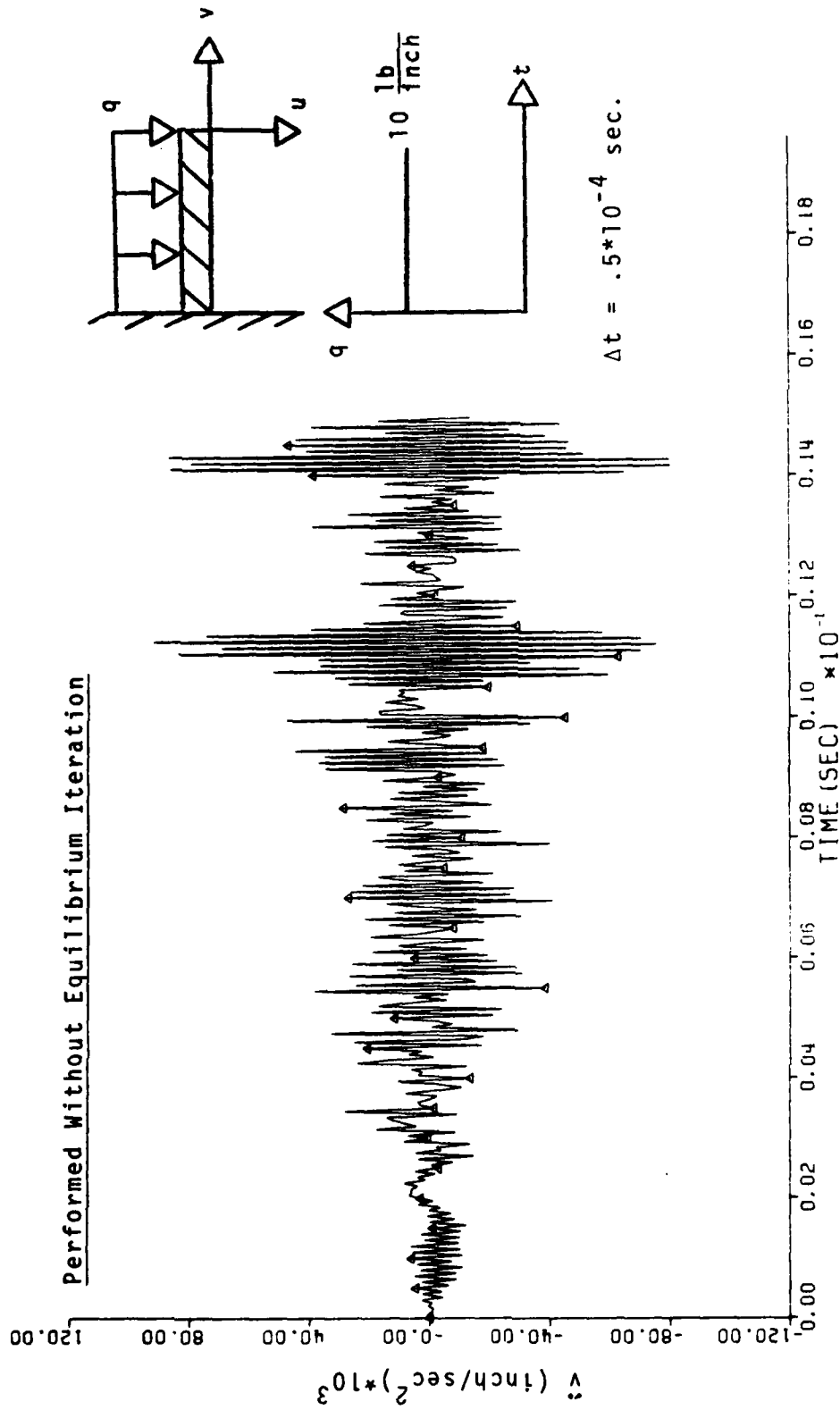


Fig. III-38  Horizontal End Acceleration of Step Loaded Elastic-Plastic
(Strain Hardening) Cantilevered Beam  (80 elements)

the solution passes the first cycle limit, progressive de-
gradation is initiated. This follows from the fact that with-
out iterative corrections, the imbalance loads cause a drift
on the solution hyper surface. Because of this, the only way
the solution can be abnormally terminated in ADINA 1977 is
via the negative pivot stop. Otherwise the calculations will
be terminated via the usual time limit check.

Increasing the problem severity further, Figures III.
39-44 illustrate the elastic-plastic cantilevered beam res-
ponse to a concentrated load. Due to the severity of the
loading, outright failure occurred when the iterative solu-
tion option was employed. To circumvent such difficulties
the reformation but no iteration option was employed to gene-
rate the results depicted in these figures. Note while ade-
quate solution behavior is obtained during the early stages
of the response, as time increases, the latter phases are
marked by progressive degradation. This can be seen from the
growing oscillations which occur in the velocity and accele-
ration fields shown in Figs. III.41-44. These culminate in
the initiation of a negative pivot stop. As noted earlier,
this is a direct outgrowth of the fact that without iterative
corrections, the load imbalance tends to grow as the time
incrementation proceeds.

Figure III.45 illustrates the geometry and material proper-
ties of the spherical cap which serves as the second benchmark of
the dynamic solution branch. As with the beam, large displace-
ment elastic-plastic behavior is admitted in the model. Whereas
the previous benchmark established solution difficulties
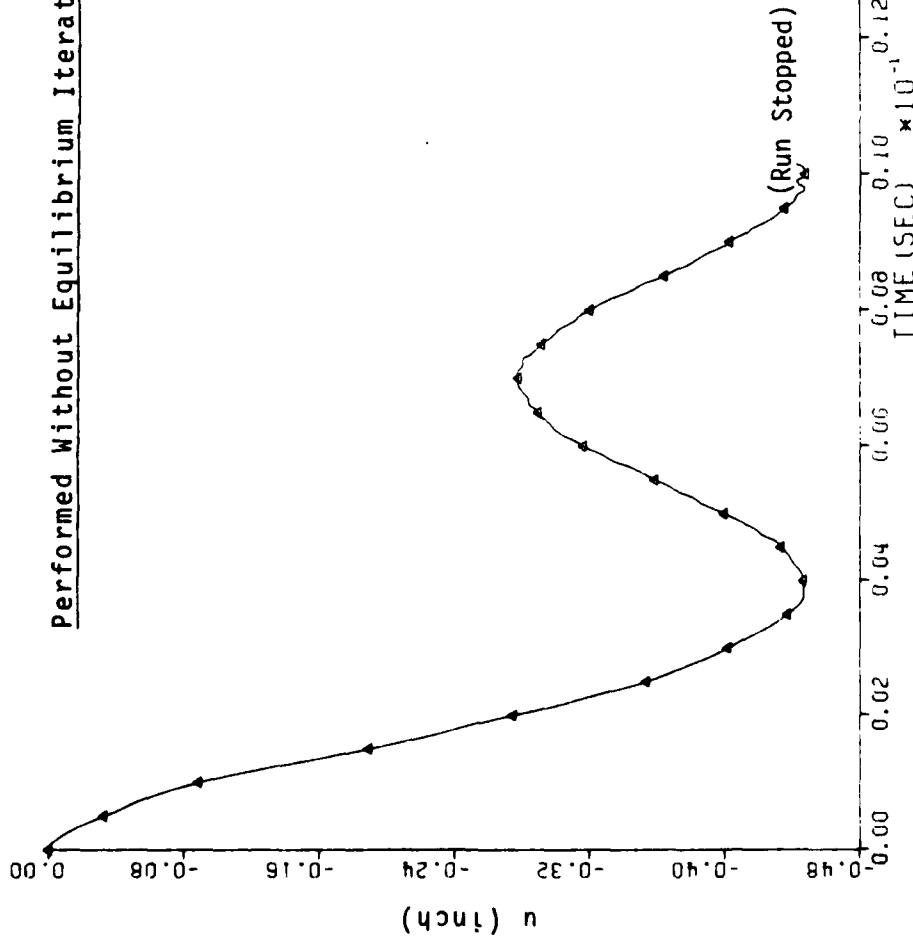
Fig. III-39  Vertical End Deflection of Step Loaded Elastic-Plastic
(Strain Hardening) Cantilevered Beam  (80 elements)

Performed Without Equilibrium Iteration

100 lbs

$\Delta t = .5*10^{-4}$ sec.

(Run Stopped)

v (inch)*10^{-1}

TIME (SEC) *10^{-1}
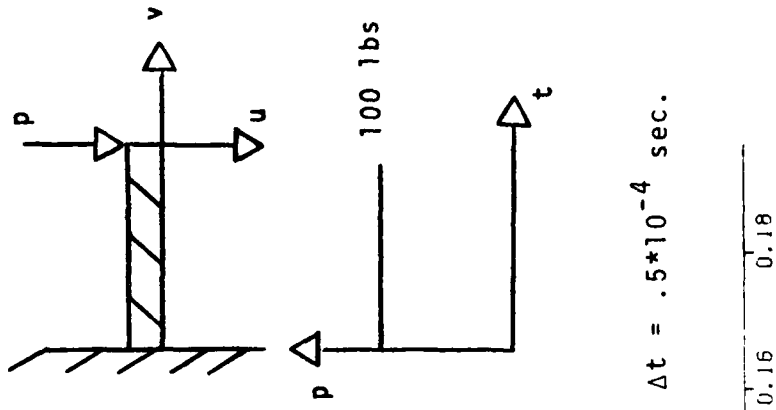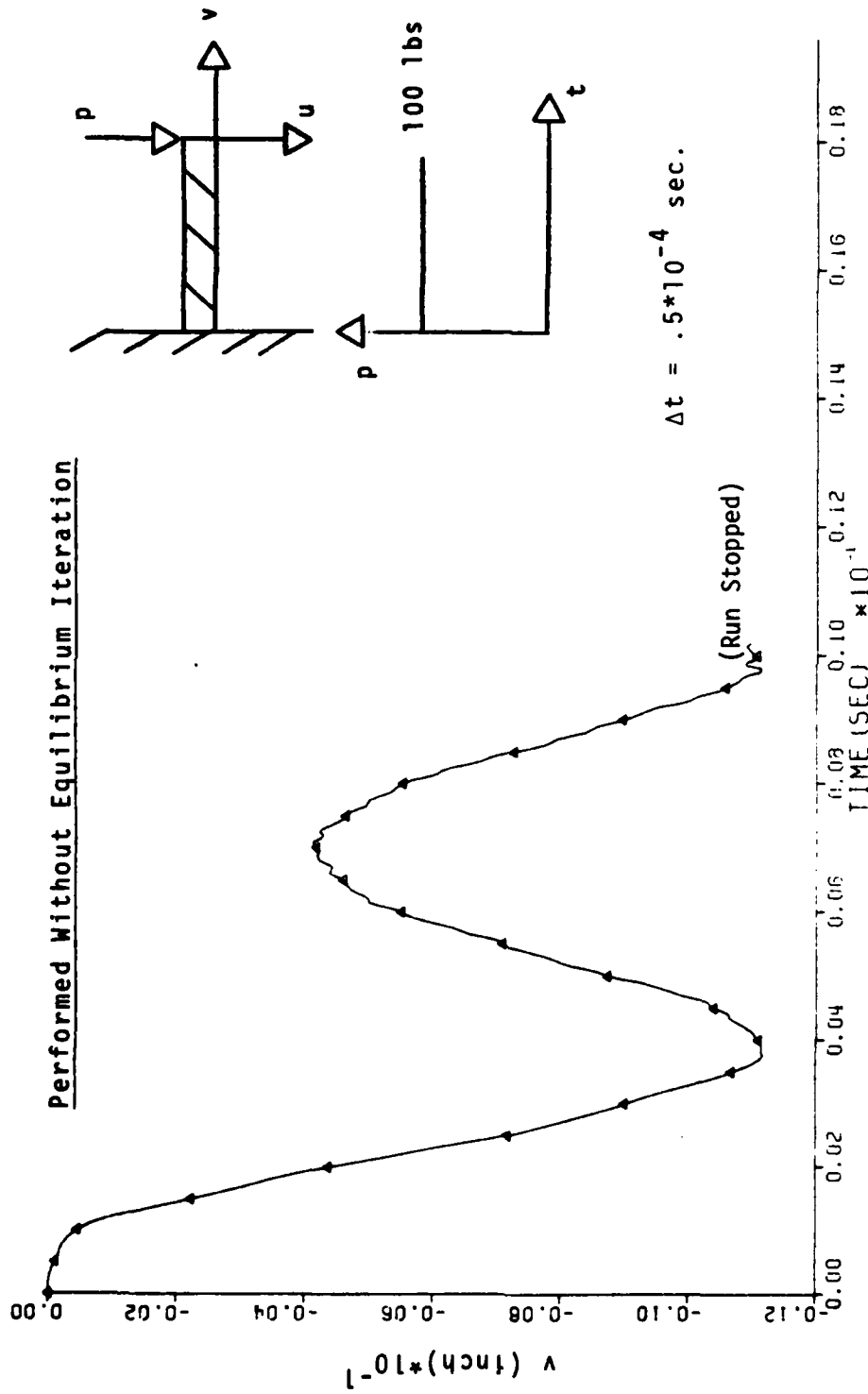
Fig. III-40 Horizontal End Deflection of Step Loaded Elastic-Plastic (Strain Hardening) Cantilevered Beam (80 elements)
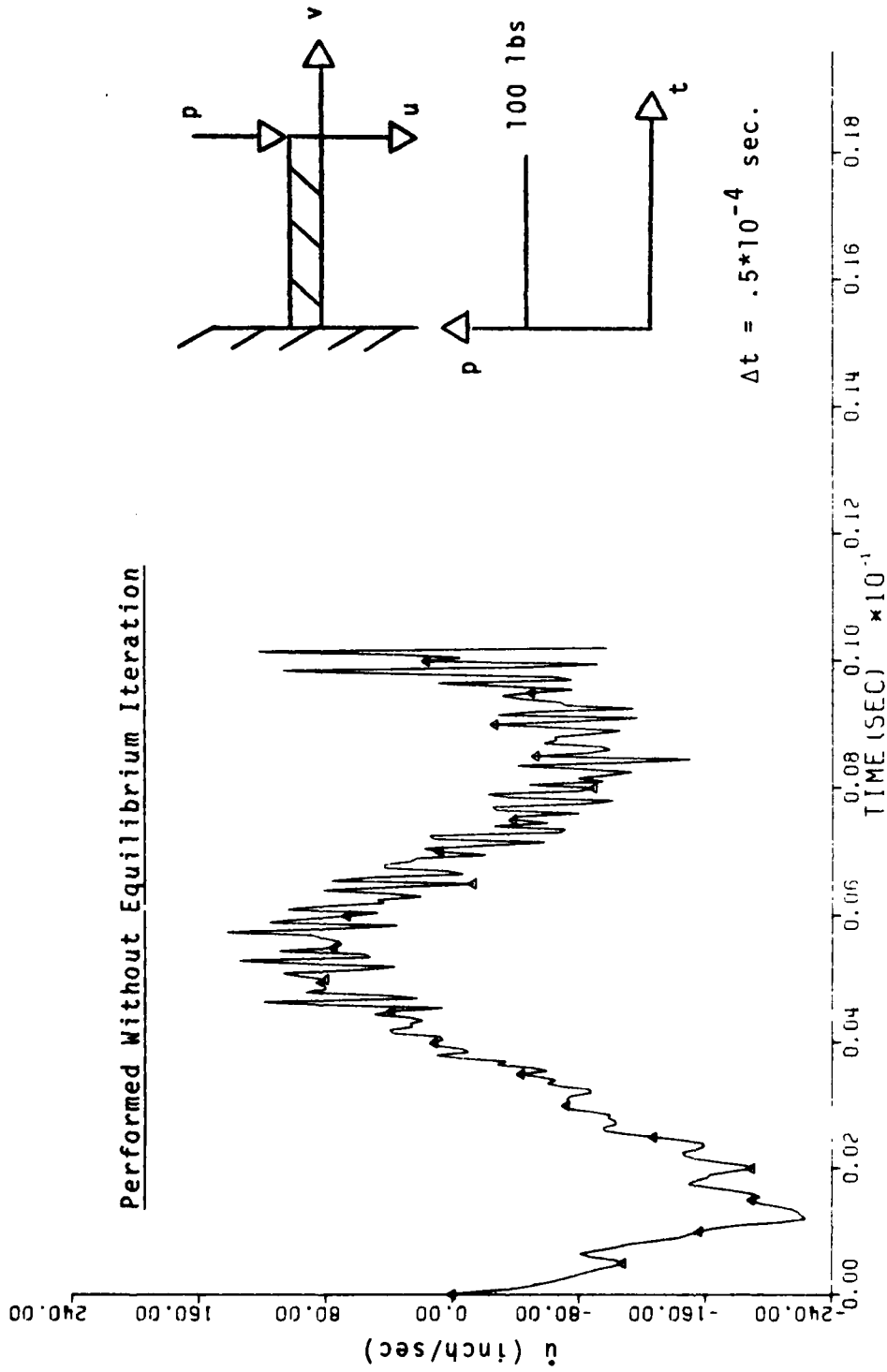
Fig. III-41  Vertical End Velocity of Step Loaded Elastic-Plastic
(Strain Hardening) Cantilevered Beam  (80 elements)
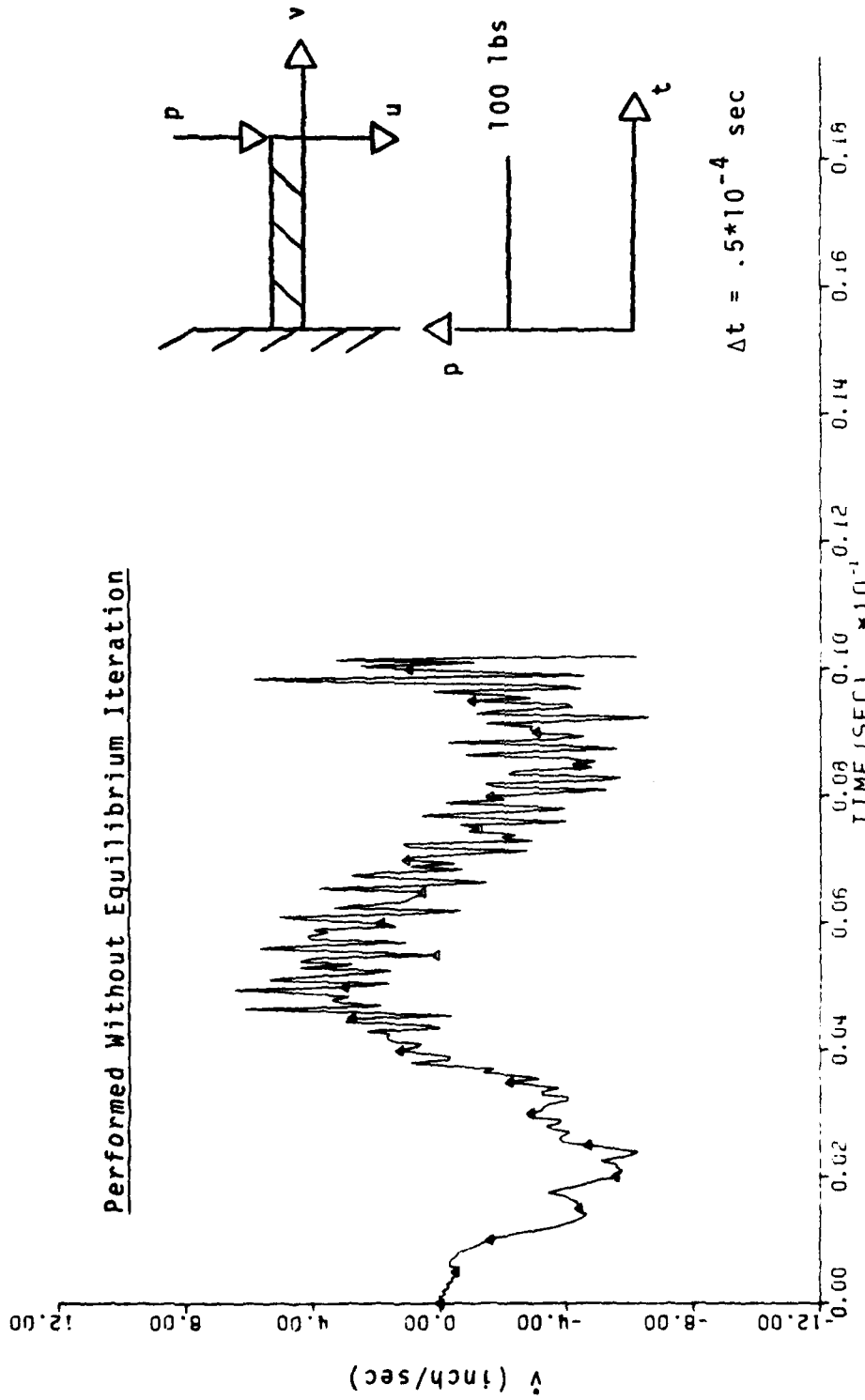
Fig. III-42   Horizontal End Velocity of Step Loaded Elastic-Plastic
(Strain Hardening) Cantilevered Beam  (80 elements)
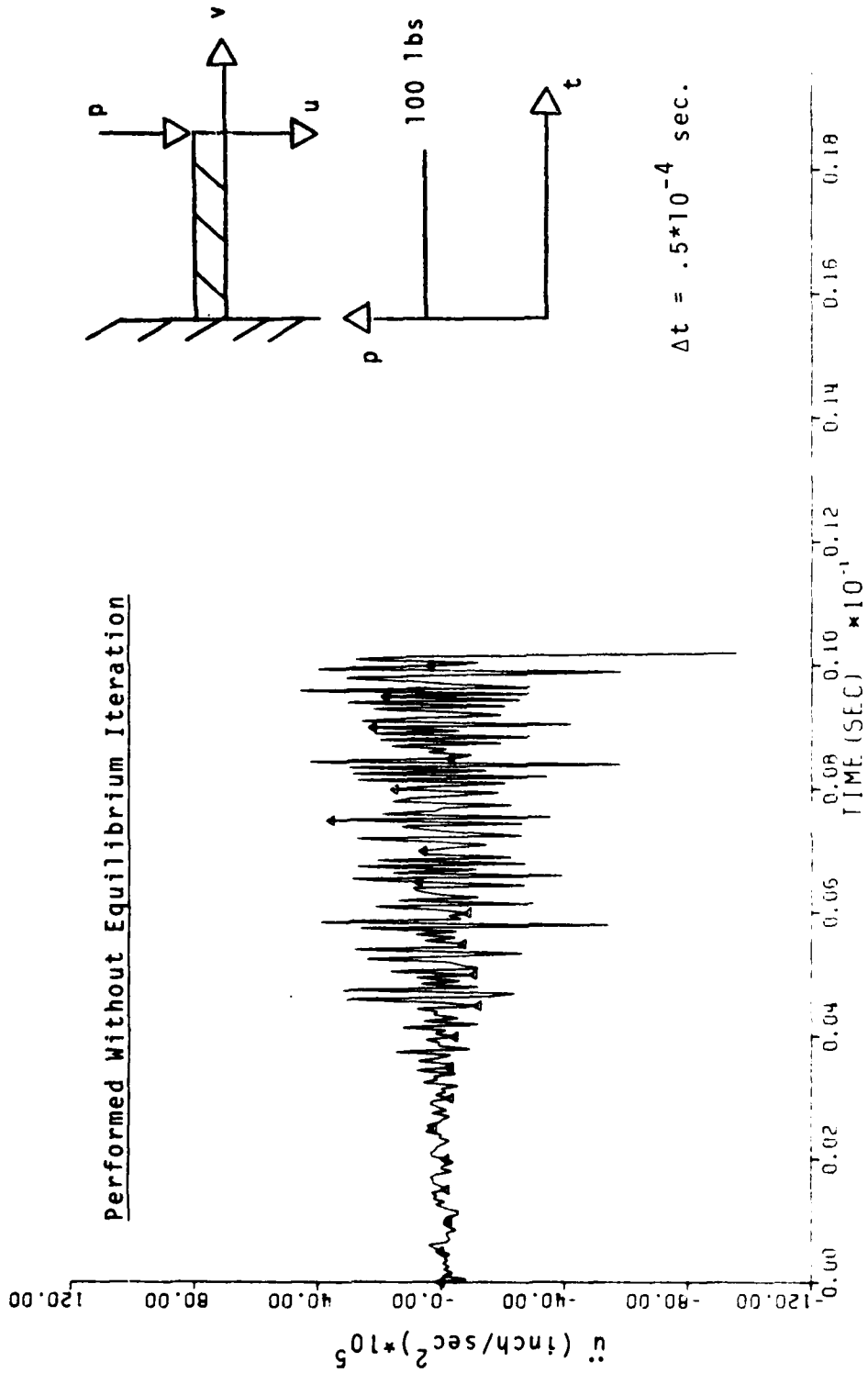
Fig. III- 43  Vertical End Acceleration of Step Loaded Elastic-Plastic
(Strain Hardening) Cantilevered Beam  (80 elements)
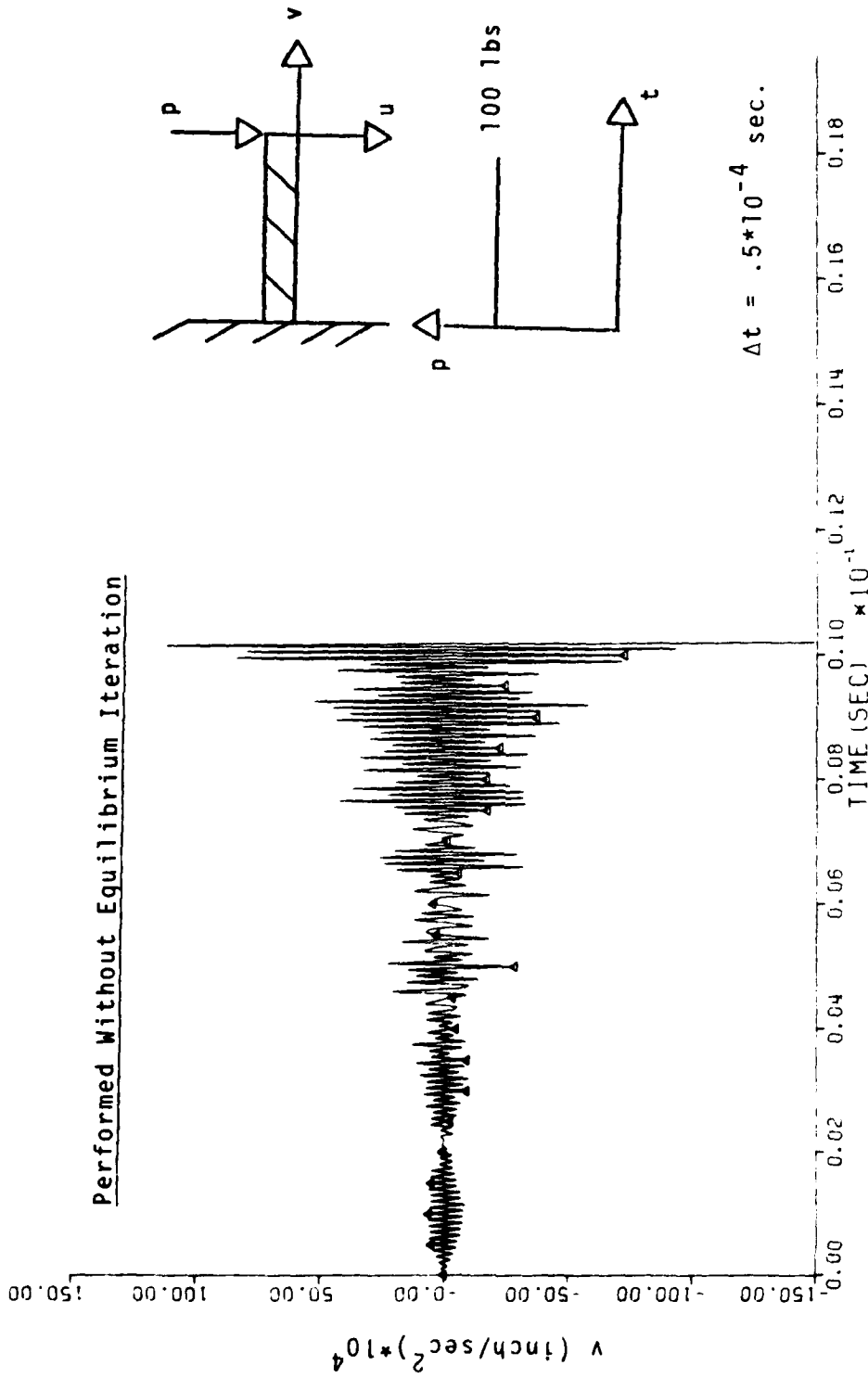
Fig. III-44  Horizontal End Acceleration of Step Loaded Elastic-Plastic
(Strain Hardening) Cantilevered Beam  (80 elements)
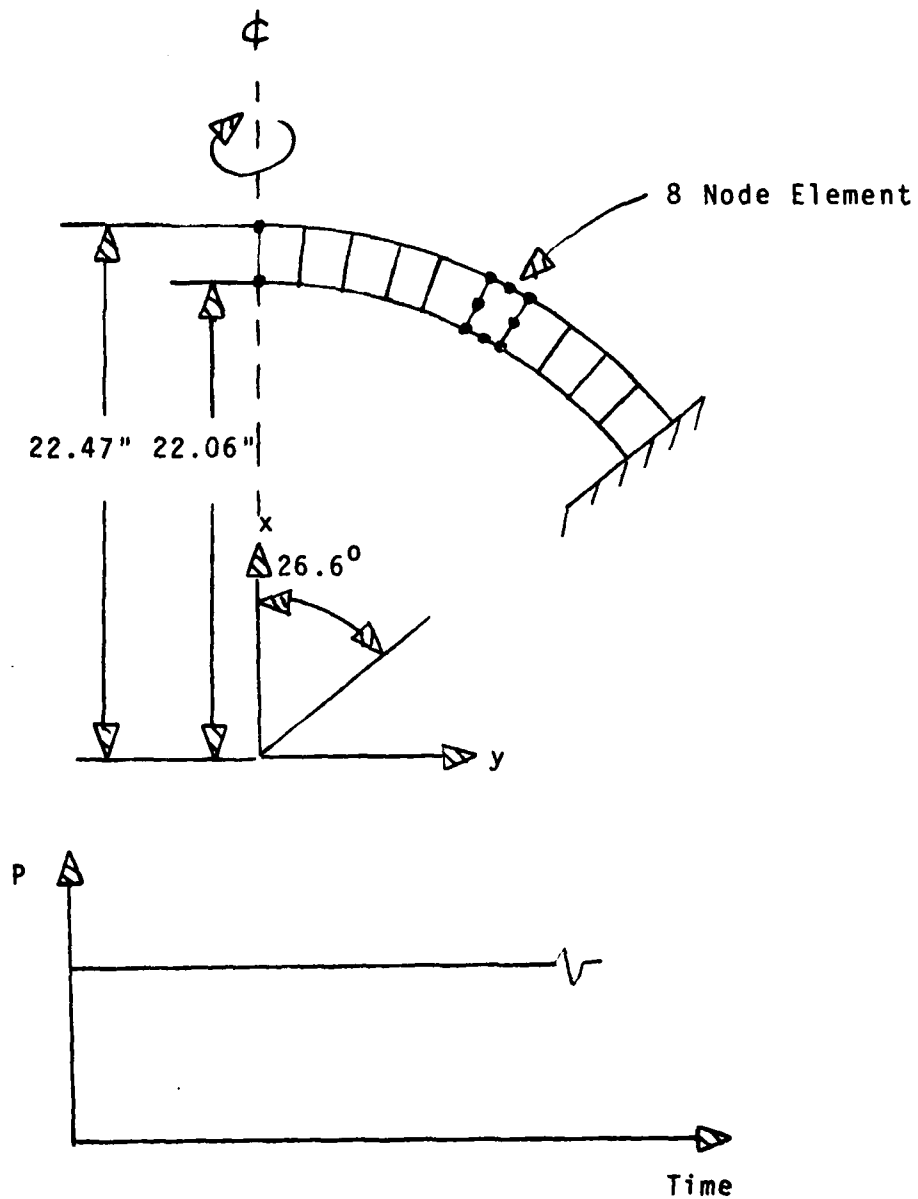
$E = 10.5 * 10^6$ psi

$\nu = .3$

$\sigma$yield $= 24 * 10^3$ psi

$\varepsilon_{tang.} = .21 * 10^6$ psi

$\rho = 2.45 * 10^{-4}$ lbm/in$^3$

Fig III.45   Spherical Cap Geometry, Material Properties
and Element Model

associated with long term behavior (several cycles), the current problem will emphasize anomalous behavior during the initial stages (first cycle) of solution.

In this context, the effects of severe nonlinearity on the choice of time step size will be considered. To achieve this end, the spherical cap will be excited by step pressure loadings of increasing magnitude. The various effects of kinematic/material nonlinearity on solution success is shown in Fig. III.46-49. Note as illustrated, three basic stages are seen to exist. These can be categorized by:

1) "Mild" nonlinear effect;

2) "Moderate" nonlinear effects and;

3) "Strong" nonlinear effects.

These stages of behavior will be considered in the context of time step sizes which are successful in describing the linear response. Before discussing such behavior, it should be noted that for loads below the critical buckling value, the cap exhibits both kinematic and material softening.

As noted earlier, time step sizes adequate to capture the inertial effects of linear problems will remain so for softening situations. For such nonlinearities, degradation typically arises as an outgrowth of the inability to track the changes in structural stiffness. For mildly nonlinear situations, since only minor changes occur in the structural stiffness, typically the linear time step is adequate. This can be seen from the results illustrated in Fig. III.46.

Employing the same time step size, Fig. III.47 illustrates the transient cap response for moderate loadings. For such

$\Delta t_1 = 5 * 10^{-5}$ sec

—— P = 200 psi

––– P = 300 psi

— — P = 400 psi

t/$\Delta t_1$

20  40  60  80

Solution
1. Newmark
2. Equilibrium Iteration
3. Timestep = .75 * $10^{-5}$ sec
4. Solution Normally Terminated

Radial Crown Deflection (Inch)
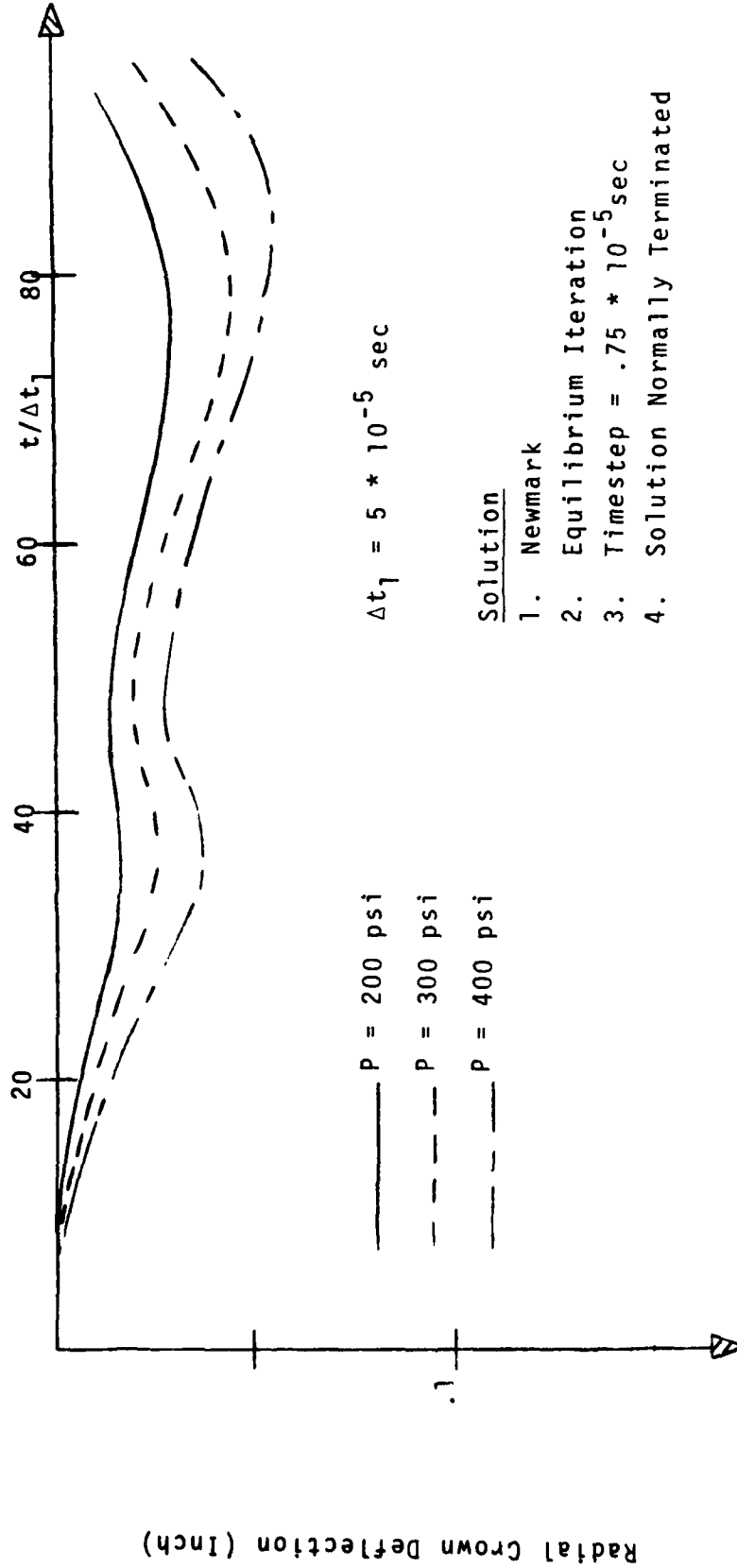
Fig III. 46  Dynamic Response of Spherical Cap Subject to Step Pressure Loading
("Mild" Nonlinearity Excited)

$\Delta t_1 = .5 * 10^{-5}$ sec

Solution

1. Newmark
2. Equilibrium Iteration
3. Timestep = $.75 * 10^{-5}$ sec
4. Solution Abnormally Terminated
   by Iteration Count Stop

P = 500 psi

P = 700 psi

P = 800 psi

t/$\Delta t_1$

Radial Crown Deflection    (Inch)
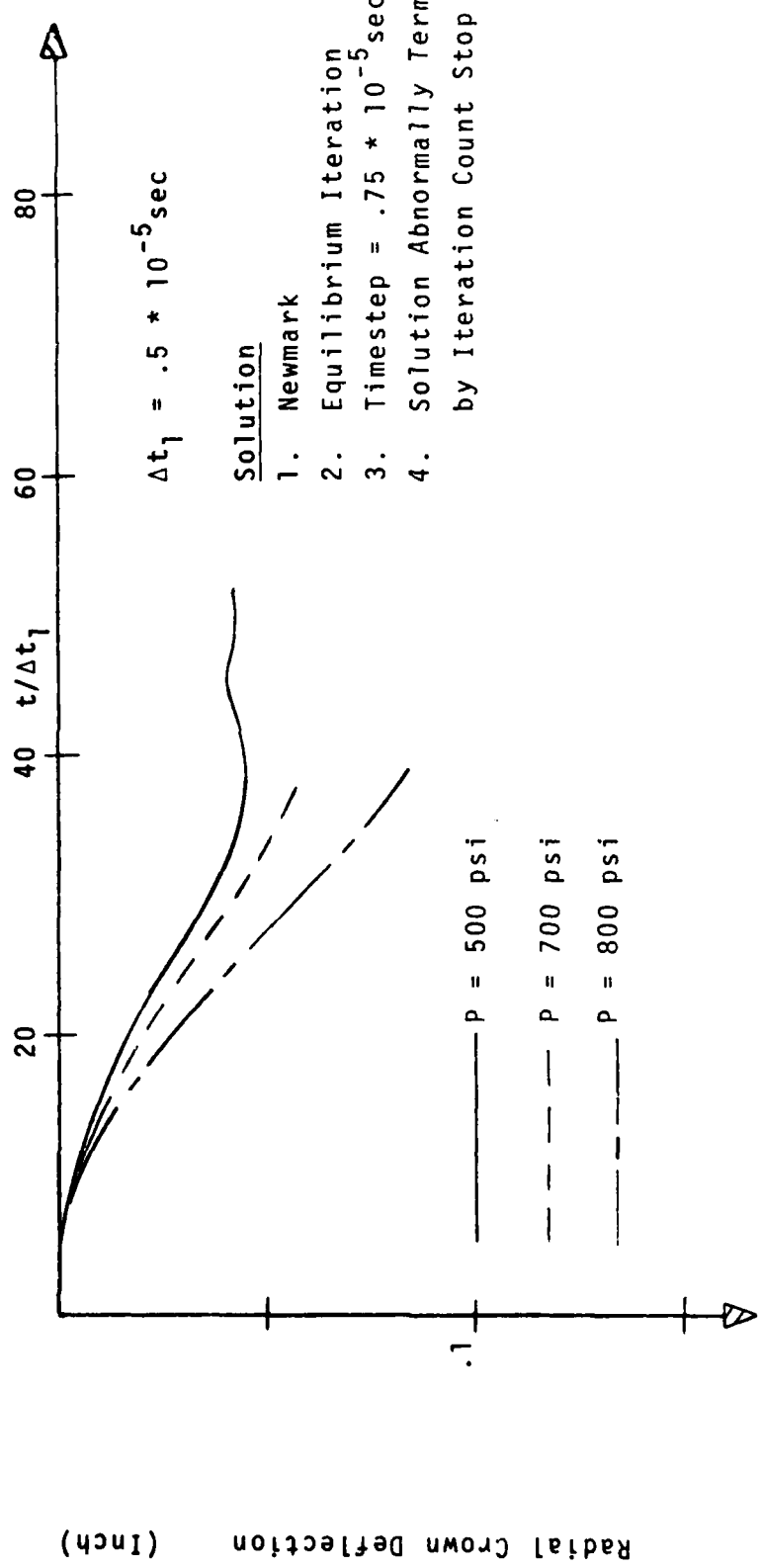
Fig III. 47   Dynamic Response of Spherical Cap Subject to Step Pressure Loading
("Moderate" Nonlinearity Excited)
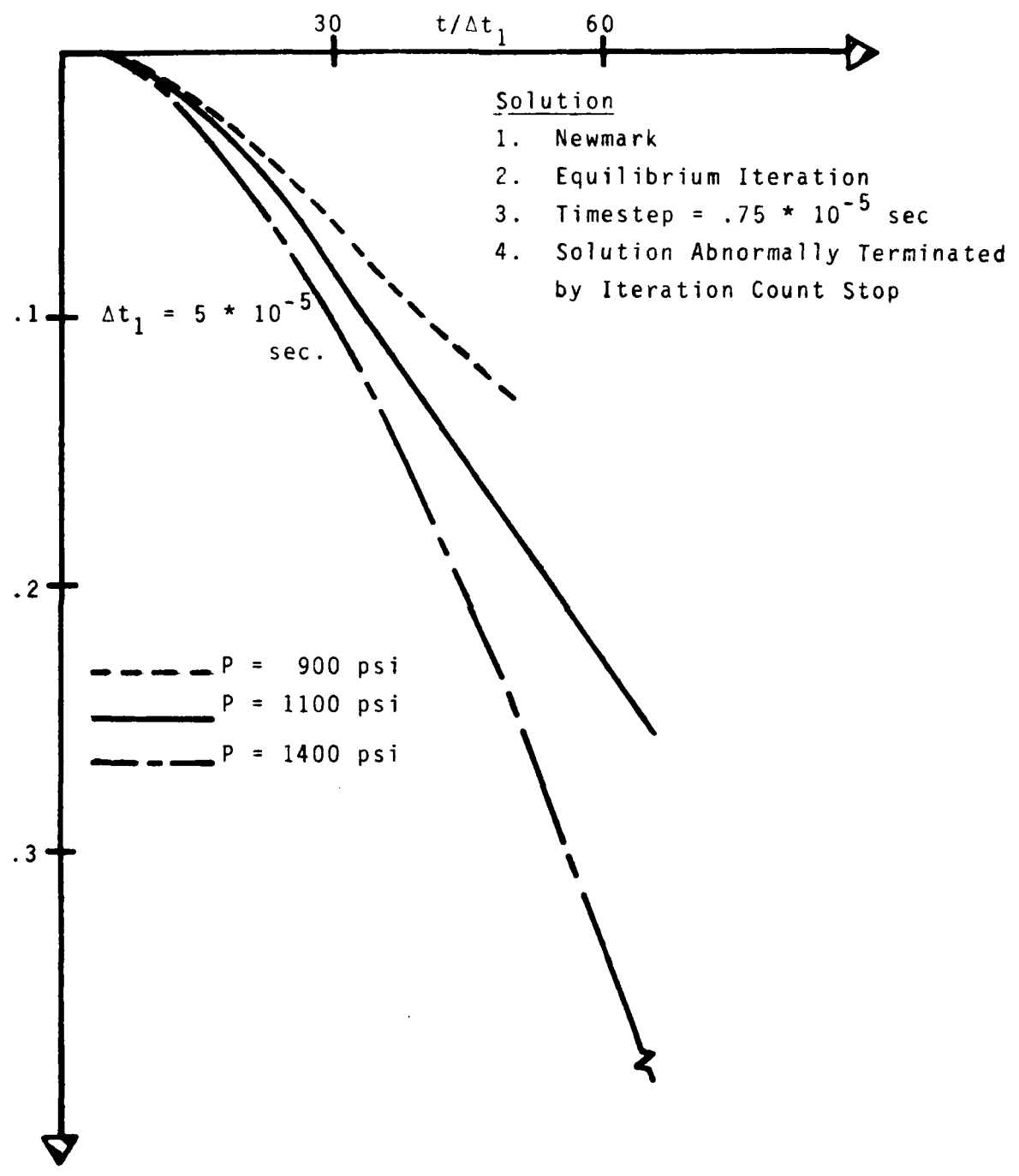
Fig. III.48  Dynamic Response of Spherical Cap to Step Pressure
Load ("Strong" Nonlinearity Excited)
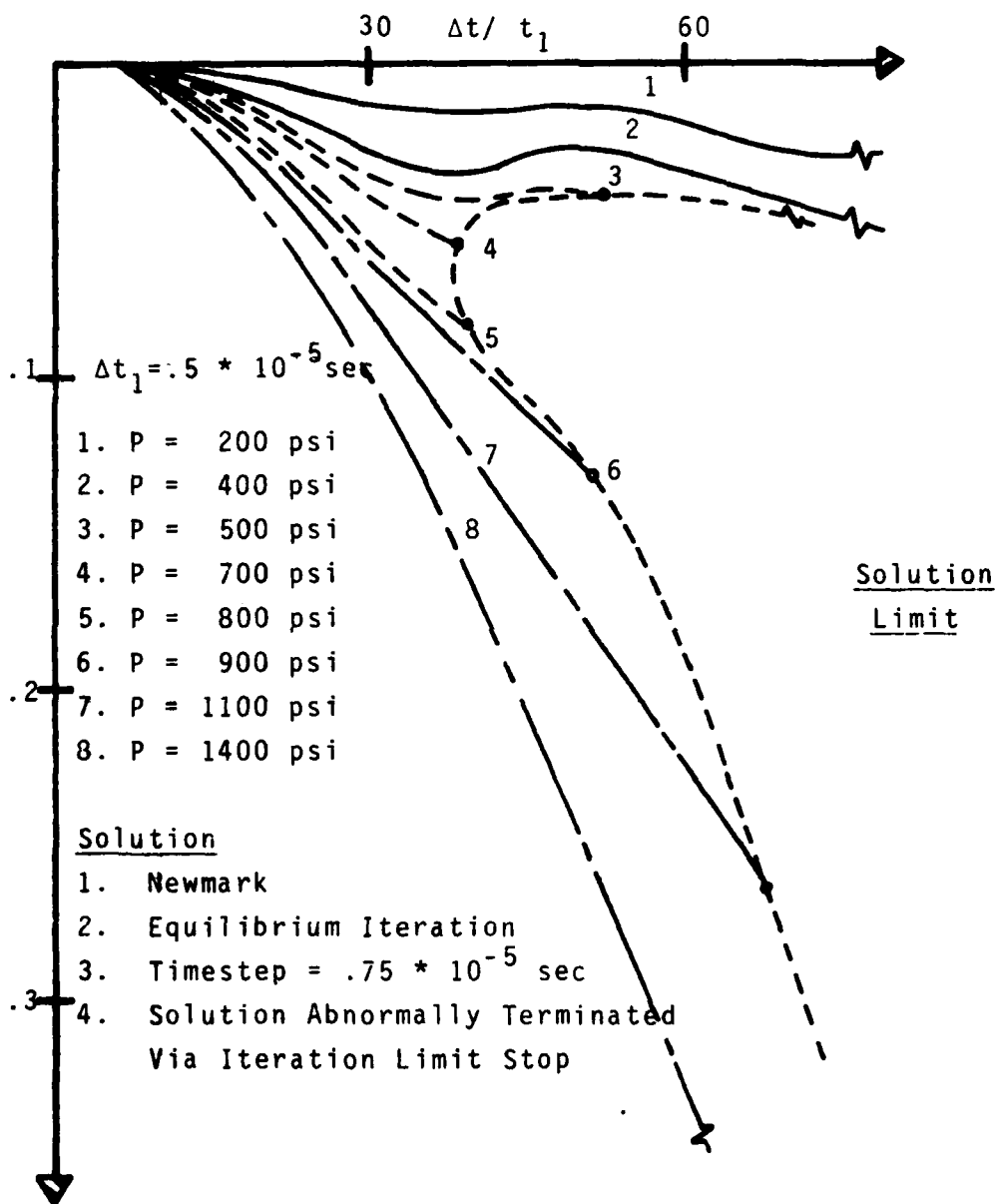
Fig. III.49   Abnormal Solution Limits for Dynamic Response of
Spherical Cap to Step Pressure Loading ('Mild",
"Moderate", and "Strongly" Nonlinear)

situations, the higher order spectral modes and the material/ geometric nonlinearity combine to cause an extensive amount of iterating to capture the overall solution. Because of this, as can be seen from Fig. 47, solution failure is initiated because of out of iteration stops. For such situations, generally any attempt to increase the number of iterations tends to fail since typically an extremely large number of steps is required. This is partially an outgrowth of the local wavyness of the solution space caused by the presence of higher order spectral modes.

For the given time size, a further increase in loading tends to excite significant amounts of plastic flow. Since such behavior causes extensive amounts of structural softening and irreversible energy conversion, much of the higher order spectral modes tend to be washed out before unloading occurs at the first cycle limit. Because of this, interestingly the solution tends to progress further before the out of iteration stop is excited. This behavior is clearly illustrated in Fig. 48.

The three stages of solution noted earlier are clearly seen from the juxtaposed results depicted in Fig. 49. Such behavior was obtained for both the Newmark and Wilson integration options.

Note, further dynamic benchmarking involving different geometries and material properties tended to initiate similar solution pathologies to those depicted by the foregoing problems. As with the static solution branch, such anomalous behavior does not appear to be generic to ADINA. Rather it

appears to be intrinsic to the tangent stiffness MNR algorithm itself. In particular, this algorithm appears to be sensitized by the interactions between structural nonlinearity and inertial effects. For moderately nonlinear problems, such factors combine cause a "wavy" solution space which tends to sensitize the tangent stiffness approach. For materials which are highly dissipative, such behavior is somewhat smoothed out as the nonlinearity is further increased.

### III.2c  Eigenvalue/Vector Extraction Algorithms

The main thrust of this subsection is to determine the computational characteristics of the eigenvalue/vector extraction algorithms inherent to ADINA (1977). In particular this will include considering such factors as the convergence properties, eigenvalue/vector deterioration and multiplicity/ separability characteristics.

To achieve these objectives, the benchmarking employed must be capable of testing the extraction algorithms for situations involving arbitrary eigenvalue spacing. In this context, the algorithmic check out considered the following types of situations namely

1. Widely-spaced frequencies;

2. Closely-spaced frequencies;

3. Widely space groups of closely spaced frequencies and;

4. Multiple frequency branches

The foregoing scenario of frequency spacings are typical of modern day support structure. The most complicated of

these usually involve main structures which have soft or stiff substructural components. Typically such components tend to lead to the occurrence of widely spaced groups of closely arranged frequency eigenvalues. For instance, supported symmetric structures are good examples of such a situation. This follows from the fact that symmetric structure in themselves usually have multiple frequency branches. Supporting such structure on soft foundation supports tends to lead to an overall frequency spectrum involving essentially two groups of eigenvalues, namely;

1. Pseudo rigid body modes involving the main structure acting rather rigidly on soft supports and;

2. Main structural modes which have been separated by the presence of the supports.

Since such structure can be made to exhibit all of the eigenspacings denoted by 1) - 4), the family of benchmarks employed herein involved such a type structural arrangement.

Before describing the actual benchmarks employed, it is appropriate to note that in order to quantify potential eigenvalue/vector deterioration, a fairly extensive number of dependable eigenvalues must be available. In this context, the approach taken herein was to chose a structure which could be solved analytically and hence have any number of known eigenvalues and associated eigenvectors.

Figures III.50-52, show the overall family of configurations used for the evaluation of the eigenvalue/vector extraction algorithm. As can be seen, the main structure of
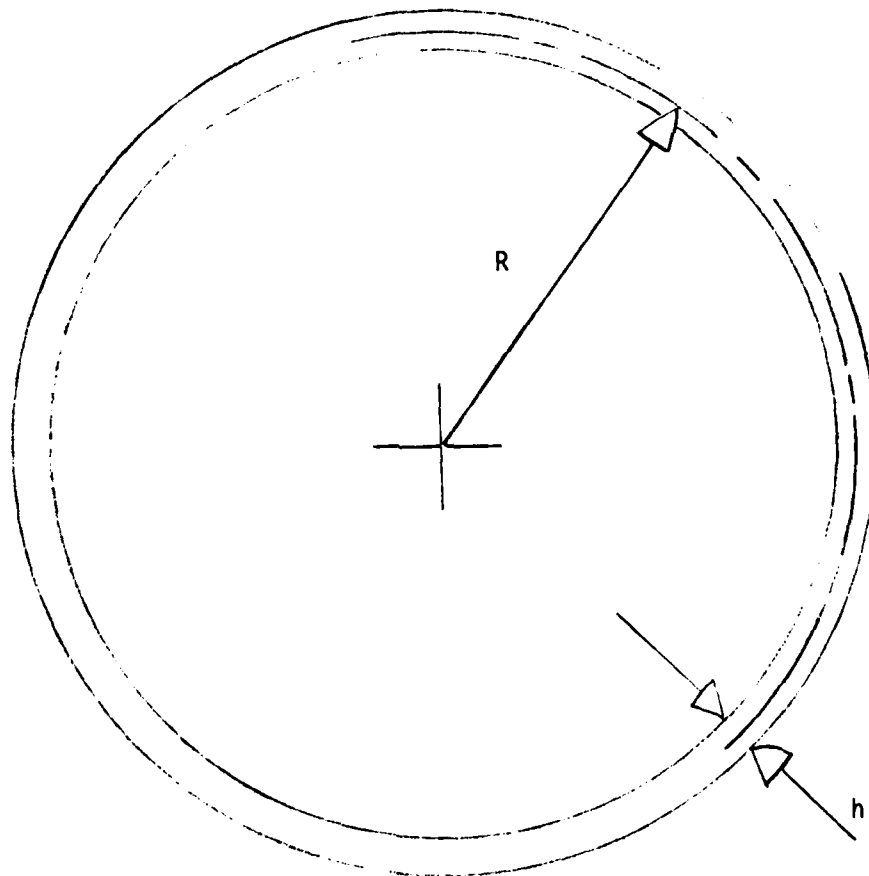
$$E = 10^8 \text{ psi} \qquad\qquad R = 15 \text{ inch}$$

$$\nu = .3 \qquad\qquad\qquad h = .1 \text{ inch}$$

$$G = E/2\ (1+\nu) \qquad \rho = .2588*10^{-3} \ 1b_m/in^3$$

Fig.III.50 Geometry of Ring

Elastic Foundation
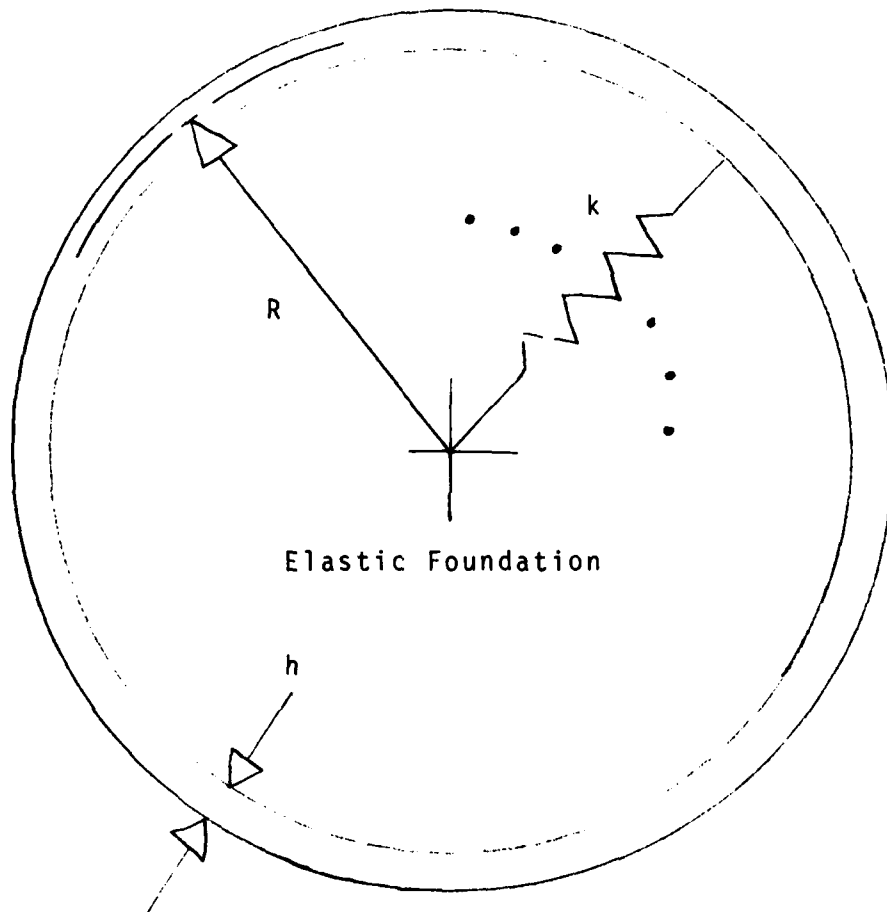
$E = 10^8$ psi          $R = 15$ inch

$\nu = .3$          $h = .1$ inch

$G = E/2\ (1+\nu)$          $\rho = .2588 * 10^{-3}$ lb$_m$/in$^3$

Fig.III.51 Geometry of Symmetrically Supported
Ring on Foundation

<u>Asymmetric Spring</u>

k

R

Elastic Foundation

h
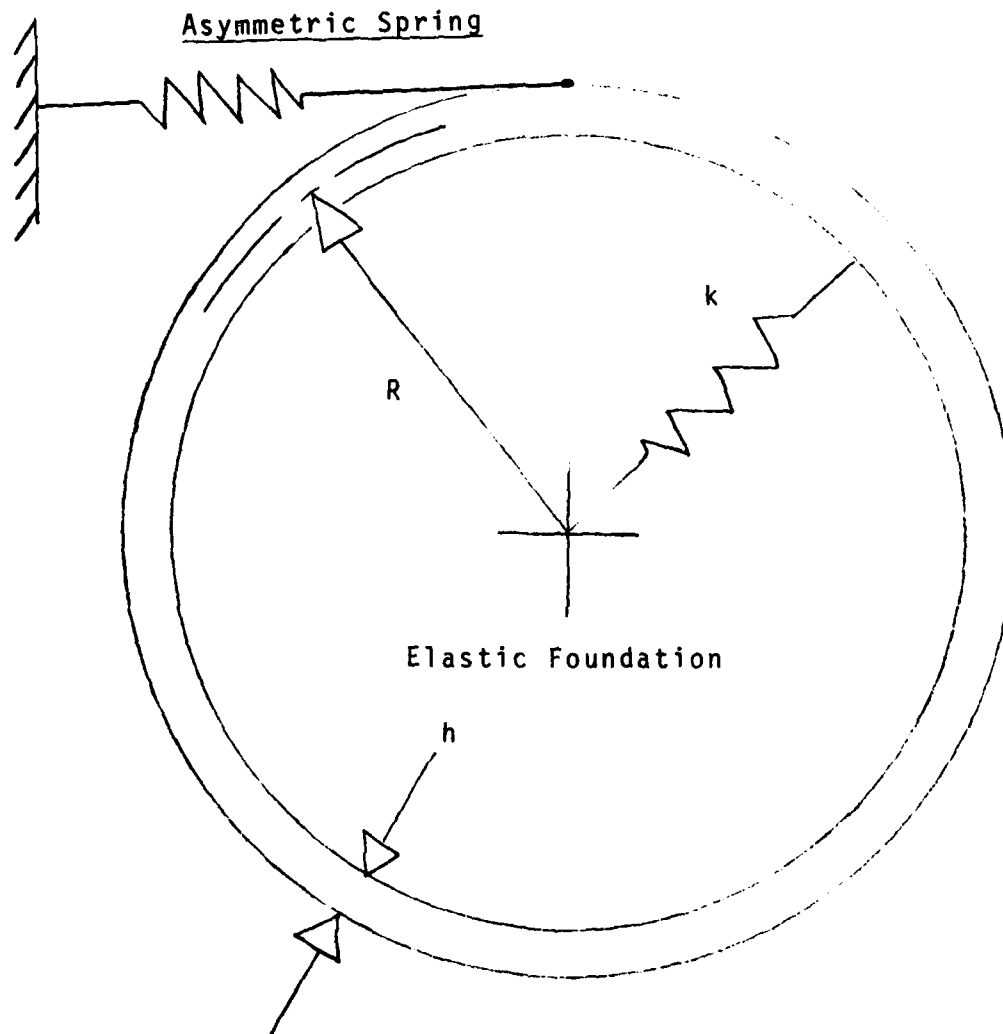
Fig.III.52Geometry of Asymmetrically Supported
Ring on Foundation

the family consists of a ring or long cylinder, Fig. III.50.
By attaching it elastically to ground via a series of radial
or tangential springs, a variety of symmetric or asymmetric
structure can be generated, Figs. III.51 and 52.

Note since the cylinder is itself axisymmetric, it
thus has multiple frequency eigenvalues of multiplicity two.
The spacings of the multiple pairs of eigenvalues of this
structure can be made to be either closely or widely spaced
depending on its radius to thickness ratio.  Such spacings
can be enhanced by attaching the cylinder to ground via a
symmetric radial spring support, Fig. III.51.

In terms of this structure, the problem of widely spaced
groups of closely/widely spaced frequency pairs can be gene-
rated by introducing asymmetrically placed tangential spring
supports as depicted in Fig. III.52.  Through the introduc-
tion of the asymmetric support springs, the multiple frequency
pairings can be made to bifurcate into separate frequency
branches.  The spacing between such branches can be made to
increase or decrease depending on the amount of asymmetric
stiffness introduced.

The choice of the foregoing benchmark family enabled a
logical and organized approach to be taken for the problem
of evaluating convergence properties, eigenvalue/vector de-
terioration and multiplicity/separability characteristics.
In performing the aforementioned benchmarking activities,
the following factors were monitored during the calculation
flow, namely:

1. The required number of iterations per eigenvalue;

2. The convergence characteristics of the eigenvalues and eigenvectors and;

3. The overall solution pathologies as the iteration process proceeded from low to high frequencies.

The first benchmark employed to study the capabilities of the extraction algorithm consisted of the cylinder on radial foundation depicted in Fig. III.51. In addition to monitoring convergence and deterioration properties, this benchmark enabled the evaluation of the multiplicity characteristics. To determine the eigenvalue/vector deterioration pathology, the cylinder was modelled by various number of elements involving either 80, 160, 300, 600 or 1000 nodes. Figure III.53 illustrates a typical mesh employed in the parametric study. Based on such models, the eigenvalues and associated vectors were calculated. In all the cases studied, the convergence characteristics were excellent. Additionally, once eigenvalue or vector deterioration was noted by comparisons to theoretical values, such pathologies could almost always be directly attributed to mesh inadequacy for the given mode.

For example, natural frequencies were obtained for a 160-element model (Fig. III.53) to illustrate the deteriorated multiple root eigenvalue family. The mode shapes associated with these multiple eigenvalues are depicted in Figs. III.54-67. As can be seen from the results illustrated, the modal and eigenvalue deterioration can be directly attributed to the lack of mesh adequacy for higher order modes.
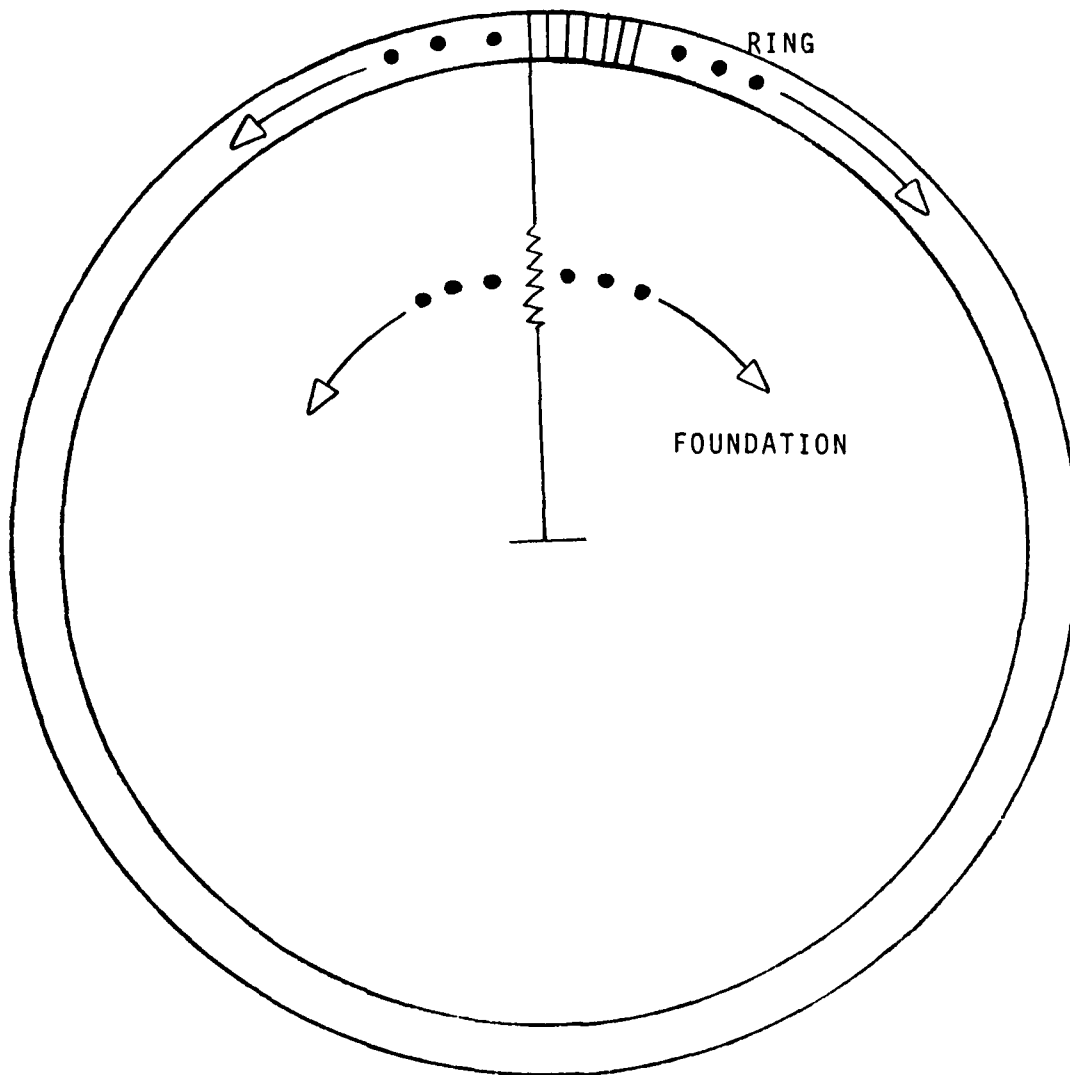
Fig III. 53    Finite Element Model of Ring on Elastic
Foundation (160 - 8 Node Elements)
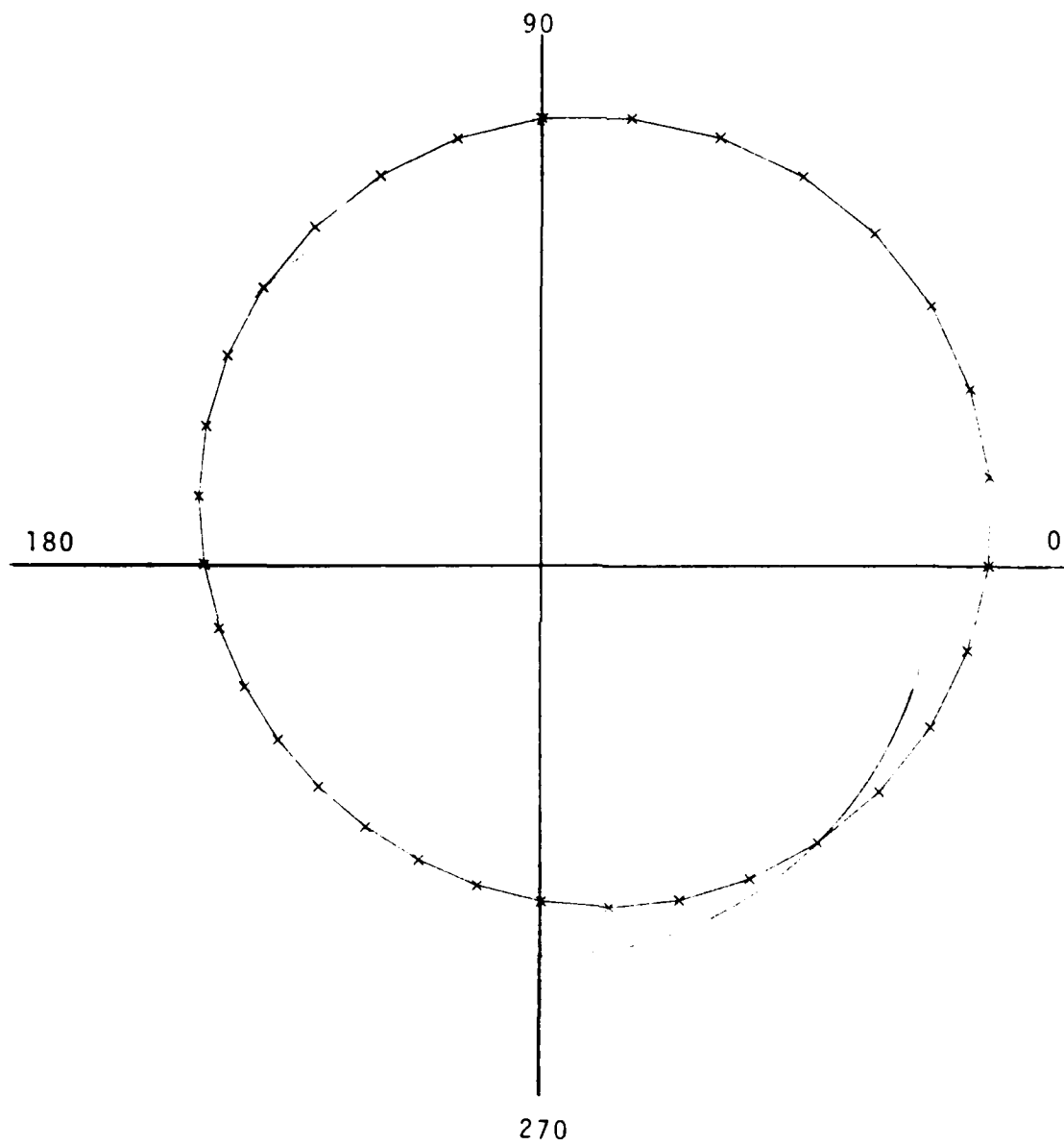
Fig. III.54  Radial Mode Shape; M = 1; $\omega_1$ = 1042 $\frac{rad}{sec}$
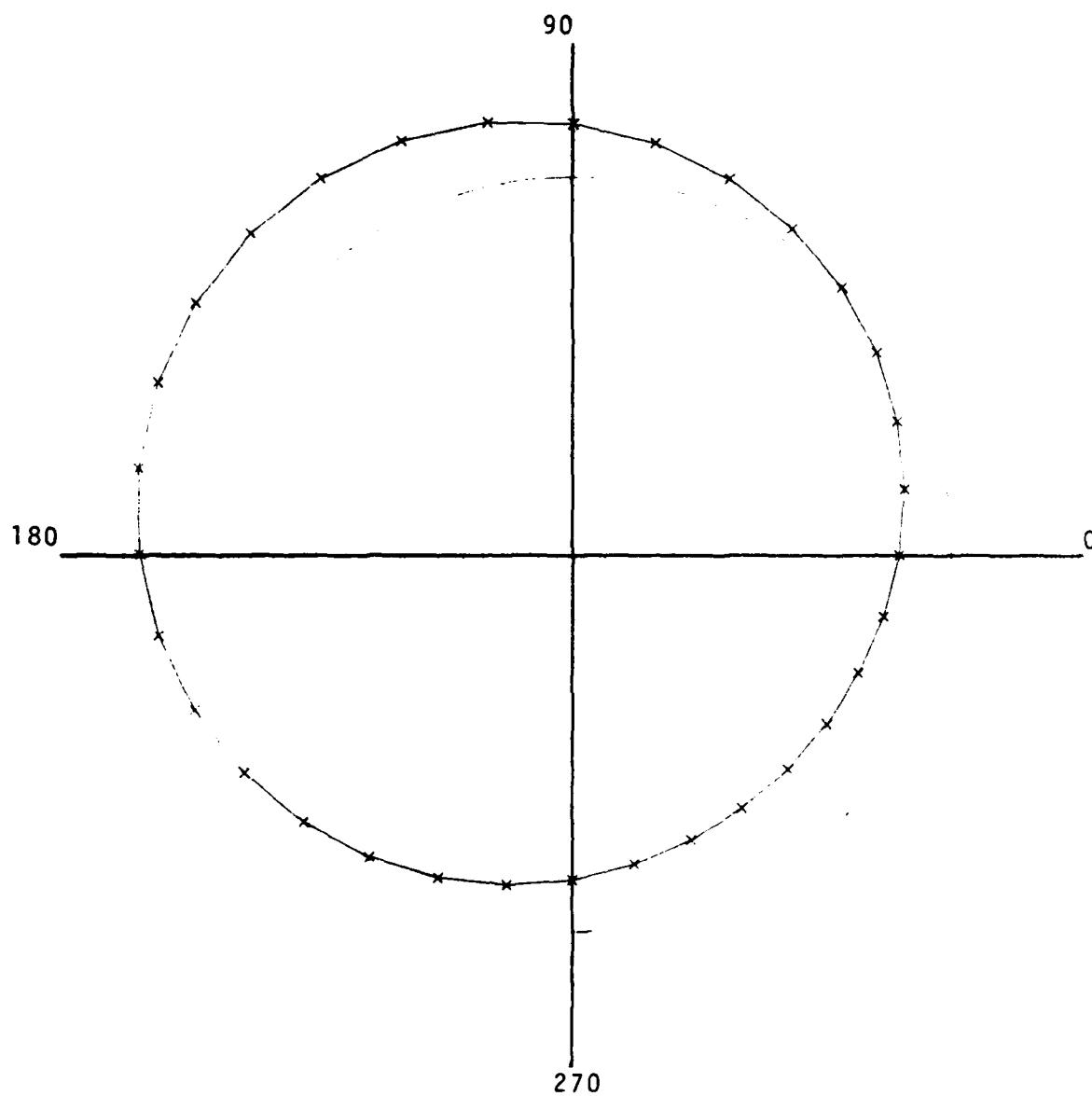
Fig. III.55 Radial Mode Shape; $M = 1$; $\omega_1 = 1042 \frac{rad}{sec}$
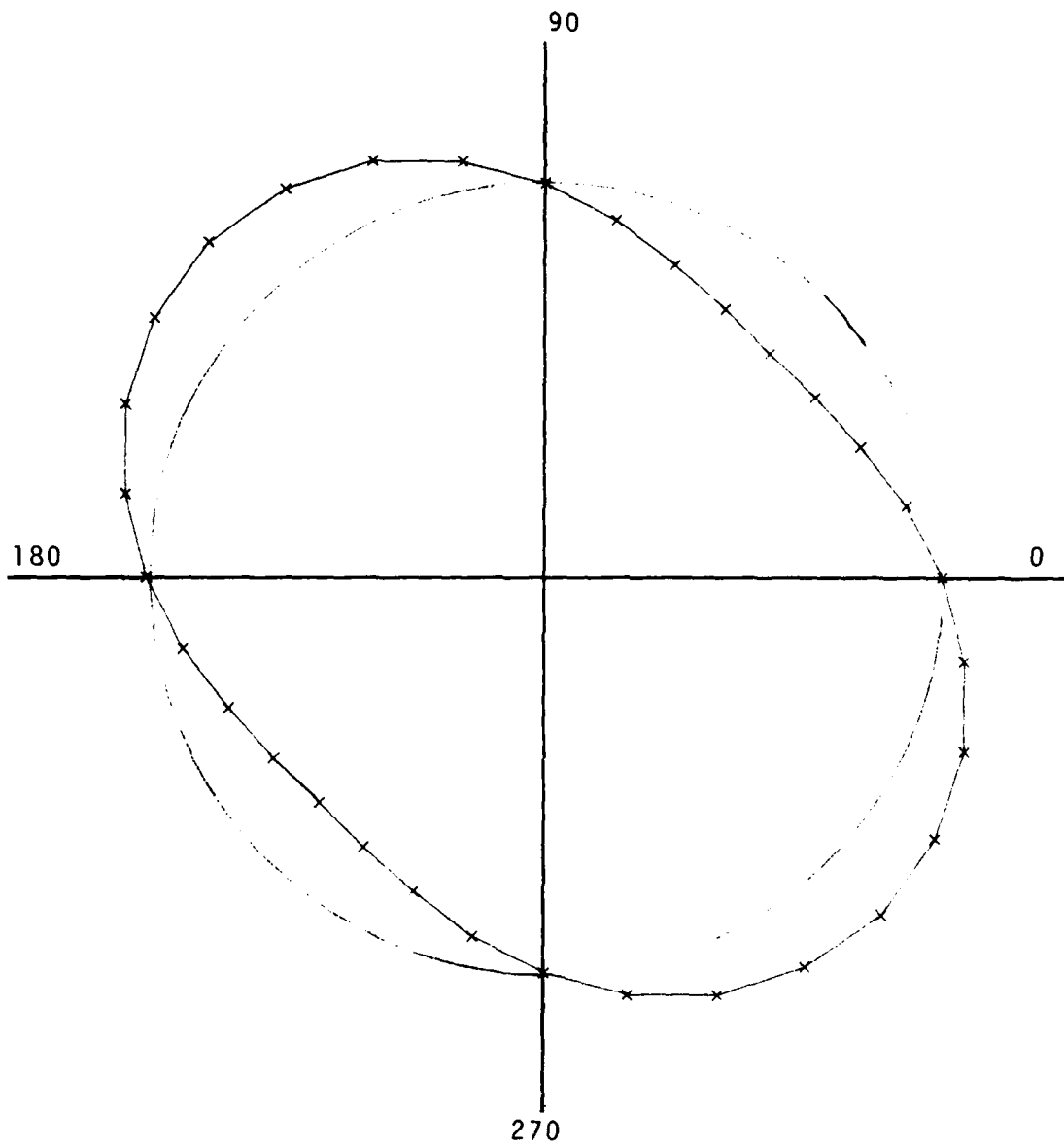
Fig. III.56 Radial Mode Shape; M = 2; $\omega_2$ = 1663 $\frac{rad}{sec}$
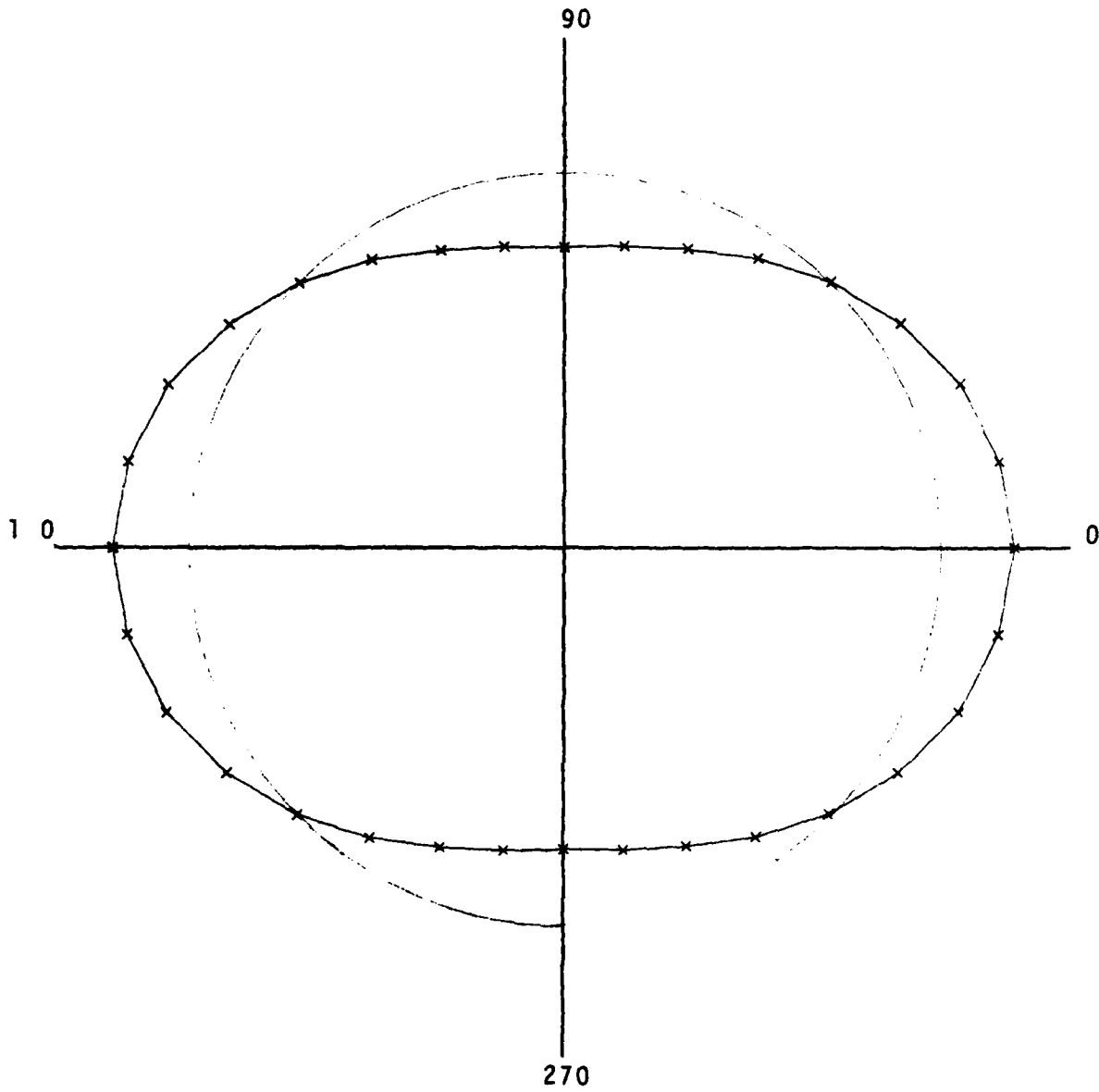
Fig.III.57 Radial Mode Shape; M = 2; $\omega_2$ = 1663 $\frac{rad}{sec}$
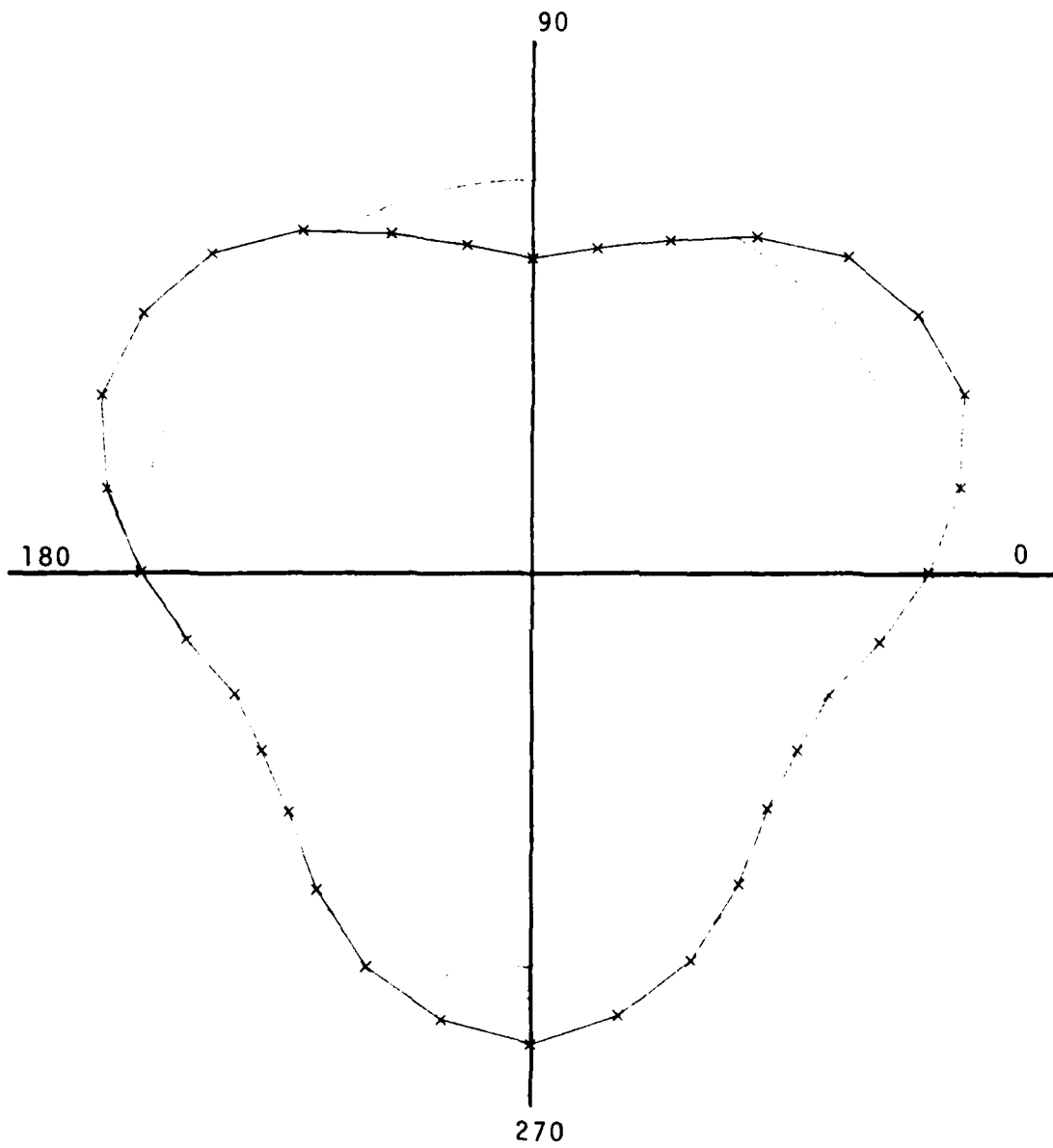
Fig.III.58 Radial Mode Shape; M = 3; $\omega_3$ = 2230 $\frac{rad}{sec}$
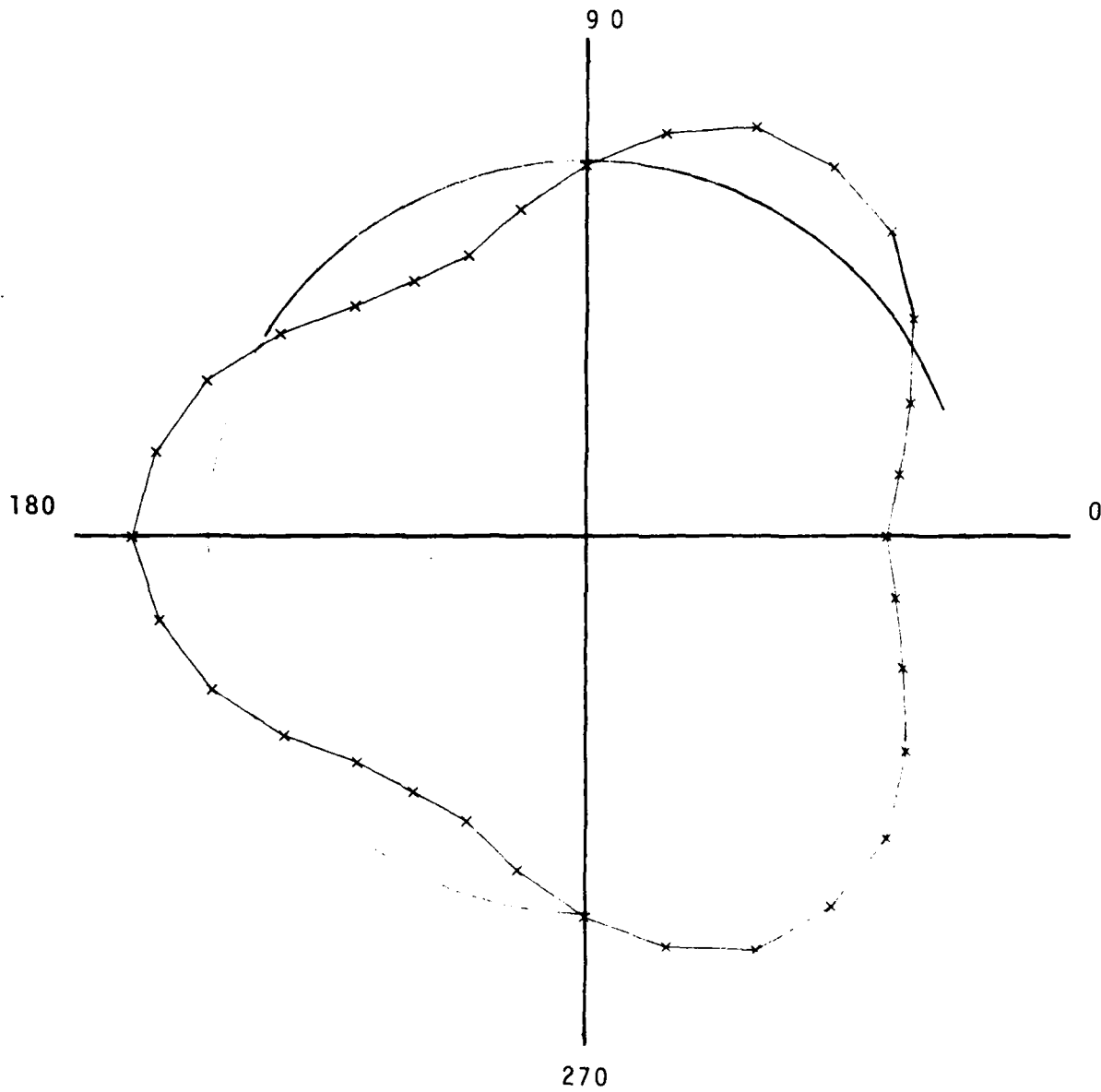
Fig.III.59 Radial Mode Shape; M = 3; $\omega_3$ = 2230 $\frac{rad}{sec}$
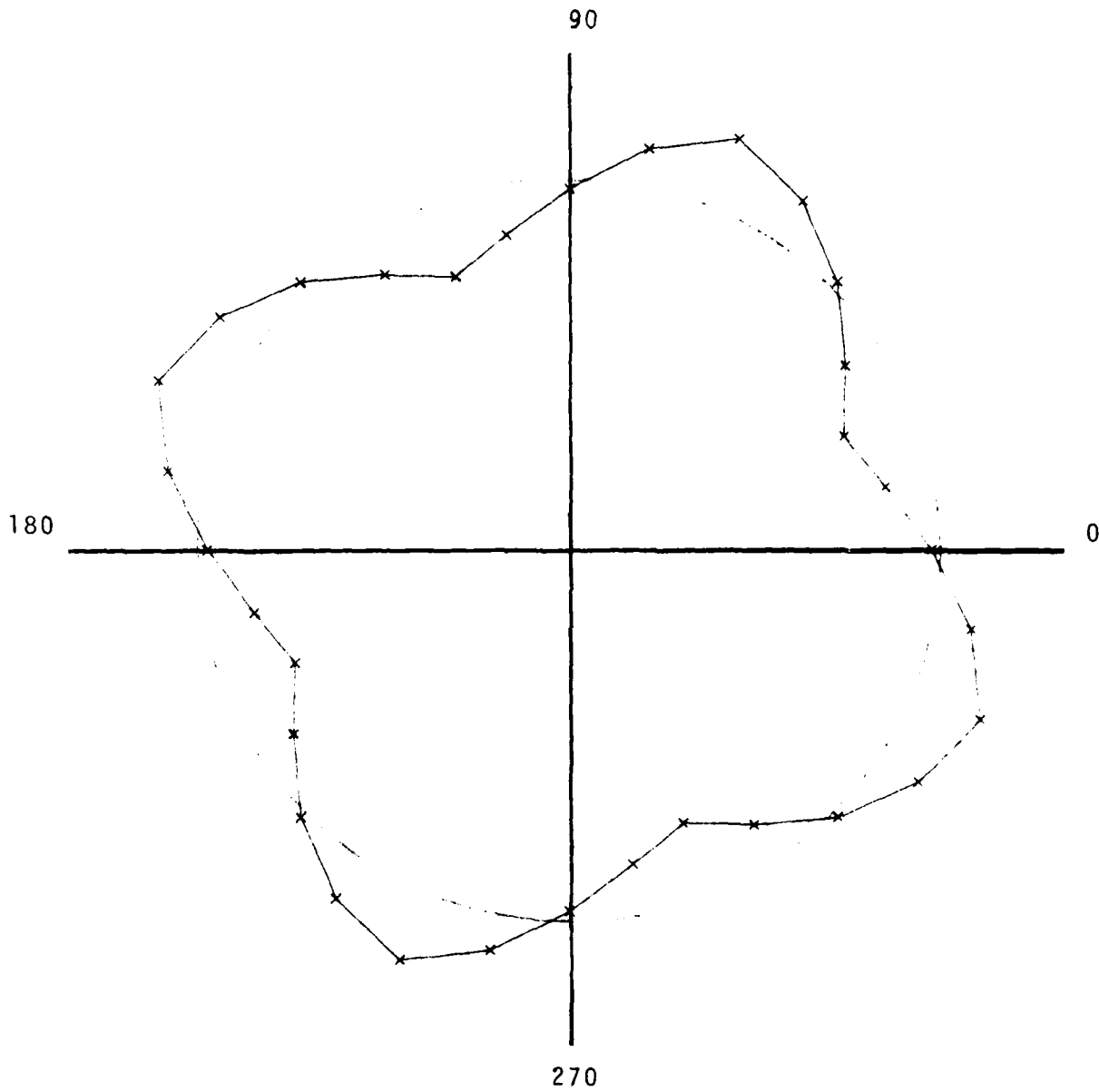
Fig. III.60 Radial Mode Shape; M = 4; $\omega_4$ = 2784 $\frac{rad}{sec}$
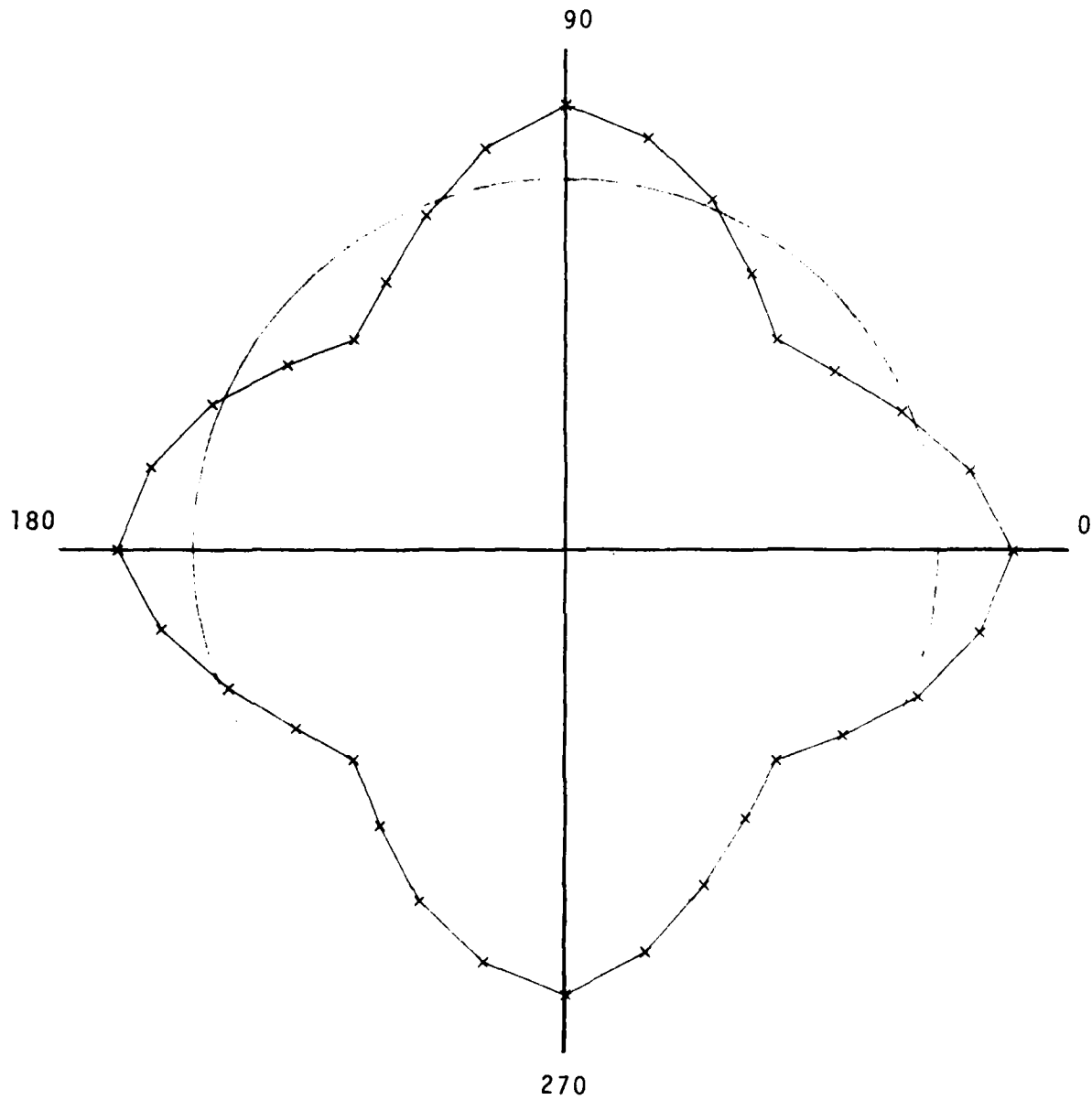
Fig. III.61 Radial Mode Shape; $n = 4$; $\omega_4 = 2784 \frac{rad}{sec}$
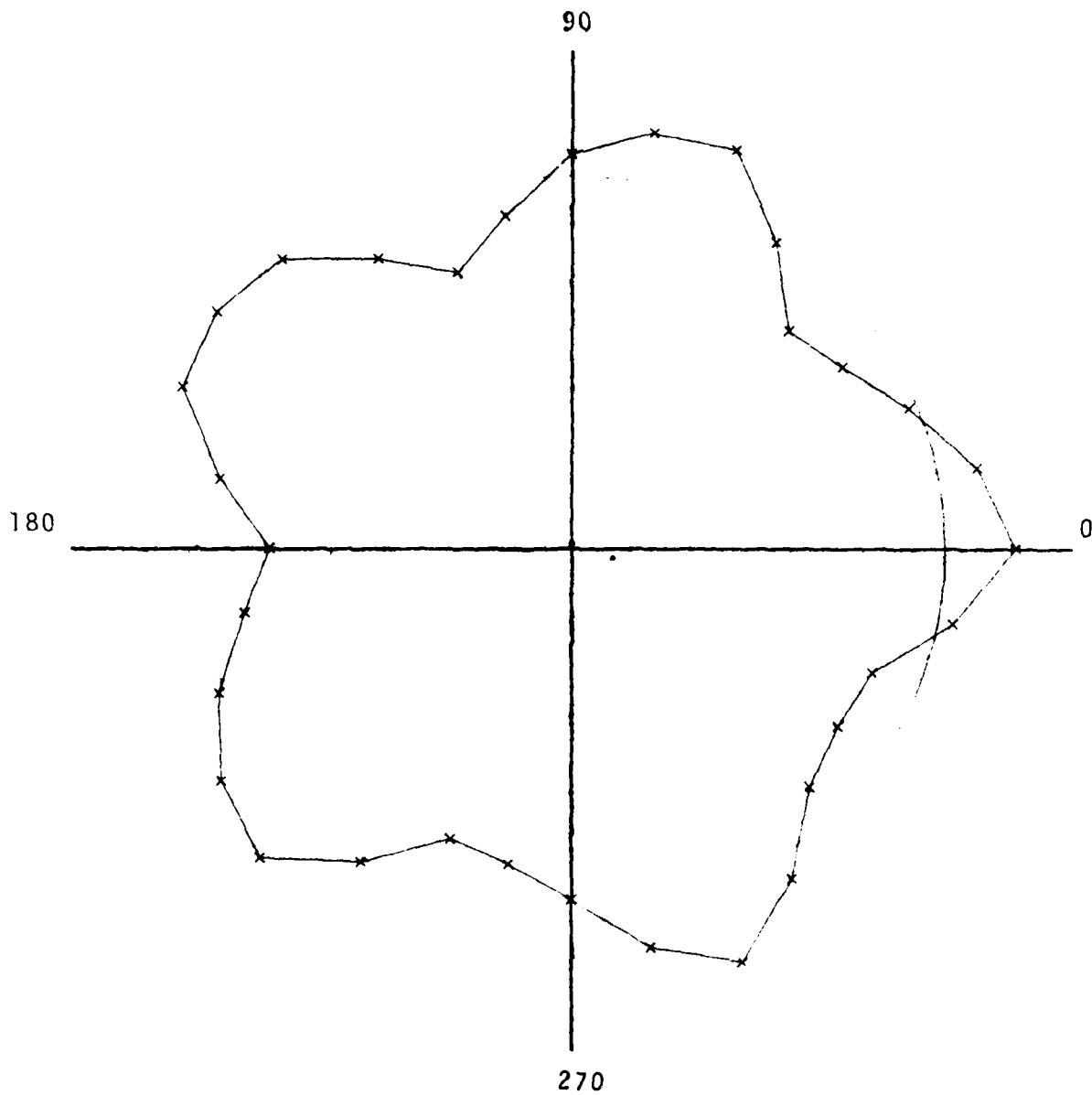
Fig. III.62 Radial Mode Shape; M = 5; $\omega_5$ 3302 $\frac{rad}{sec}$
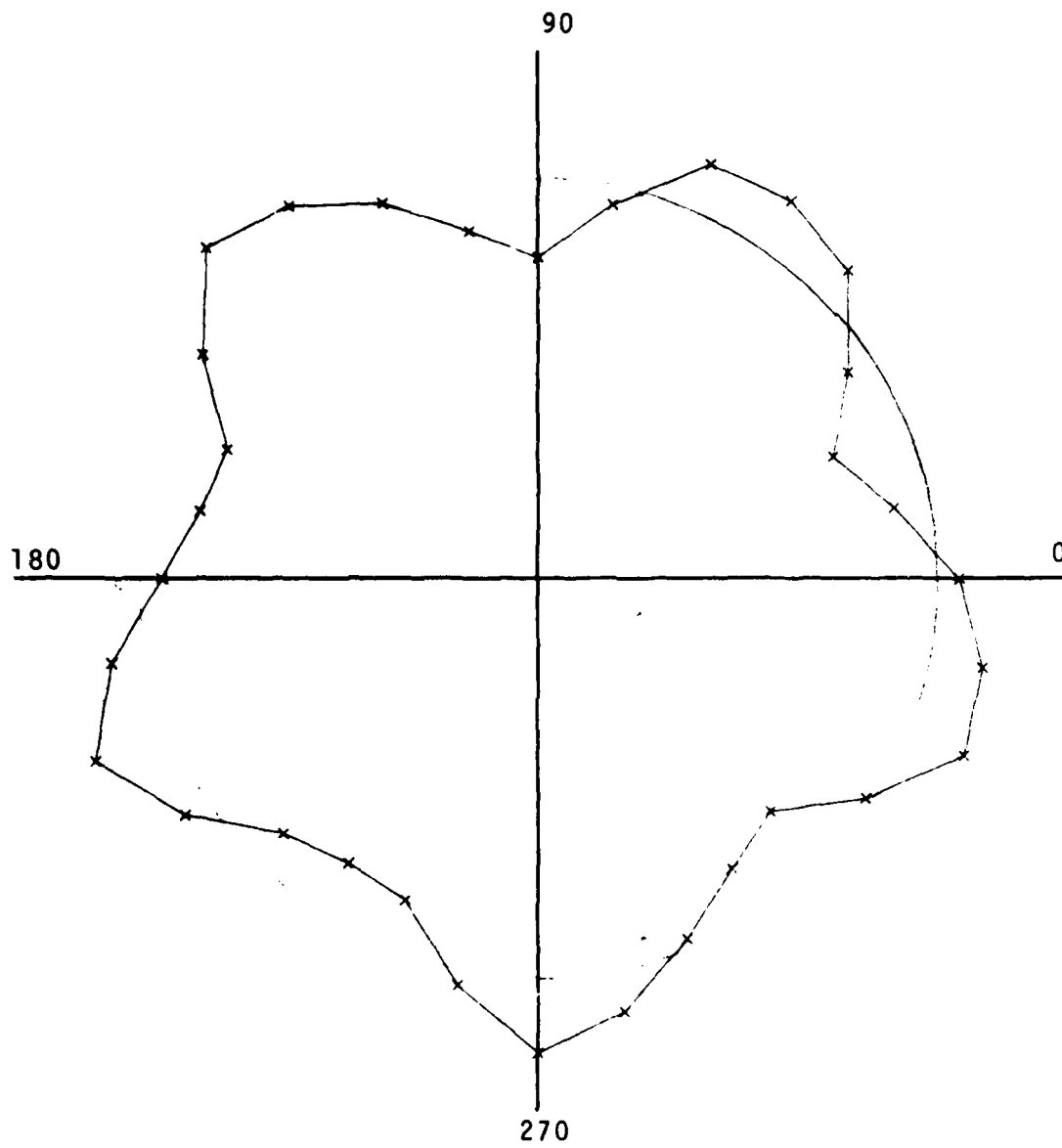
Fig.III.63 Radial Mode Shape; M = 5; $\omega_5$ = 3302 $\frac{rad}{sec}$
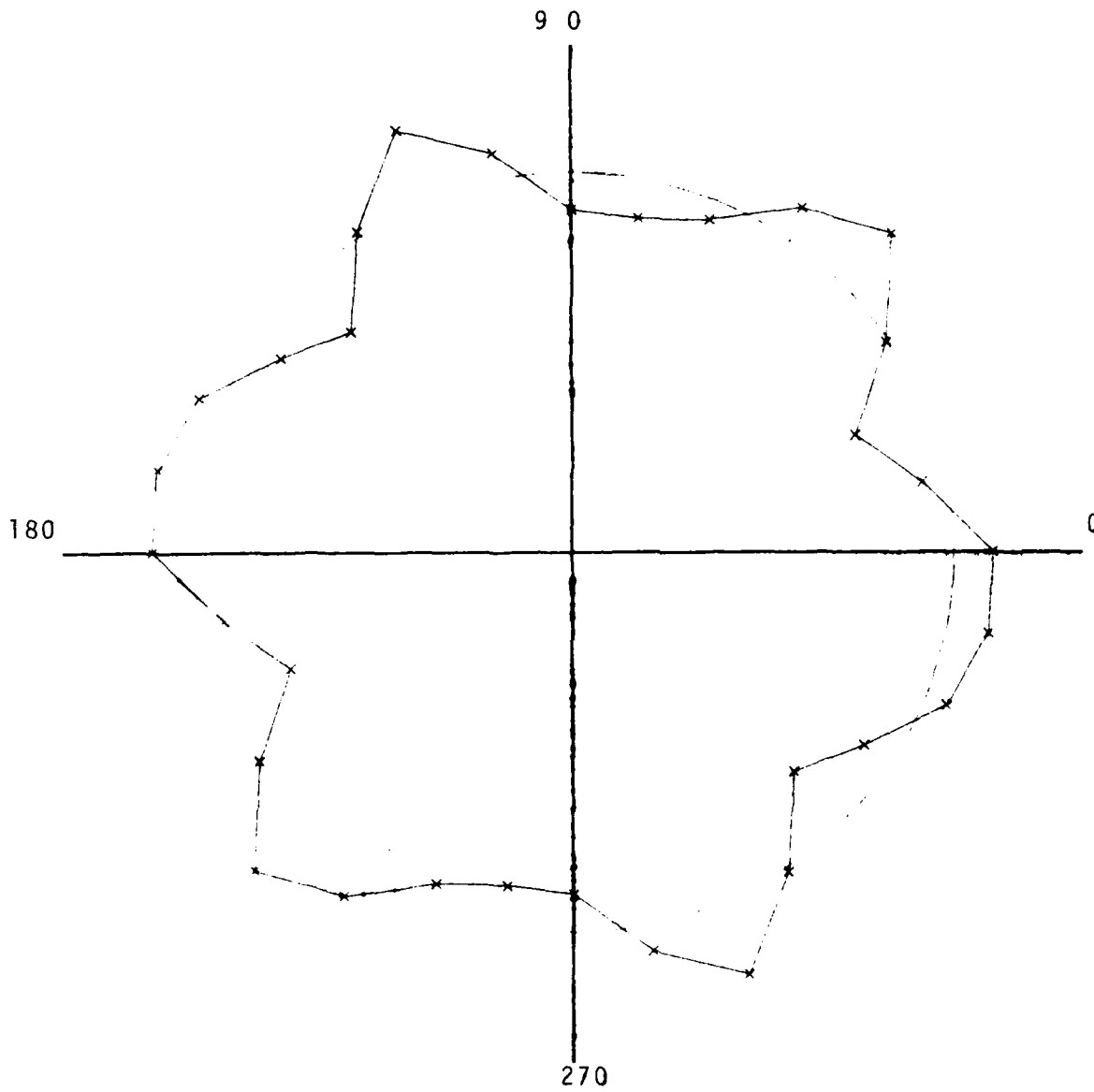
Fig.III.64 Radial Mode Shape; M = 6; $\omega_6 = 3744 \frac{rad}{sec}$
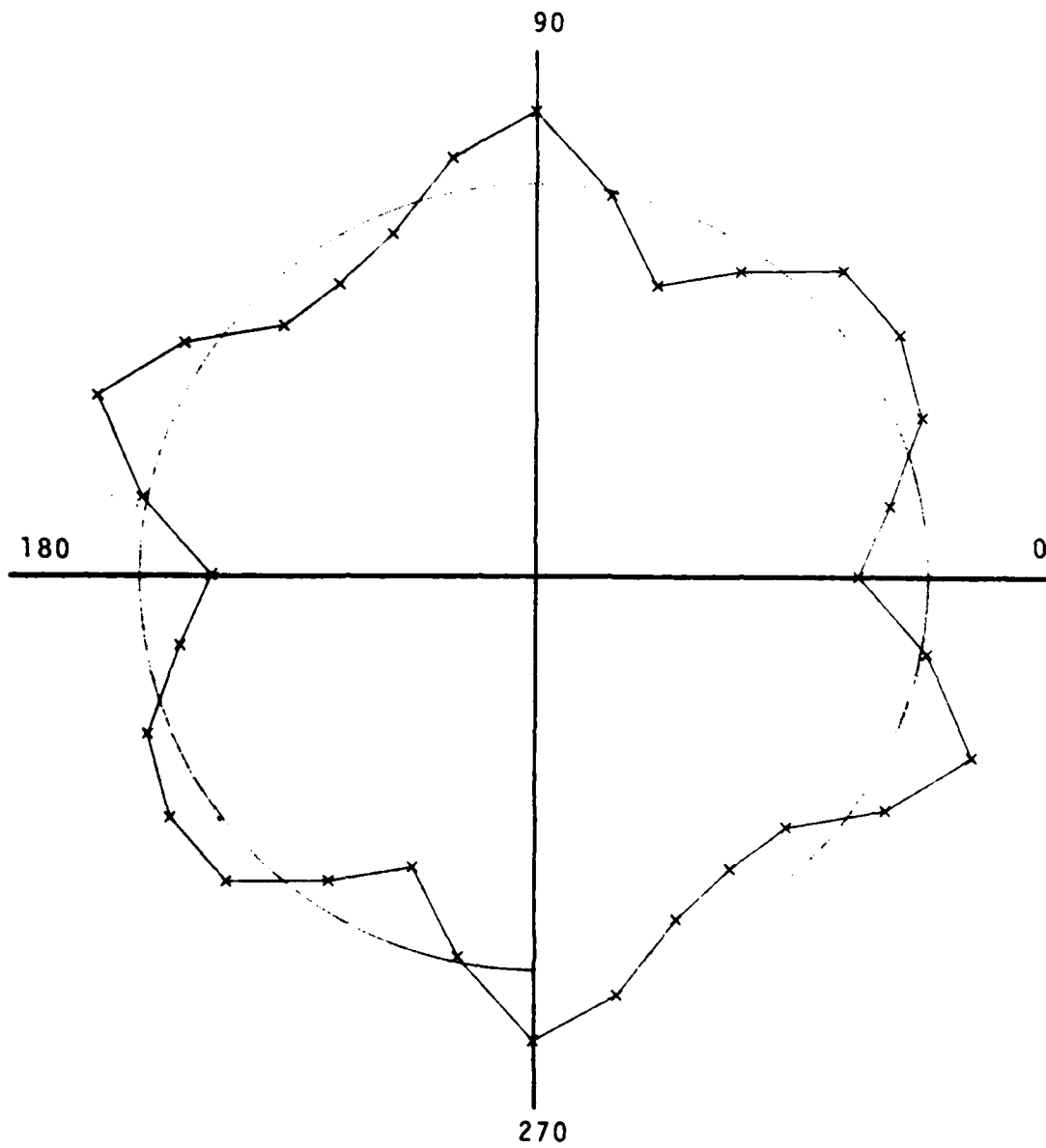
Fig.III.65  Radial Mode Shape; M = 6; $\omega_6$ = 3744 $\frac{rad}{sec}$
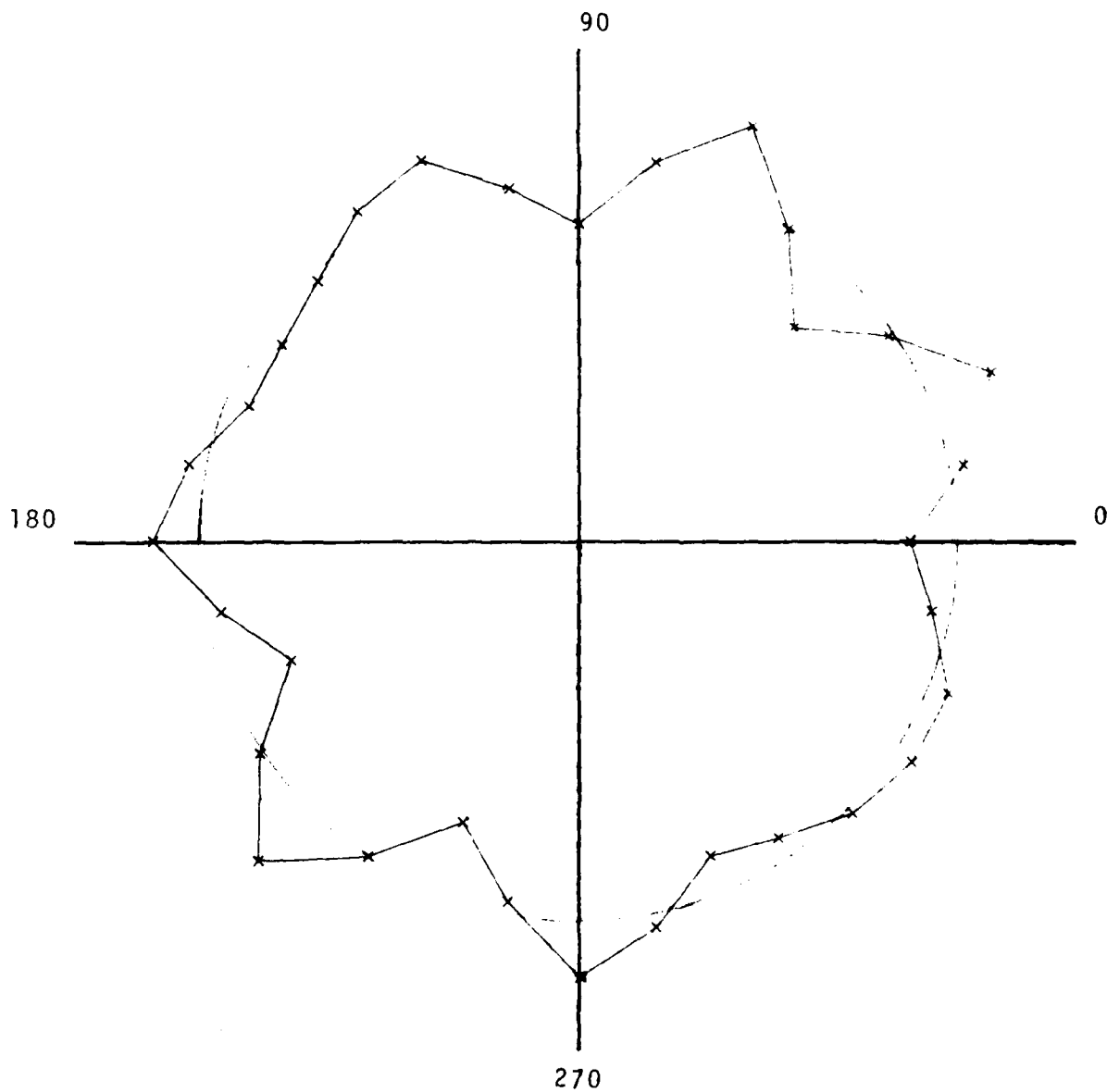
Fig. III.66 Radial Mode Shape; $M = 7$; $\omega_7 = 4054 \frac{rad}{sec}$
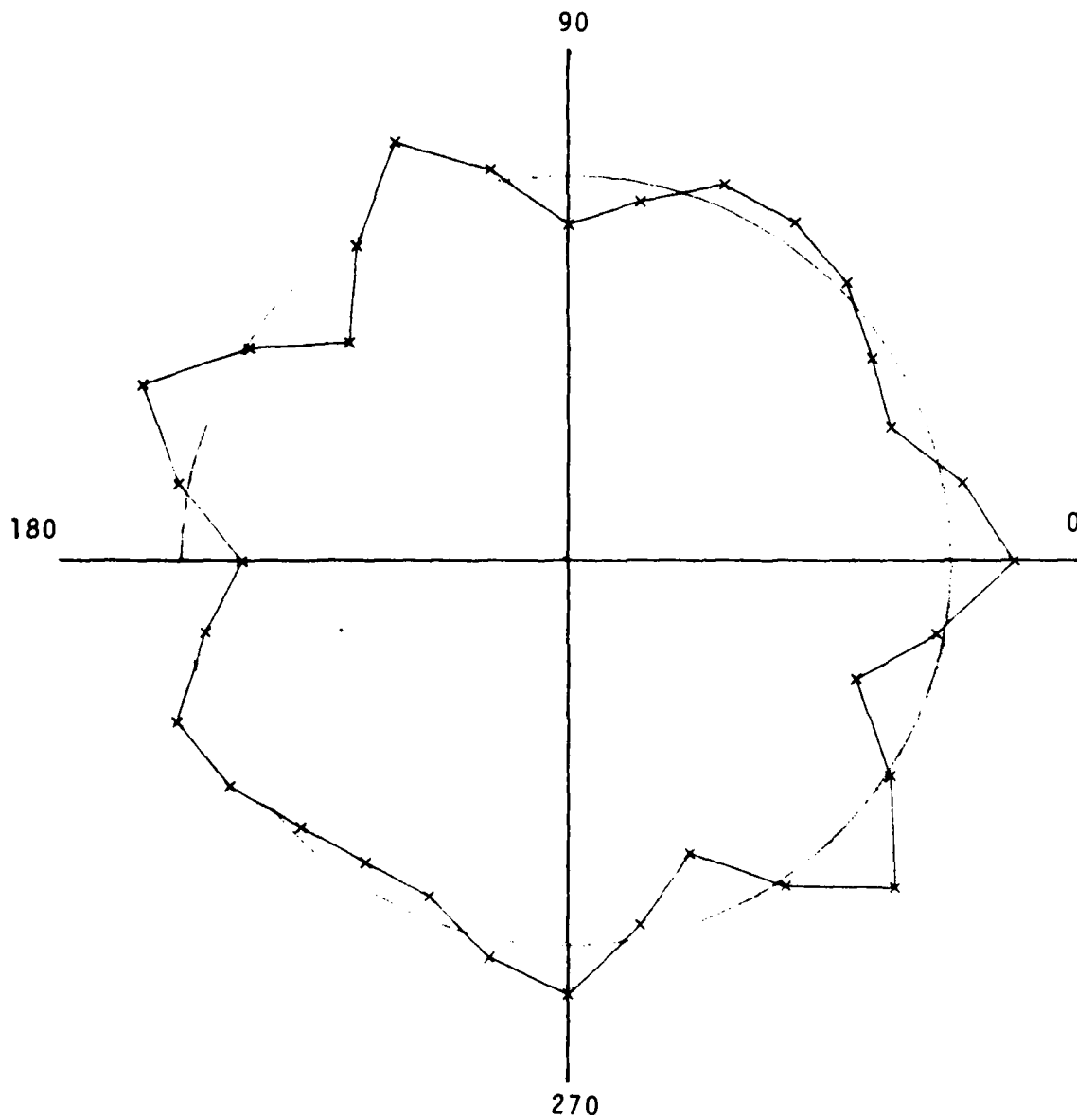
Fig.III.67  Radial Mode Shape; M = 7; $\omega_7$ = 4054 $\frac{rad}{sec}$

The only difficulties encountered with this benchmark involved problems with large numbers of elements. For such cases, as noted by the ADINA manual itself, the out of core solution proved somewhat costly. This can be directly attributed to the necessity of using low speed storage (disks) reads and writes to pack and unpack the various blocks of the global stiffness matrix.

Figure III.52 illustrates the asymmetrically supported cylinder. By adjusting the various foundations of this model, the eigenvalue spacing was varied over an extensive range of separations. This enabled a further evaluation of the multiplicity and separability characteristics. As in the previous case, the cylinder was modelled by various numbers of elements involving either 80, 160, 300, 600 or 1000 nodes. In the parametric studies performed with these models, the convergence characteristics were good for all the ranges of separability tested. Whenever eigenvalue or vector deterioration was encountered, it could generally be attributed to the lack of model accuracy. Namely, the lack of proper numbers of elements required to adequately define a given mode shape.

As a consequence of the foregoing parametric benchmark studies, it follows that the ADINA eigenvalue/vector extraction algorithm has good convergence characteristics for most typically occurring ranges of frequency spacing. The only difficulties encountered were associated with out of core solutions wherein slow secondary storage was involved. Note by increasing the size of the dynamic allocation array, larger

in-core problems can be handled thus enabling faster run
times. This raises an interesting point concerning the
ADINA overlay structure and the MVS environment typical
of IBM systems. While such studies were not run, it would
be interesting to determine the advantages of totally in
core Vrs out of core solutions in an MVS storage environment.
In this regard, it was found that for the benchmarks run
for the study, the purely in core approach involving large
storage dynamic allocations ran faster than small dynamic
allocations involving the out of core option. While this
might seem obvious at first, it must be remembered that in
the MVS environment, portions of the program are paged in and
out of the central core during the course of running. Such
an operation can be likened to a machine generated overlay
structure. In this context, it would be worthwhile to de-
termine in future studies the pros and cons of in core vrs
out-of-core program architecture in an MVS environment.

### III.2d  Numerical Integration of Element Stiffness

In the evaluation of element stiffness for isoparametric
elements, the general practice is to use Gauss quadrature nu-
merical integration. Ordinarily, the degree of accuracy in
numerical integration is affected by the integration order cho-
sen consistent with the approximating shape functions used for
the element. For example, for an element of quadratic displace-
ment field, the exact numerical integration order is "3" [7].
However, the choice of integration order is also complicated by
other factors, i.e., variation of material properties over the

element (elastic-plastic material), incompressibility constraints,
presence of shear stresses in thin-wall structure, etc. In this
section, some numerical difficulty of the 3/D continuum element
is revealed when it is used for bending analysis.

The problem considered is a square plate simply supported
along its four edges, and constrained from horizontal motion in
the directions perpendicular to the edges of the supports. The
plate is subjected to a uniformly distributed load. Material
properties were assumed to be linearly elastic and isotropic, i.e.

$$\text{Young's Modulus} \quad E = 2.1 \times 10^6 \text{ Kg/cm}^2$$

$$\text{Poisson ratio} \quad \nu = 0.3$$

The 20 node 3/D continuum element was used to model the bending
action of the plate. From symmetry, only one quarter of the
plate was modeled by 9 elements with 96 nodes as shown in Fig.
68. The plate was loaded well into the large deflection range
so that membrane action of the plate became predominating. Seve-
ral computer runs were made by varying the thickness-ratio (or
aspect ratio, t/a) of the plate ranging from 0.1 to $10^{-5}$. For
each thickness ratio, two numerical integration orders were
chosen for the evaluation of element stiffness; namely, 3x3x2
(exact) and 2x2x2 (reduced) orders, two integration points in
the thickness direction for both cases. The load - deflection
responses of the plate with two different aspect ratios are plotted
in Figs. 69 and 70. In the analysis, the results obtained from
the exact integration order represent convergent solution under
equilibrium iterations are totally erroneous as seen in Figs.
69 and 70. On the other hand, the reduced integration scheme

gave a more satisfactory result as compared to the analytical solution [8]. The non-dimensionalized maximum deflection of the plate vs. various aspect ratios for the load factor $\frac{Pa^4}{Et^4}$=4.6,50, and 208 are plotted in Figs. 71 and 73, respectively. From these plots, one can clearly see that the use of 3/D continuum elements with exact integration order fails to give any reasonable solution for thin plates with an aspect ratio smaller than $10^{-3}$. In order to overcome this numerical problem, reduced integration order must be used for either small deformation or large deformation analysis. It is also noted that as the plate thickness becomes very thin (t/a less than $10^{-4}$), no solution can be obtained even the reduced integration was used.

## IV.  Potential Algorithmic Improvement

Finite element simulations of statically and dynamically loaded structures composed of general materials undergoing large displacements usually lead to nonlinear field equations. Since the types of nonlinearity exhibited by such field equations are both diverse and complex, the question of the best choice of an appropriate solution algorithm inevitably arises. While many alternatives are available, generally the various solution procedures may have special advantages for certain classes of problems but may exhibit poor

a = 60 cm

t = thickness
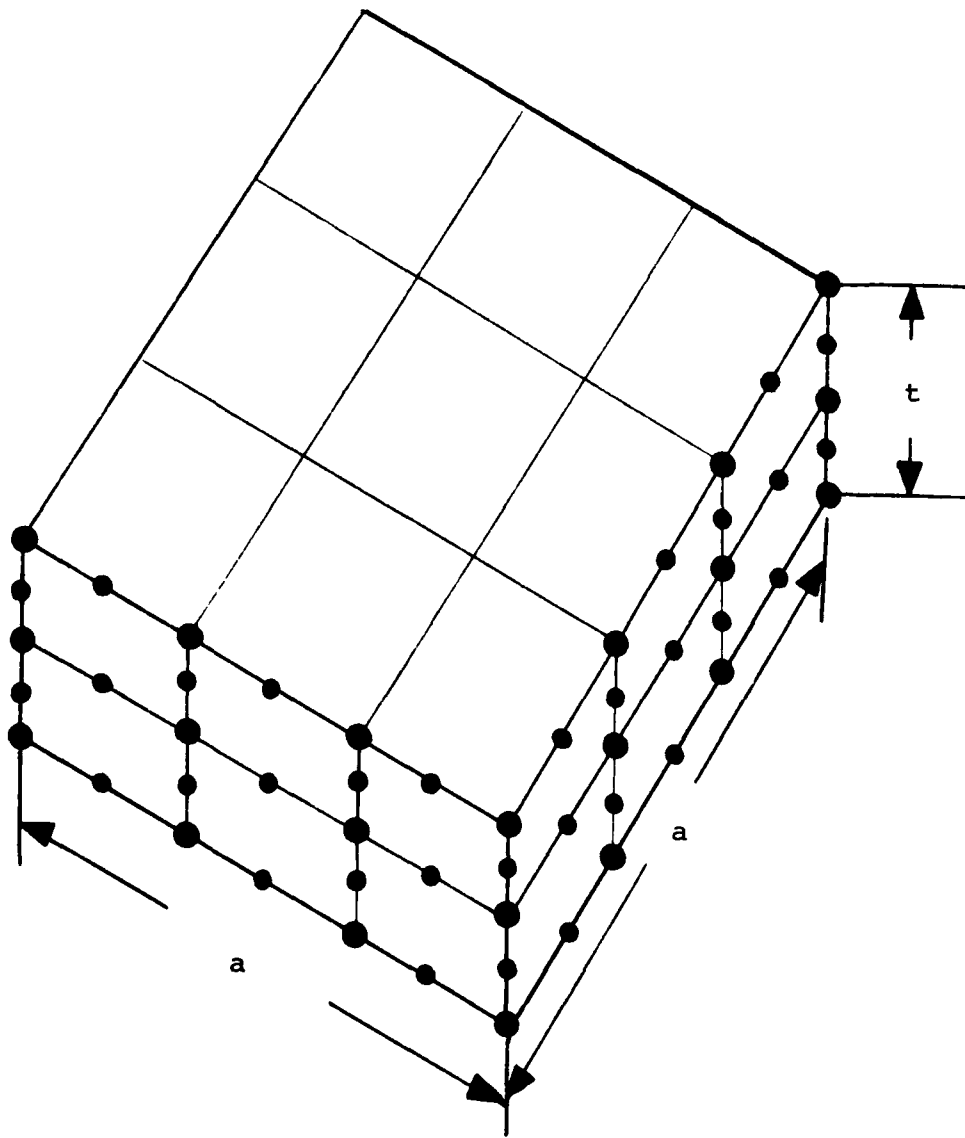


Fig. III.68 Finite Element Model for a Plate
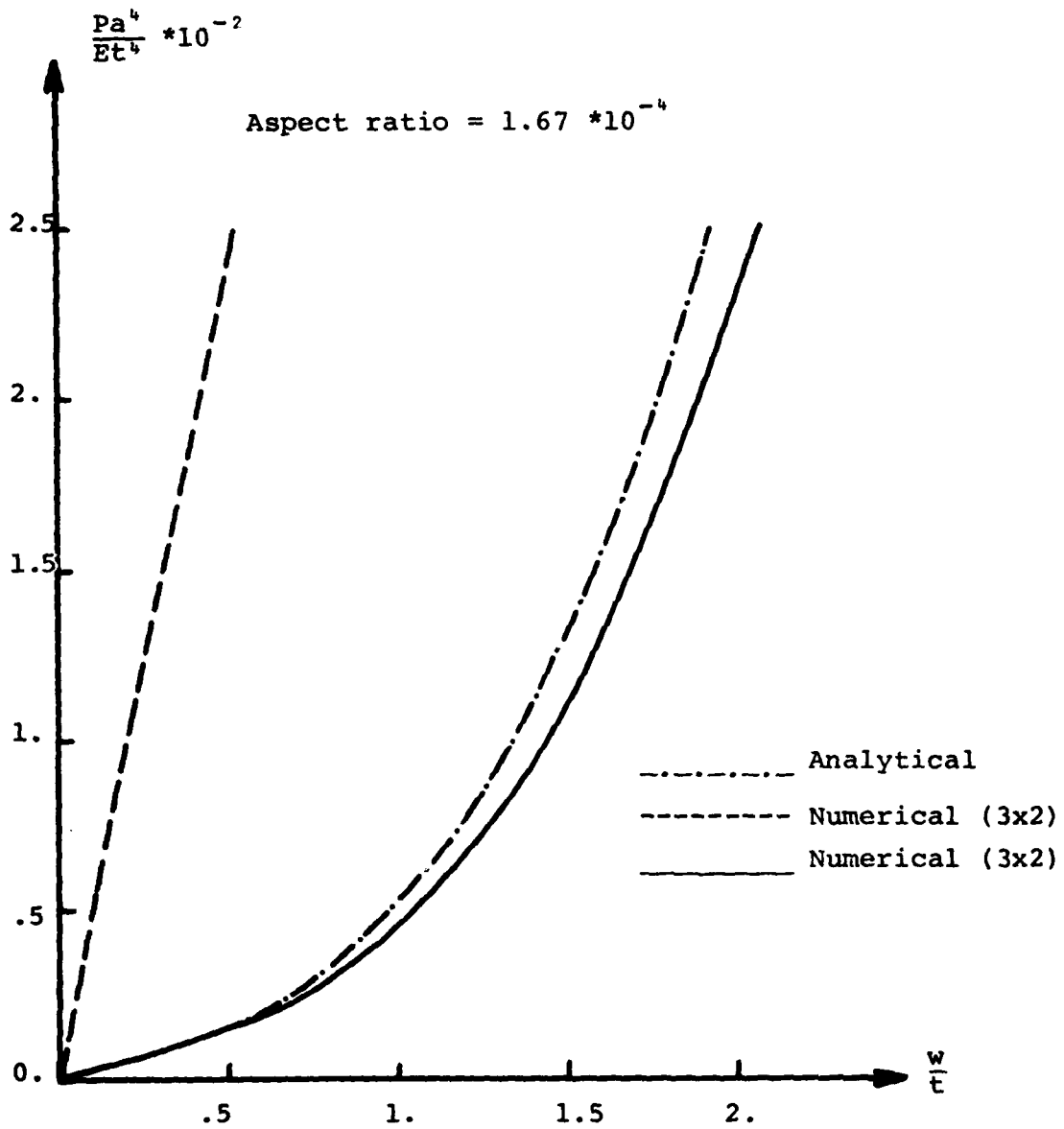
Fig. III.69    Load Deflection Response of Plate
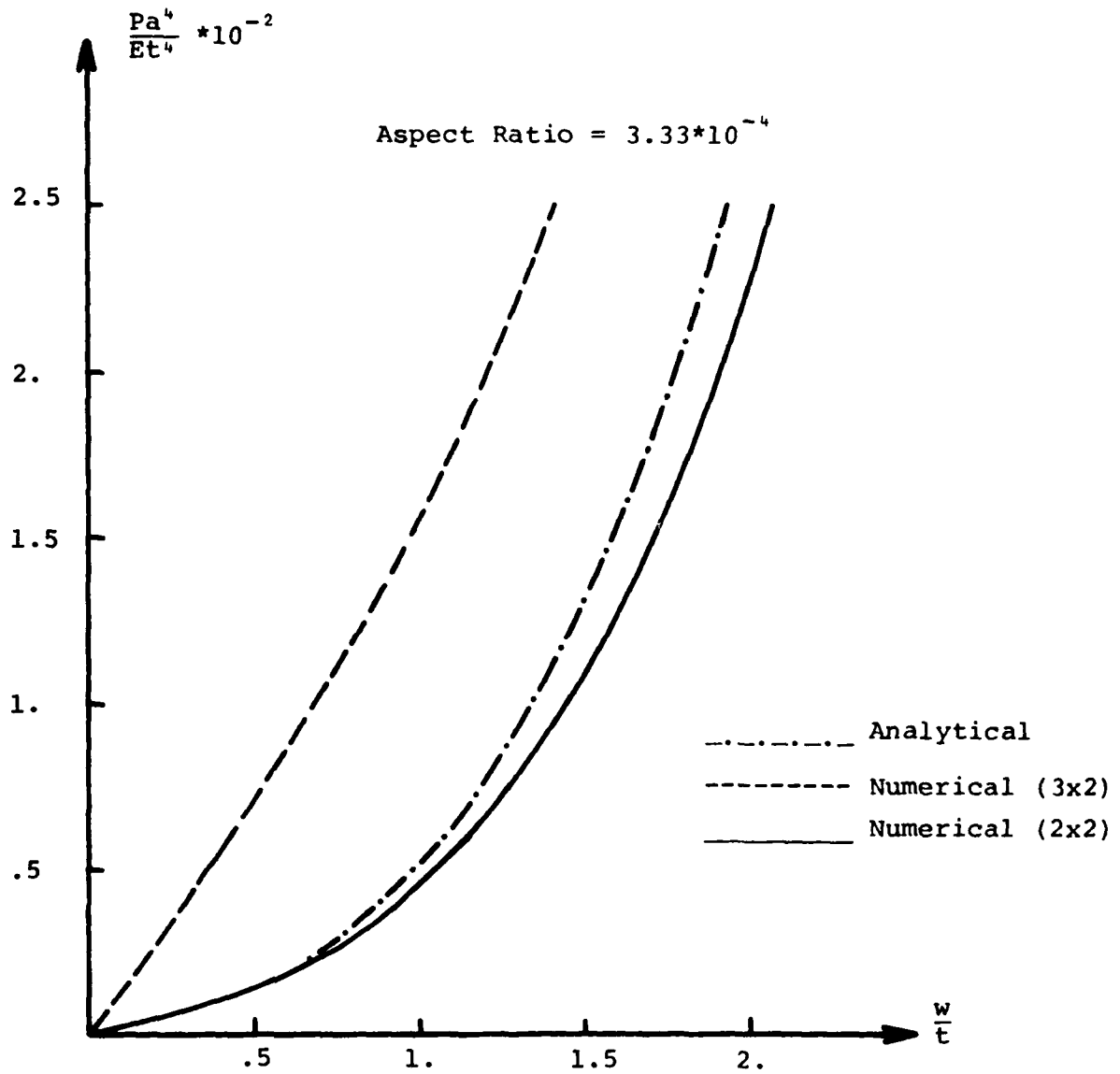
Fig. III.70    Load Deflection Response of Plate
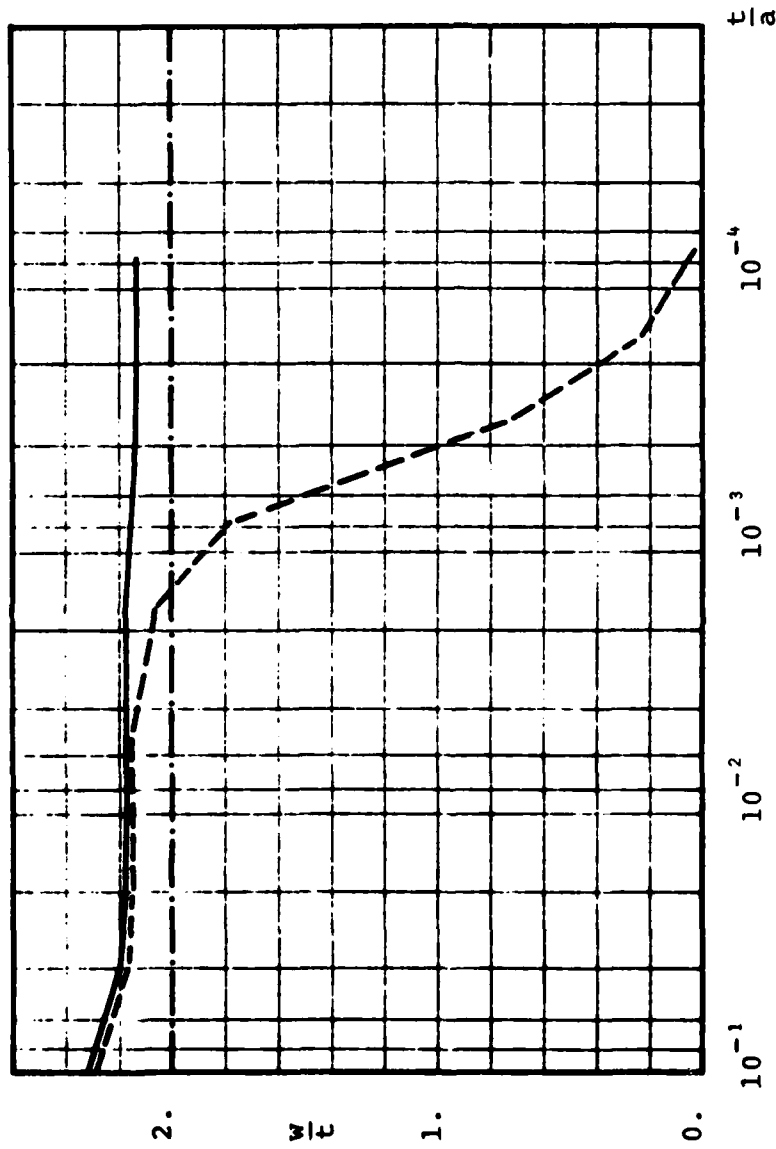
Fig.III.7)    Effect of Aspect Ratio on Plate Response
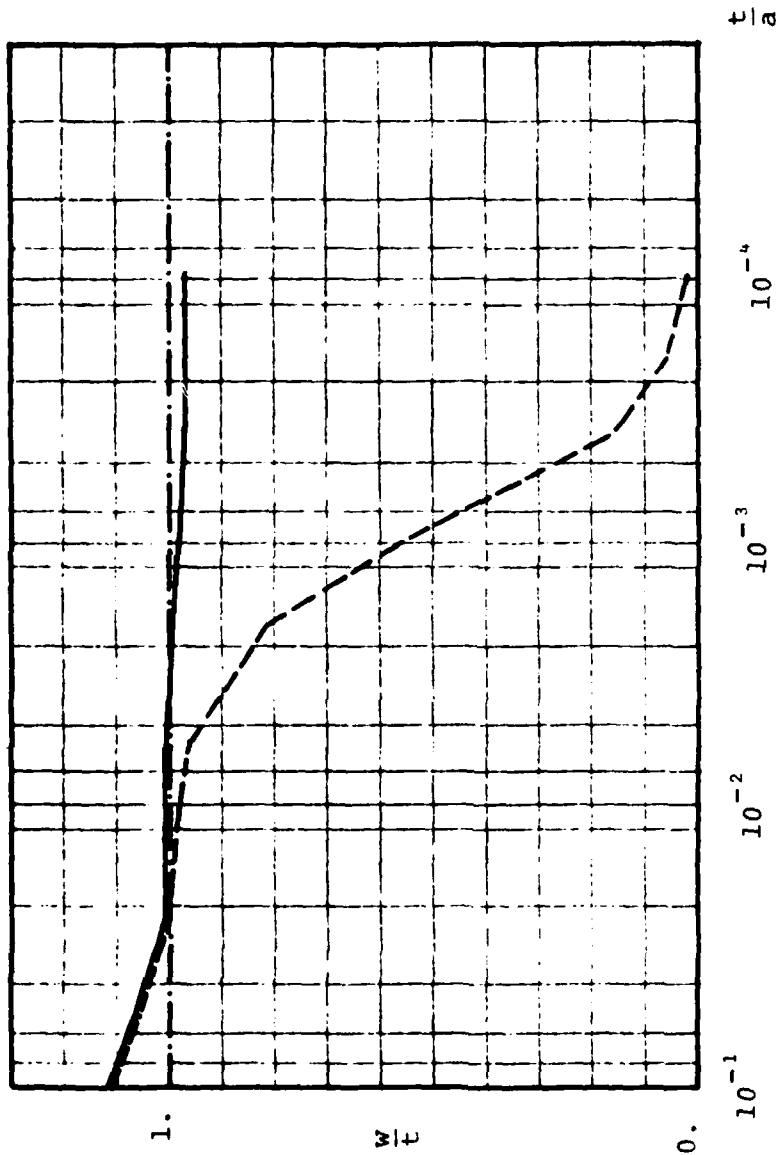
Fig.III.72   Effect of Aspect Ratio on Plate Response

120
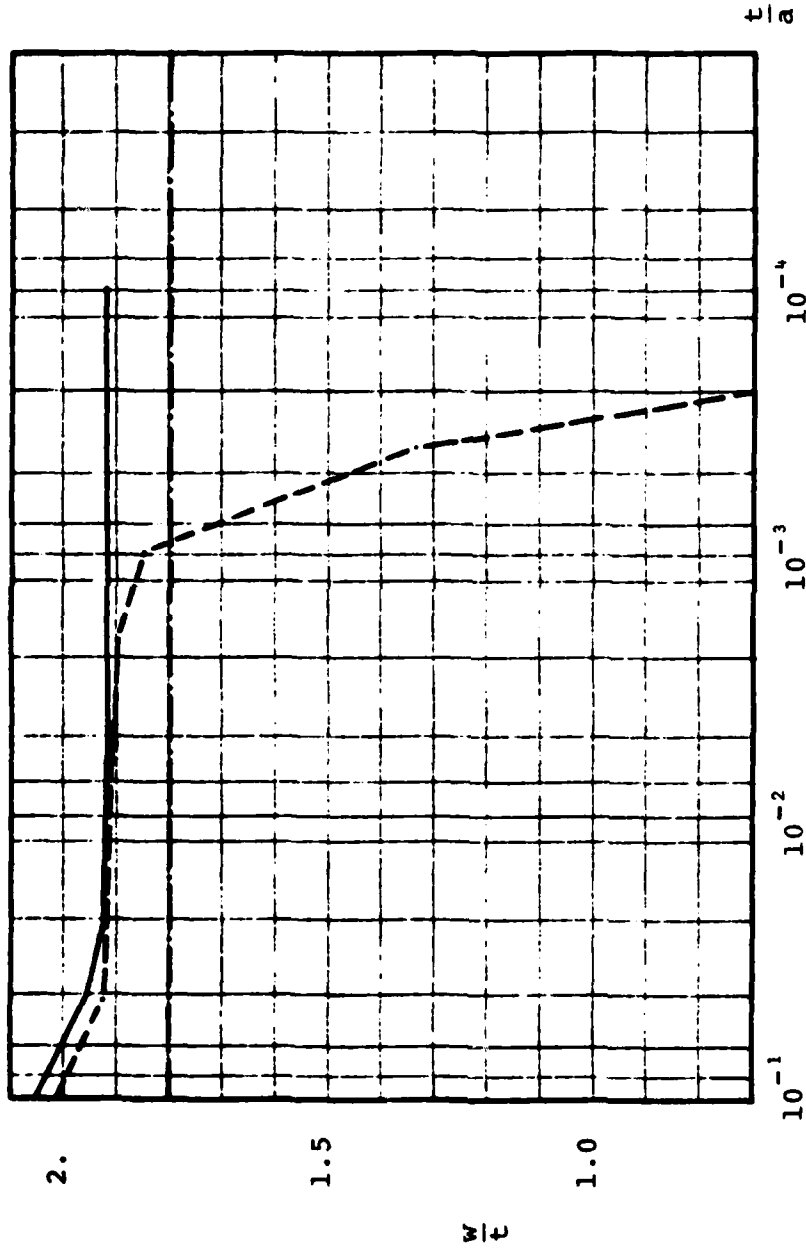
Fig. III.73    Effect of Aspect Ratio on Plate Response

convergence for other situations. For example, the ideal general purpose nonlinear finite element code should have several algorithmic options augmented with a degree of artificial intelligence. Namely, the problem solving capability should involve a heuristically guided trial and error search in the space of possible solution via an automatically structured algorithm. Unfortunately, currently available general purpose finite element codes of which ADINA is an example, do not have heuristic (self-adaptive) capabilities. In particular, because of its wide applicability, like ADINA most such codes employ some primitive (non-self-adaptive) variant of either the full or modified incremental Newton Raphson (MNR) algorithmic procedure. This applies to both the static and transient solution branches. In particular, the various transient algorithms such as Wilson, Newmark, Houbolt and central difference are usually developed around the primitive MNR algorithm and hence do not in themselves possess heuristic (self-adaptive) capabilities.

While the ADINA code presents the user with far-reaching and accurately programed capabilities, without apriori physical insight, expensive parametric studies are oftentimes necessary to assure adequate solution convergence. This is particularly true for unqualified users who do not have the proper training in nonlinear mechanics theory. As has been seen in the previous section, unless the proper load or time incrementation is employed, either poor convergence or out-of-balance loads are generally encountered. Such anomalous solution behavior is not an outgrowth of improper programing practice or illchosen field

<u>representation, but rather is generic to all nonlinear F.E.</u>
<u>codes employing non-self-adaptive MNR algorithms</u>. In view
of such shortcomings, this section will overview a series of
suggested changes to the ADINA algorithmic strategies aimed
at increasing the efficiency of the code as well as decreasing
the need for direct user intervention which is generally
quite time-consuming and costly.

From an overview point of view, the main thrust of the
discussion is to establish a three level strategy in parti-
cular:

    i)    Level 1:    Preliminary solution development via
                            primitive algorithms;

    ii)    Level 2:    Solution monitoring via validity/con-
                            vergence tests and;

    iii)    Level 3:    Self-adaptive strategies (Heuristic
                            programming).

Like the current ADINA equation solver, the first level should
employ primitive ( MNR,  NR etc.) operators to generate the
solution in the usual manner. The second level should involve
the constant monitoring of the different stages of solution
via a variety of validity/convergence tests. The last level
should consist of various self-adaptive strategies which are
triggered by the tests initiated by the level two surveillance
process. Note these strategies should be arrayed so that the
correct validity/convergence tests initiate the strategy with
the appropriate degree of sophistication.

To quantify the particulars of the suggested algorithmic
improvements, the following subsection will briefly outline

the main intent of the various phases of solution strategy noted above.

## IV.1  Level 1:  Primitive Operators

As noted earlier, the first level should employ primitive operators to generate the solution.  So as not to cause major changes in the ADINA architecture, such operators should involve various versions of the  NR algorithm namely:

1.  Full NR with constant reformation of tangent stiffness matrix during iteration;

2.  NR  algorithm with intermittent updating during iteration;

3.  Modified  NR algorithm with tangent stiffness reformation at beginning of load step but not during iteration (currently available);

4.  NR algorithm with iteration but no reformation (currently available);

5.  NR algorithm with reformation but no iteration (currently available) and lastly;

6.  NR algorithm with no reformation and iteration (currently available).

In the context of Fig. II.1, Fig. IV.1 defines the overall logic needed to implement the calculation flow associated with the  NR adaptions noted by items 1-6 listed above.

Such an addition could be achieved through minor modification to the EQUIT subroutine wherein the iterative loop is programmed.  Additionally, new control parameters would be
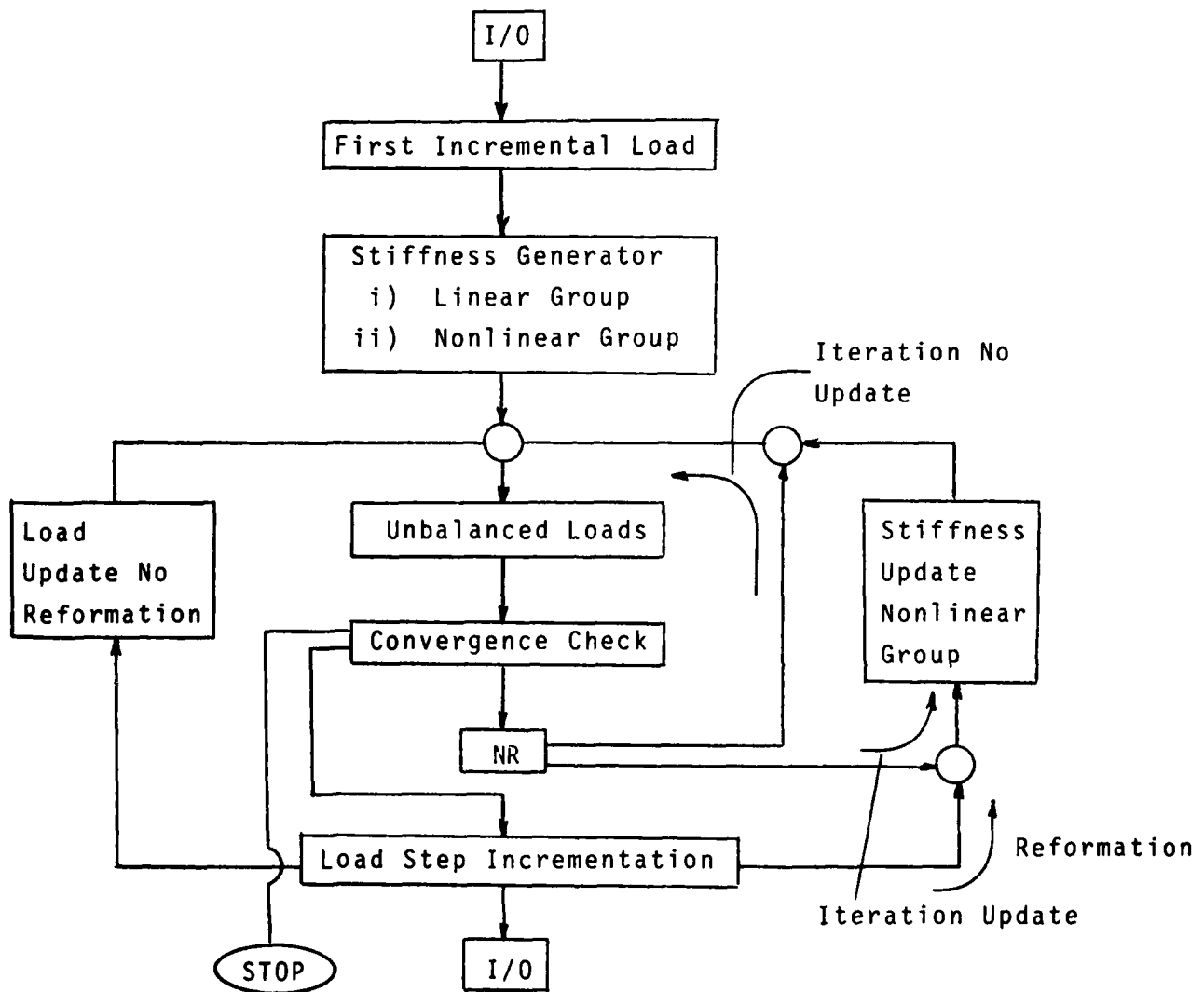
Fig. IV.1  Flow Diagram of Newton Raphson Algorithm
          Including Continuous Stiffness Updating
          Branch

necessary in such subroutines as TDFE, QUADS etc. to allow
for constant and/or intermittent updating of the tangent
stiffness matrix. As most of all the necessary arrays of
data are available in EQUIT, no real changes in code archi-
tecture would be involved apart from the incorporation of:

1. New variables to control the choice of the appro-
   priate NR algorithm;

2. New logic to allow for the proper packing of the
   reformed stiffness in secondary storage.

## IV.2   Level 2:   Validity/Convergence Tests

The validity/convergence tests should be the core of
the modification to ADINA. For the present purposes, the
discussion will be organized in three main categories namely:

1. Classical convergence tests;

2. "Quality" of convergence tests;

3. Degree of "nonlinearity tests".

The first group should be of the classical normed type
pass or fail variety as typified by the convergence test
currently programmed in ADINA, namely:

i)   the out of balance norm test;

ii)   nodal displacement norm test.

The main intent of such tests is essentially to monitor the
success or failure of the iterative procedure. While such
tests are efficient and well adapted to this prupose, they
cannot really forecast potential difficulties until outright
failure occurs. Because of this, if the restart option is
employed, depending on the problem, much of the solution

generated up to the failure point may have to be scratched so as to proceed further. In this context, what is necessary are so-called validity checks which enable a constant monitoring of the solution so as to determine whether the direction of convergence is proper.

In the context of the foregoing, the second group of tests should be concerned with the quality of convergence namely the rate, monotonicity, positive, negative and semi-definiteness, etc. Such information should obviously be used to trigger various modifications in the primitive iterative strategy depicted in level 1. As can be seen from the results outlined in Section III, various aspects of the system energy could be employed to serve as validity checks.

In addition to serving as a quality of convergence test, monitoring various aspects of the energy should serve as a good measure of the degree of nonlinearity excited by successive load/time increments. The importance of such tests follows from the fact that although finite element simulations of structures composed of general media undergoing large deflections are inherently nonlinear, the degree of non-linearity excited varies from point to point as well as from load/time increment to load/time increment. As it is possible that large portions of a structure may exhibit basically linear behavior, the third phase of quality/convergence testing will enable the automatic partitioning of the structure by allowing for preferential updates of the tangent stiffness depending on the amount of local nonlinearity excited. Such preferential updating obviously represents a more significant

modification in ADINA's architecture than the first two phases of quality/convergence testing. In particular, to accomodate the preferentially updating of particular stiffness partitions, such a change would entail a modification in the dynamic allocation scheme.

## IV.3 Level 3: Heuristic/Self-adaptive Strategies

Since the core of the ADINA solution strategy is based on the tangent modulus approach, any Heuristic programming modifications should obviously be centered around the NR family of algorithms. In the context of the inherent features of the NR algorithm, the adaptive strategy should incorporate one or more of the following basic options namely:

1) Adaptive tangent stiffness updates;

2) Adaptive incremental load adjustments;

3) Adaptive incremental time adjustments.

As noted earlier, the various self adaptive strategies should be programmed so as to be triggered by various of the previously discussed validity/convergence tests. The hierarchy of such modifications should be arrayed so that the quality of convergence test can be used to initiate the algorithm with the requisite degree of sophistication and efficiency required by the solution difficulties encountered.

The adaptive stiffness updates can themselves be organized in three main categories namely:

a) Global updates,

b) Local updates and

c) Partial updates.

The global stiffness updates should be based on either the degree of global geometric and material nonlinearity excited or because of poor solution convergence as determined by the validity/convergence test. The initiation of local updates should depend on the degree of local element nonlinearity excited. The incorporation of the local update option would obviously enhance the overall efficiency of the calculations. While the global and local preferential updates represent higher order solution fixes, pseudo updates such as the BFGS [ 9 ]* may represent a less costly self-adaption for certain classes of problems wherein only minor changes in stiffness may be encountered. Obviously for such problems as plastic loading and unloading, pseudo updates such as the BFGS are apt to yield erroneous results.

The adaptive incremental load and time adjustments can also be organized in several main categories namely:

    a)   Increment expansion;

    b)   Increment contraction;

    c)   Corrective incrementation.

Increment expansion for either static or dynamic problems can be initialized by various of the quality of convergence checks. Since the solution quality can be constantly monitored, any degradation initiated by increment expansion can be followed by a subsequent contraction. The contraction process should iteself be based on various checks such as:

    1)   Poor quality of convergence (non-monotonicity; nonpositive definiteness, etc.);

---

*Currently available in ADINA 1978

2)   Level of nonlinearity excited;

3)   Nearness to bifurcation points as monitored by nonlinearity and energy checks.

Note, a high level of local nonlinearity may be used to initiate local modification of incrementation.  Obviously in order to do this, special bookkeeping routines must be initiated to keep track of the status of the loading.

Note for load increments for which significant solution divergence is encountered, corrective load incrementation should be initiated.  In particular, negative load incrementation should be employed to retrace a portion of load history wherein a lower order algorithmic strategy yielded poorly converged results.  For time dependent problems, corrective incrementation should be initiated to retrace a portion of time history.

## V.     Summary

As noted earlier, the primary emphasis of this part
of the ISEG evaluation study was to establish the compu-
tational capabilities/shortcomings of the numerical algori-
thms inherent to ADINA (1977).  For this study, it was
achieved by utilizing specialized benchmark problems with
the two-fold purpose of;

    i)   Performing code check-out; and more importantly

    ii)  Establishing the algorithmic sensitivities, con-
        vergence characteristics and typical solution
        failure modes generic to the ADINA algorithmic
        apparatus.

Since ADINA has the capability to handle both kinematic and
material nonlinearity, special emphasis was given to ascer-
taining the operating characteristics in the presence of
softening, hardening, elastic/plastic and load/unload situa-
tions.

In this context, the benchmarking served to establish
the sensitivity/pathological behavior of the various non-
linear algorithms to changes in:

    i)    Convergence criteria;

    ii)   Time step size;

    iii)  Load increment size;

    iv)   Material models;

    v)    Order of integration of element stiffness, etc.

To enable the evaluation of the various behavioral patho-
logies, specialized coding was programmed into ADINA to allow

the strain energy, potential energy and kinetic energy histories to be evaluated during the various stages of calculation. This allowed for the monitoring of the initiation characteristics of anomalous pathological solution behavior.

The typical types of solution stops encountered during the degradation process most often involved either:

i) Out-of-balance loads;

ii) Negative pivots or;

iii) Iteration limit stops;

All other types of stops (zero Jacobian etc.) could be attributed most often to input errors in the data preparation or to the use of the code outside its range of capabilities. For instance, application of the code to bifurcation problems involving changes from positive to negative definite tangent stiffness are outside the range of application of the solution algorithm. Hence, care must be taken in dealing with problems involving statically or dynamically generated postbuckling behavior.

Typically it was found that the nature of degradation is dependent on the relative magnitude of load/time increment size. Usually three basic types of solution pathologies were encountered. Specifically:

i) Immediate and strong nonmonotonicity;

ii) Moderate but progressively increasing non-monotonicity and nonpositive definiteness; and

iii) Mild monotonicity with either very gradual increases or decreases in solution oscillation.

The first two types were found to give rise to out-of-balance loads and negative pivots (bifurcation problems) while the third type caused iteration limit stops.

As noted earlier, such anomalous behavior is <u>not</u> an outgrowth of any shortcomings in the ADINA architecture and coding practice. Rather, they are due to the intrinsic properties of the modified NR procedure used to solve the nonlinear field equations arising in both the static and dynamic branches. Furthermore, as an outgrowth of fairly extensive code check-out benchmarking, apart from minor bugs, the algorithmic apparatus inherent to ADINA (1977) is both honestly and accurately programmed.

Due to the results of the sensitivity studies, it has been observed that while ADINA can generally be forced to generate a solution to highly nonlinear problems via the various restart and time block options, such an approach is typically expensive and time consuming. Because of this and the adaptability of the coding and architecture, some heuristic type algorithmic capabilities should be incorporated in ADINA to streamline the process of solution generation in highly nonlinear problems.

## VI. REFERENCES

1. Bathe, R.J. and Wilson, E.L. "Stability and Accuracy Analysis of Direction Integration Methods", Int. Jr. Earth of Engrg. Struct. Vol. 1, p. 283 (1973).

2. Newmark, N.M. "A Method of Computation for Structural Dynamics", J. Eng. Mech. Div., ASCE, Vol. 85, EM3, 1959, pp. 67-94.

3. Collatz, L., The Numerical Treatment of Differential Equations, Springer-Verlag, New York (1966).

4. Bathe, R. J. and Wilson, E. L., Numerical Methods in Finite Element Analysis, Prentice Hall Inc. New Jersey (1976).

5. Green, A. E. and Zerna, W., Theoretical Elasticity, Oxford Press, England (1968).

6. Meirovitch, L., Analytical Methods in Vibrations, MacMillan Company, New York (1967).

7. Zienkiewicz, O. C., "The Finite Element Method", McGraw Hill, (1977).

8. Donnell, L. H., Beams, Plates and Shells, McGraw-Hill Book Co., New York, (1976).

9. Mathies, H. and Strang, G., "The Solution of Nonlinear Finite Element Equations," Int. J. Num. Meth. Engng., Vol. 14, pp.1613-1626 (1979).

## APPENDIX 1:   Energy Calculations

As was first noted in Chapter III, the local and global
strain energy are used to monitor the computational capa-
bilities and shortcomings of the algorithms inherent to ADINA
(1977).  For the present purposes, the TL version of the energy
functionals will be derived.  The development will include both
the local element and global versions.

To start, we turn to the  NR algorithm defined by

$$[K_T \, (\underset{\sim}{Y})] \Delta \underset{\sim}{Y} = \Delta \underset{\sim}{R} \qquad (A-1)$$

where here $\Delta \underset{\sim}{Y}$ denotes the increment of displacement associated
with a given unbalanced load $\Delta \underset{\sim}{R}$ and $[K_T]$ is the current tangent
stiffness matrix.  For a given load step, the iterative solu-
tion of (A-1) obviously leads to the overall incremental res-
ponse.  Graphically, the results of the iterative process is
defined in the scalar analogy given in Fig. A1-1. The incre-
mental energy stored during a given iteration step is es-
sentially the shaded area illustrated in this figure.  Reali-
zing that the ordinate values of the true solution surface are
given by the relation[7]

$$\underset{\sim}{F} = \int_V [B \, (\underset{\sim}{Y})]^T \underset{\sim}{\sigma}(\underset{\sim}{Y}) \, dV \qquad (A-2)$$

it follows that the incremental energy stored during the $k^{th}$
iteration step can be approximated by the inner product
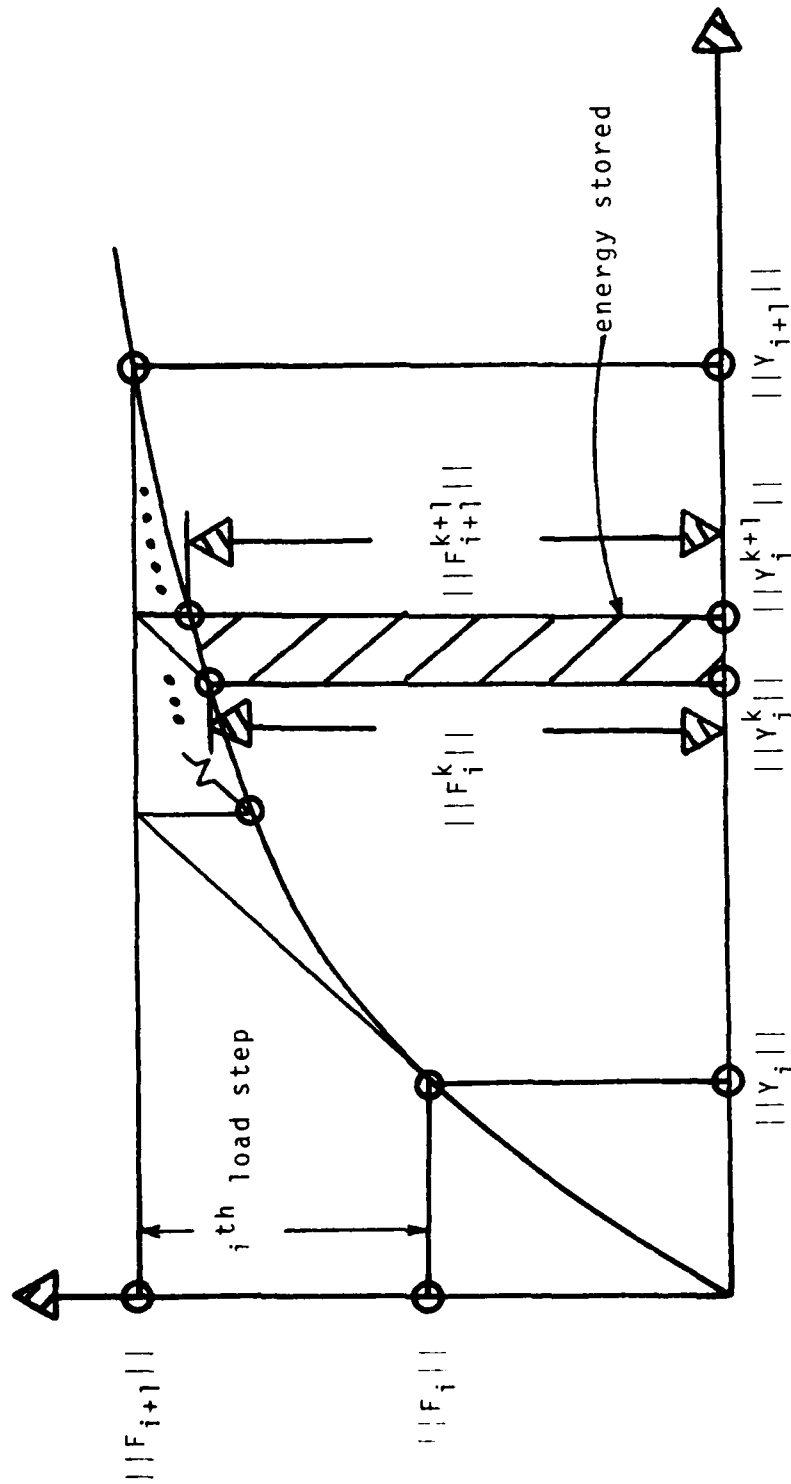
Fig. Al-1   Energy Stored During $k^{th}$ Iteration of $_i^{th}$ Load Step

$$E_i^k = \frac{1}{2}(F_{\sim i}^k + F_{\sim i}^{k+1})^T \Delta \gamma_{\sim i}^k$$

$$= \frac{1}{2}\left(\int_0^R [B(\gamma_{\sim i}^k)]^T \sigma_k(\gamma_{\sim i}^k)\, dV + \int_0^R [B(\gamma_{\sim i}^{k+1})]^T \sigma_k(\gamma_i^{k+1})\, dV\right)^T \Delta\gamma_{\sim i}^k \qquad (A-3)$$

where $(\ )^T$ denotes matrix transposition, and B is the element strain-nodal displacement transformation matrix.

In terms of Fig. (A1-2), assuming that a total of $K^i$ iteration steps are associated with the $i^{th}$ load step, then the following expression can be developed for the energy stored namely

$$E_i = \sum_{k=1}^{K^i} E_i^k$$

$$= \frac{1}{2}\sum_{k=1}^{K^i} (F_{\sim i}^k + F_{\sim i}^{k+1})^T \Delta\gamma_{\sim i}^k$$

$$= \frac{1}{2}\sum_{k=1}^{K^i}\left(\int_0^R [B(\gamma_{\sim i}^k)]^T \sigma(\gamma_{\sim i}^k)\, dV + \int_0^R [B(\gamma_{\sim i}^{k+1})]^T \sigma(\gamma_{\sim i}^{k+1})\, dV\right)^T \Delta\gamma_{\sim i}^k \qquad (A-4)$$

Summing (A-4) over the entire set of I load steps yields the requisite overall strain energy stored for a given problem namely
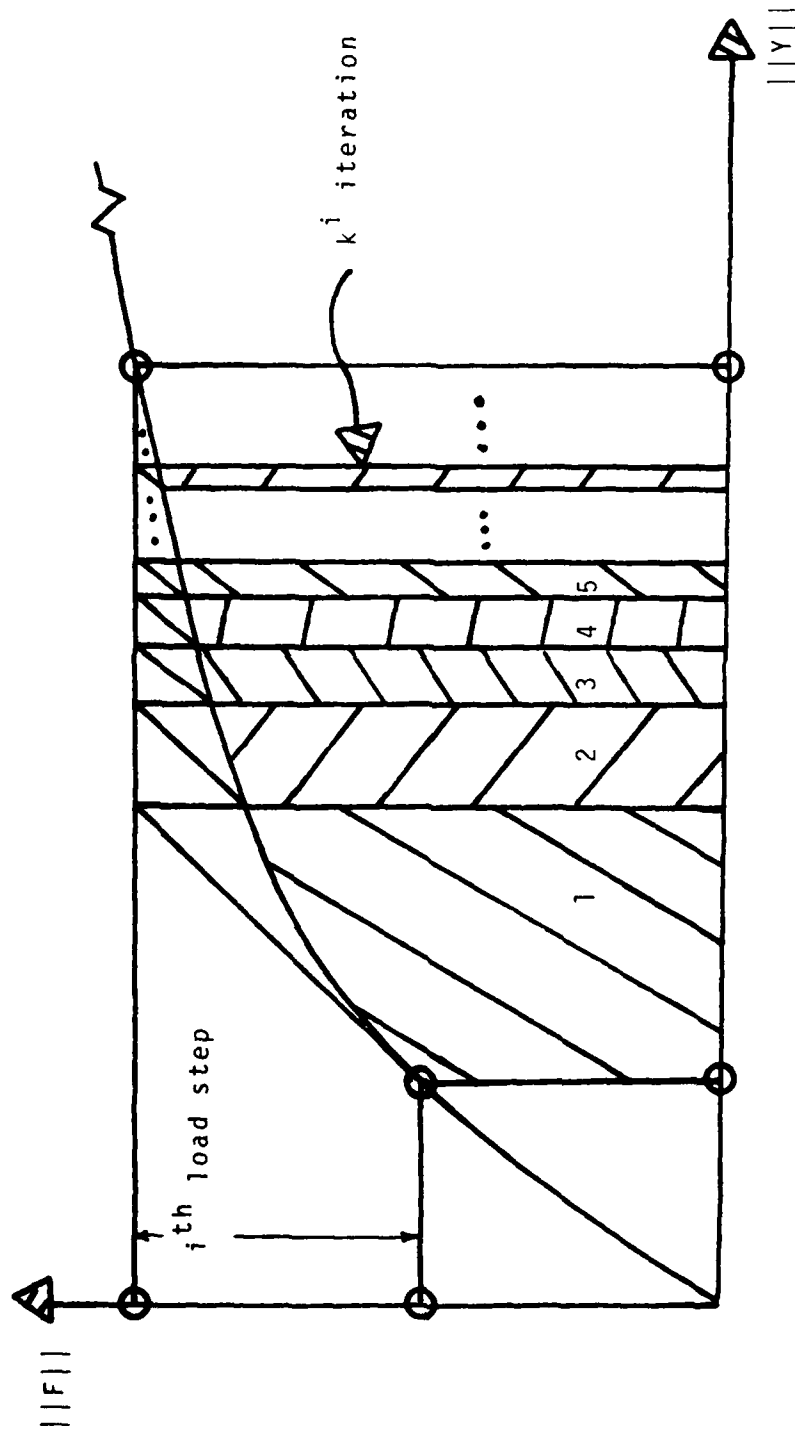
Fig. A1-2  Energy Stored During $i^{th}$ Load Step

$$E_t = \sum_{i=1}^{I} E_i$$

$$= \frac{1}{2} \sum_{i=1}^{I} \sum_{k=1}^{K^i} (\underset{\sim}{F}_i^k + \underset{\sim}{F}_i^{k+1})^T \Delta \underset{\sim}{Y}_i^k$$

$$= \frac{1}{2} \sum_{i=1}^{I} \sum_{k=1}^{K^i} \left( \int_{o^R} [B\,(\underset{\sim}{Y}_i^k)]^T \underset{\sim}{\sigma}(\underset{\sim}{Y}_i^k)\, dV - \right.$$

$$\left. \int_{o^R} [B*(\underset{\sim}{Y}_i^{k=1})]^T \underset{\sim}{\sigma}(\underset{\sim}{Y}_i^{k+1})\, dV \right)^T \Delta \underset{\sim}{Y}_i^k \qquad (A-5)$$

To obtain the element strain energies from (A-5), the various nodal displacement and force vectors must be interpreted from a local point of view namely

$$E_t = \frac{1}{2} \sum_{i=1}^{I} \sum_{k=1}^{k^i} \left( \int_{o^{R_e}} [B\,(\underset{\sim}{Y}_{ie}^k)]^T \underset{\sim}{\sigma}(\underset{\sim}{Y}_{ie}^k)\, dV - \right.$$

$$\left. \int_{o^{R_e}} [B\,(\underset{\sim}{Y}_{ie}^{k+1})]^T \underset{\sim}{\sigma}(\underset{\sim}{Y}_{ie}^{k+1})\, dV \right) \Delta \underset{\sim}{Y}_{ie}^k \qquad (A-6)$$

where here $\underset{\sim}{Y}_{ie}^k$ $\underset{\sim}{Y}_{ie_k}^{k+1}$ and $\Delta \underset{\sim}{Y}_{ie}^k$ denote local element partitions of $\underset{\sim}{Y}_i^k$, $\underset{\sim}{Y}_i^{k+1}$ and $\Delta \underset{\sim}{Y}_i^k$ and $_o R_e$ is the region occupied by the $e^{th}$ element.

Because of the form of either (A-5) or (A-6), any form of tangent stiffness type constitutive law can be accomodated. This is particularly true for those inherent to ADINA (1977).

The actual calculations programmed into the ADINA's algorithmic flow are depicted in Appendix 3. As noted earlier, such options include the capability of handling:

1) Multiple element groups;

2) In/out of core solution options;

3) All available material property options and;

4) All algorithmic options (static and dynamic).

APPENDIX 2 : Code Checkout

The various benchmarks that were run strictly for
preliminary code check out will be briefly discussed in
this Appendix.  The problem types employed fell into three
main structural categories namely:

1)   Beam/truss type structure;

2)   2-D continuum and;

3)   3-D continuum.

The analyses ran consisted of static, dynamic and eigenvalue/
vector problems.

For check out pruposes, NFAP, NONSAP, STRUDL and NASTRAN*
were employed to perform parallel runs.  This enabled both
linear and nonlinear verifications to be performed on well tried
and readily available "general" purpose codes.

Note the linear benchmarks with STRUDL and NASTRAN en-
abled a thorough determination of any anomalies in much of the
ADINA bookkeeping associated with:

1.   In/out of core solutions;

2.   Handling of various boundary conditions;

3.   Handling of different;

   i)   element groups

  ii)   material properties

 iii)   node sequencing etc.

Additionally, such tests permitted the benchmarking of the
initial structure stiffness.

_____

*Cosmic version levels 16. and 17.5

Once such factors were verified, the various geometric
and material nonlinearities were benchmarked within the capa-
bilities of NONSAP and its derivative NFAP.

The primary source of benchmarks was drawn from the
ADINA sample problems.  Whenever possible, their results were
verified via either NONSAP, NFAP or the linear initial stiff-
ness results via STRUDL and NASTRAN.  The benchmarks con-
sisted of the following list of problems namely:

1. Tower Cable;

   i)  static

   ii)  frequency

2. Rubber sheet; Mooney Rivlin material, small/
   large deformation

   i)  static

   ii)  dynamic

   iii)  frequency (linear)

3. Spherical shell; elastic, plastic, concrete,
   small/large deformation

   i)  static

   ii)  dynamic

   iii)  frequency (linear)

   iv)  onset of static/dynamic buckling

4. Thick walled cylinder; thermo-elastic-plastic,
   small/large deformation

   i)  static

   ii)  dynamic

5. Simply supported plate; elastic, plastic, concrete, small/large deformation

    i) static

    ii) dynamic

    iii) frequency/linear

6. Arch; elastic, plastic, concrete, small/large deformation

    i) static

    ii) dynamic

    iii) frequency (linear)

    iv) onset of static/dynamic buckling

7. Cyclic creep analysis of a thick walled cylinder.

8. Underground opening, elastic, plastic, concrete, static analysis.

9. Reinforced concrete beam

    i) static

    ii) dynamic

    iii) frequency

10. Pipewhip; dynamic response.

During the initial attempts to run the foregoing problems, benchmarks 1-7 yielded successful solutions for all the various analyses performed (static, dynamic, frequency, etc.). Such was not the case for problems 8-10. In particular, in our version of ADINA (1977), negative pivots were initially encountered. After some debugging, dynamic allocation problems were found in the MAXA array. Once

corrected, all the above listed problems yielded successful solutions for the various analyses performed.

To check the various bookkeeping features of ADINA alluded to earlier, (in/out of core solutions, etc.), the foregoing problems were modified in several different ways namely;

1. Elementing increased/decreased

2. Element type changed

3. Node sequencing changed

4. Changes introduced in

    i) Material types

    ii) Boundary conditions

    iii) Loadings etc.

In order to verify the in and out of core features, the dynamic allocation and block size was increased and decreased. Such an approach allowed the same problem to be run in and out of core. For all the foregoing manipulations, apart from the minor allocation difficulties associated with the MAXA array, no difficulties or aberration were encountered in either the beam, 2-D or 3-D elements.

In addition to the foregoing problems, several additional code check out benchmarks were considered. The main thrust of this group of problems was to establish the capability of ADINA to predict the onset of static and dynamic structural instability. In this context, buckling problems involving beams, arches, rings and spherical caps were considered. This

included:

1.  Offset loaded beam/columns with varying boundary conditions;

2.  Arches with varying depths and boundary conditions;

3.  Radially loaded rings and;

4.  Spherical caps with varying depths and boundary conditions.

The results of the above noted "stability" problems were compared with NONSAP and NFAP for independent verification. Note within the limits of the tangent modulus/MNR approach, good resolution was obtained for such problems. Such was not the case though for the beam element. In particular, for offset column type buckling problem, immediate solution failure was encountered. From the nature of the program stop, (negative pivot), the difficulty appears to be isolated to the beam element. This also follows from the fact that good buckling predictions were obtained via the 2-D TL and UL formulation of the same problem. Apart from the foregoing difficulties, ADINA (1977) appears to be largely error free.

<u>Appendix 3   Input Data Echoes for Selected Sample Problems</u>

1) Static Analysis of a Rubber Sheet

2) Dynamic Analysis of a Spherical Cap

3) Dynamically Loaded Cantilever Beam

```
                    C O L U M N   N U M B E R
        1         2         3         4         5         6         7
1234567890123456789012345678901234567890123456789012345678901234567890

        STATIC ANALYSIS OF A RUBBER SHEET 1.
        48100111  1  1  4

CARD
NUMBER
------
  1              1    1   50
  2              1
  3
  4
  5
  6
  7
  8
  9
 10
 11
 12      1      -1
 13      2       1   -1
 14      3       1    1   -1
 15      4       1    1
 16      5       1    1
 17     45                      1.01
 18      6                     11.11    1.52
 19     10                      1.01    3.00
 20     14                      2.02    4.46
 21     18                      3.03
 22     22                      4.04    1.16
 23     26                      5.05    0.92
 24     30                      6.06    0.74
 25     46                      7.07    0.62
 26      7                     11.11    0.56
 27     11                      1.01    0.52
 28     15                      2.02    0.50
 29     19                      3.03    0.50
 30     23                      4.04    2.32
 31     27                      5.05    1.86
 32     31                      6.06    1.54
 33     35                      7.07    1.34
 34     39                      8.08    1.20
 35     47                      9.09    1.19
 36      8                     11.11    1.04
 37     12                      1.01    1.02
 38     16                      2.02    1.00
 39     20                      3.03    1.06
 40     24                      4.04    3.42
 41     28                      5.05    2.76
 42     32                      6.06    2.28
 43     36                      7.07    2.04
                               8.08    1.80
                                       1.66
                                       1.58
                                       1.54
```

```
                      C O L U M N   N U M B E R
         1         2         3         4         5         6         7
1234567890123456789012345678901234567890123456789012345678901234567890
----------------------------------------------------------------------
                                                    9.09              1.50
                                                   11.11         13   1 1.50
                                                              1

     1    2              2

     1.0    2
  21.605 15.74650
     1    4    1    4
     6    2    5    1
    11    4    1    1
    46   42   45    4                     0.125
    12    4    2    1                     0.125
     7    3    6    4                     0.125
    22    4    1    1                     0.125
    47   43   46    4                     0.125
    23    4    1    1                     0.125
     8    4    7    4
    33    4    1    1
    48   44   47    1
     1    2    2              4.9   40.90
    45    2    1  0.166667
    46    2    1  0.333333
    47    2    1  0.333333
    48    2    1  0.166667
```

CARD NUMBER
44
45
46
47
48
49
50
51
52
53
54
55
56
57
58
59
60
61
62
63
64
65
66
67
68

```
                    C O L U M N   N U M B E R
         1         2         3         4         5         6         7
1234567890123456789012345678901234567890123456789012345678901234567890
----------------------------------------------------------------------
DYNAMIC RESPONSE OF A SPHERICAL CAP USING NEWMARK (NONLINEAR ANALYSIS)
```



| CARD NUMBER | | |
|---|---|---|
| 1 | 53100111 | |
| 2 | | 1 1 100 .000005 |
| 3 | | 1 |
| 4 | | |
| 5 | 1 | |
| 6 | 1 1 | |
| 7 | 1 1 | 1 |
| 8 | | 1 |
| 9 | | |
| 10 | | |
| 11 | | |
| 12 | 52 | 2 |
| 13 | 1 | x   22.065   63.33   1 |
| 14 | 3 1 | x   22.475   63.33 |
| 15 | 4 1 | x   22.065   64.6635   5 |
| 16 | 49 | x   22.065   88.6665 |
| 17 | 6 | x   22.065   65.9970   5 |
| 18 | 46 | x   22.065   87.3330 |
| 19 | 7 | x   22.270   65.9970   5 |
| 20 | 47 | x   22.270   87.3330 |
| 21 | 5 | x   22.475   64.6635 |
| 22 | 50 | x   22.475   88.6665   5 |
| 23 | 8 | x   22.475   65.9970 |
| 24 | 48 1 | x   22.475   87.3330   5 |
| 25 | 51 1 | x   22.065   90.0 |
| 26 | 53 2 | x   22.475   90.0   1 |
| 27 | | 10 |
| 28 | | |
| 29 | | |
| 30 | 2 10 2 | 8   1 |
| 31 | .000245 | |
| 32 | 10500000. 0.3 | 24000.   21000. |
| 33 | 1 6 | 5   5 |
| 34 | 8 1 | 5   7   4   2 |
| 35 | 10 | |
| 36 | 48 53 46 | 50 52 49 47 |
| 37 | 1 2 | .004 |
| 38 | 1200. | 1200. |
| 39 | 3 8 5 | |
| 40 | 1.0 1.0 1.0 | 5 |
| 41 | 1 48 53 50 | |
| | 1.0 1.0 | |
```

```
                              COLUMN  NUMBER
                 1         2         3         4         5         6         7
         1234567890123456789012345678901234567890123456789012345678901234567890
CARD     ----------------------------------------------------------------------
NUMBER
------
  1      **DYNAMICALLY LOADED CANTILEVER BEAM**
  2      12110111 1 1 1000 0.00005
  3         2
  4
  5
  6          1
  7          1      1
  8
  9
 10
 11          11     1        1        1
 12          1      1        1        1                      1.00     0.25
 13          2      1        1        1                      10.0     0.75
 14          11     1        1        1                               0.25
 15          12     1        1        1                               3.0
 16          1      2
 17
 18      4   10    2                   1   1          2   1
 19          1     0.0007305
 20      3.0E07    0.27     0.5               4.4E04  3.0E05
 21          1      2   12   1     4
 22      10  16    11  12   1     4
 23          1      2
 24                -170.0            30.0 -170.0
 25          11     3    1   1.0
 26      STOP
```

| REPORT DOCUMENTATION PAGE | READ INSTRUCTIONS BEFORE COMPLETING FORM |
|---|---|

| 1. REPORT NUMBER | 2. GOVT ACCESSION NO. | 3. RECIPIENT'S CATALOG NUMBER |
|---|---|---|
| AUE-802 | AD-A096 681 | |

| 4. TITLE (and Subtitle) | 5. TYPE OF REPORT & PERIOD COVERED |
|---|---|
| Evaluation of ADINA: PART II - Operating Characteristics | Technical Report |
| | 6. PERFORMING ORG. REPORT NUMBER |

| 7. AUTHOR(s) | 8. CONTRACT OR GRANT NUMBER(s) |
|---|---|
| J. Padovan and T. Y. Chang | N00014-78-C-0691 |

| 9. PERFORMING ORGANIZATION NAME AND ADDRESS | 10. PROGRAM ELEMENT, PROJECT, TASK AREA & WORK UNIT NUMBERS |
|---|---|
| College of Engineering The University of Akron Akron, Ohio 44325 | |

| 11. CONTROLLING OFFICE NAME AND ADDRESS | 12. REPORT DATE |
|---|---|
| Office of Naval Research Arlington, VA | June 8, 1980 |
| | 13. NUMBER OF PAGES |

| 14. MONITORING AGENCY NAME & ADDRESS(if different from Controlling Office) | 15. SECURITY CLASS. (of this report) |
|---|---|
| | Unclassified |
| | 15a. DECLASSIFICATION/DOWNGRADING SCHEDULE |

**16. DISTRIBUTION STATEMENT (of this Report)**

Distribution of this report is unlimited.

**17. DISTRIBUTION STATEMENT (of the abstract entered in Block 20, if different from Report)**

**18. SUPPLEMENTARY NOTES**

**19. KEY WORDS (Continue on reverse side if necessary and identify by block number)**

Nonlinear Finite Element Analysis, Static and Dynamic Responses, Convergence test, Benchmark Problems, Numerical Algorithms.

**20. ABSTRACT (Continue on reverse side if necessary and identify by block number)**

An advanced evaluation of the various solution algorithms available in the 1977 ADINA was made. The main objective of the evaluation work is to assess the inherent characteristics of the nonlinear static, dynamic and eigenvalue solution branches of the program. Several benchmark problems were run to establish the numerical characteristics of the solution algorithms adopted by ADINA.

DD FORM 1473 EDITION OF 1 NOV 65 IS OBSOLETE
1 JAN 73

S/N 0102-LF-014-6601

DATE
ILMED
-8